The effect of the acid sphingomyelinase/ceramidase system on bacterial induced colitis

Inaugural-Dissertation

zur

Erlangung des Doktorgrades

Dr. rer. nat.

der Fakultät für

Biologie

an der

Universität Duisburg-Essen

vorgelegt von

Jana Meiners

aus Achim

Februar 2019

DOI: 10.17185/duepublico/70151
URN: urn:nbn:de:hbz:464-20190606-080456-9

Die der vorliegenden Arbeit zugrunde liegenden Experimente wurden am Institut für Medizinische Mikrobiologie der Universität Duisburg-Essen durchgeführt.

1. Gutachter: Prof. Dr. Astrid Westendorf
2. Gutachter: PD Dr. Katrin Becker-Flegler

Vorsitzender des Prüfungsausschusses: Prof. Dr. Ulf Dittmer

Tag der mündlichen Prüfung: 10.05.2019

Table of Content

Summary

Sphingolipids are complex structures, which are shown to be involved in the maintenance of the intestinal integrity. Increasing evidence implicates a function of sphingolipids in intestinal diseases such as inflammatory bowel disease (IBD). Interestingly, the activation of various phospholipases and sphingomyelinases were shown to be altered through inflammatory cytokine secretion. However, little is known about the role of sphingolipids, such as ceramide, and sphingomyelin in the context of bacterial induced inflammation. In the present study, we determined the function of the acid sphingomyelinase (Asm) and acid ceramidase (Ac) during the bacterial induced colitis using the *Citrobacter (C.) rodentium* infection model. *C. rodentium* is a natural mouse gram-negative mucosal pathogen that induces colonic inflammation. Importantly, sphingomyelin and ceramide concentrations were significantly decreased in the colon of *C. rodentium* infected mice. However, treatment with amitriptyline to inhibit Asm and Ac activity during infection as well as infection of Asm KO or Ac cKO mice led to an increase in sphingomyelin and ceramide in the colon within 6 to 10 days post infection. This increase was accompanied by an enhanced histopathological score. Interestingly, Asm KO, as well as Ac cKO mice showed enhanced bacterial translocation of the normally non-invasive *C. rodentium* into the liver and the spleen compared to infected wildtype mice. Flow cytometry analysis revealed that neither the frequencies of macrophages, as part of the first line of defence from the innate immune system, nor the MHCII expression by macrophages were impaired in wildtype compared to amitriptyline treated mice. Furthermore, uptake capability of macrophages generated from bone marrow of ASM KO or Ac cKO, as well as killing activity was not dysregulated compared to BMDMs isolated from wildtype littermates. Intriguingly, increased cell infiltration of adaptive immune cells, such as T_h1 and T_h17, into lamina propria (LP) was detected during *C. rodentium* infection in mice lacking Asm and Ac activity due to amitriptyline treatment compared to wildtype littermates. In contrast, frequencies of T_{regs} were reduced in colonic tissue at the peak of infection in amitriptyline treated mice compared to wildtype littermates. However, the differentiation capacity of T_h1 and T_h17 cells *in vitro* was not altered after loss of Asm.

In summary, loss of Asm and Ac leads to a dysregulated immune response during *C. rodentium* infection. Reduced frequencies of colonic T_{regs} in Asm/Ac inhibited mice allowed the uncontrolled expansion of T_h1 and T_h17 cells, thereby inducing severe pathology in the colon.

We showed for the first time that Asm and Ac possess a protective function during bacterial induced colitis. Intriguingly, Asm and Ac shape the adaptive immune response to effectively fight invading *C. rodentium* and protect the mice against severe intestinal pathology.

Zusammenfassung

Sphingolipide besitzen auf Grund ihrer diversen und grundlegenden Funktion in Membranen ein großes wissenschaftliches Potential. In unterschiedlichen Studien wurde bereits der Einfluss von Sphingolipiden auf die intestinale Homöostase und auf Entzündungsprozesse im Gastrointestinaltrakt beschrieben. Bisher ist jedoch wenig über die Funktion der sauren Sphingomyelinase (eng. Acid sphingomyelinase, Asm) und der sauren Ceramidase (eng. Acid ceramidase, Ac) während einer bakteriell induzierten Kolitis bekannt.

In dieser Arbeit wurden daher erstmals die Funktionen der sauren Sphingomyelinase und sauren Ceramidase während der *Citrobacter* (*C*) *rodentium* induzierten Kolitis untersucht. *C. rodentium* ist ein gram-negatives Bakterium, welches ähnliche Entzündungsreaktionen hervorruft, die auch in Patienten mit chronisch-entzündlichen Darmerkrankungen beobachtet werden. Im Verlaufe einer 10-tägigen Infektion mit *C. rodentium* von Wildtyp-Mäusen zeigte sich eine signifikante Abnahme der Sphingomyelin und Ceramide Konzentrationen im Kolon. Im Gegensatz dazu führte die Infektion von Asm KO und auch Ac cKO Mäusen zu einem Anstieg der Sphingomyelin und Ceramide Konzentrationen. Interessanterweise, zeigten *C. rodentium* infizierte Asm KO und Ac cKo Mäuse insgesamt einen verschlechterten Habitus und erhöhte Entzündungsparameter im Kolon im Vergleich zu infizierten Wildtyp-Mäuse. Besonders auffällig war die erhöhte systemische Ausbreitung des normalerweise nicht-invasiven Bakteriums in die Leber und Milz von Asm KO und Ac cKO Tieren. Intestinale Makrophagen stellen die erste immunologische Verteidigungslinie gegen pathogene Erreger des Darms dar. Interessanterweise führte die Inhibition von Asm und Ac in Mäusen weder zu einer unterschiedlichen Frequenz von Makrophagen, noch zur Veränderungen in der Phagozytose-Aktivität. Ebenfalls konnten keine Unterschiede in der Effektivität bei der Abtötung von phagozytierten Bakterien festgestellt werden.

Die vollständige Eliminierung der *C. rodentium* Infektion benötigt eine effiziente adaptive Immunantwort. Dabei spielen vor allem T_h1 und T_h17 Zellen in der Lamina Propria (LP) eine entscheidende Rolle. Interessanterweise, führte die Inhibition von Asm/Ac mittels Amitriptylin zu einer signifikant erhöhten Infiltration der LP mit T_h1 und T_h17 Zellen. Im Gegensatz dazu war die Frequenz an regulatorischen T-Zellen (T_{regs}) in diesen Tieren im Vergleich zu infizierten Wildtyp-Tieren reduziert. Dieses Ungleichgewicht zwischen Effektorzellen und T_{regs} während der *C. rodentium* Infektion bei Asm/Ac Inhibition ist vermutlich die Ursache für die unkontrollierte Darmpatholgie.

Zusammengefasst konnte erstmals eine protektive Funktion von Asm und Ac in der bakteriell-induzierten Kolitis gezeigt werden. Der maßgebliche Einfluss dieser Enzyme auf die erworbene Immunantwort ist essentiell für eine erfolgreiche Eliminierung von *C. rodentium*.

Introduction

3.1 Intestinal homeostasis

The human body is constantly exposed to the external environment and thus permanently in close contact with a vast number of microorganisms. Epithelial surfaces, such as the skin epithelium and intestinal epithelium, are adapted uniquely to prevent invasion of microorganisms [1]. By far the largest surface area can be found in the gastrointestinal tract, with an approximate surface area of 400 m^2 [2]. The intestine as a part of the gastrointestinal tract can be further divided into small and large intestine. Both, the small and large intestine, have the primary function of absorbing nutrients and water. The gastrointestinal tract is in close contact with a large number of commensal bacteria, which are tolerated by the gastrointestinal tract. These commensal bacteria are essential to keep up a symbiotic relationship, in which substantial metabolic, immunological and gut protective functions are supported in the healthy gut environment. However, pathogens preferentially invade the host through the gastrointestinal tract, thereby exposing the gastrointestinal tract not only to commensal bacteria but also to pathogens [3].

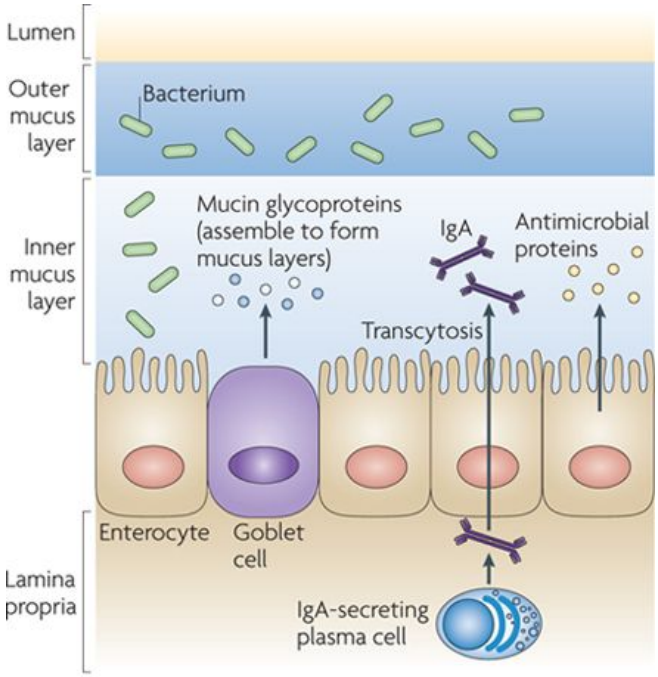

Figure 3.1: Overview of the outer mucus layer, the inner mucus layer and the epithelium.
The outer mucus layer, the inner mucus layer and the epithelium protect the lamina propria from invading bacteria. Bacteria can be commonly found in the outer mucus layer, whereas bacteria are absent in the inner mucus layer. The inner mucus layer is produced by the secretion of antimicrobial peptides by enterocytes, goblet cells, and Paneth cells, to further ensure the elimination of bacteria from the inner mucus layer. IgA is produced by plasma cells in the lamina propria and is transported via transcytoses across the epithelial cell layer. After secretion of IgA from the apical surface of epithelial cells, IgA limits the numbers of mucosa-associated bacteria and prevents bacterial penetration of host tissue (adapted from [4]).

The gastrointestinal system is adapted to these unique circumstances, by limiting direct bacterial contact to the epithelial cell surface, by rapid detection and killing of invading bacteria, and by minimizing the exposure of commensal bacteria to the immune system [4]. Histologically, the intestine is composed of three layers, the outer mucus layer, the inner mucus layer and the epithelium itself, protecting the central lamina propria from the exposure of bacteria (Figure 3.1) [5].

The outer mucus layer contains large numbers of bacteria, whereas bacteria are scarce in the inner mucus layer and epithelia [6]. The vast amount of approximately 10^{14} bacteria as well as the vast diversity of at least 1000 distinct bacteria species in the outer mucus aid in the degradation of dietary polysaccharides [7-9]. The mucus layer is produced by the secretion of a protective coat of mucus containing antimicrobial peptides by the epithelial cells, including enterocytes, goblet cells, and Paneth cells [10]. However, the outer and inner mucus layer can be distinguished in terms of their polymeric glycoproteins, as in the inner layer these glycoproteins are tightly stacked, whereas in the outer layer the structure is looser [11].The inner mucus layer is composed of defensins and serine leukocyte protease inhibitors, which restrict microbial translocation [12]. Furthermore, the non-inflammatory antibody immunoglobulin A (IgA) is released by IgA-secreting plasma cells in the lamina propria and transported via transcytosis to the inner mucus layer, where IgA also functions as an inflammation mediator [13].

As mentioned afore, the epithelial layer consists of enterocytes, goblet cells, and Paneth cells, which form a biochemical and physical layer to prevent bacteria from invading the lamina propria. The epithelial layer is constantly renewed by pluripotent intestinal epithelial cells that reside in the base of the intestinal crypts. New cells then migrate to the top of the crypt, where old cells are shed off and exposed into the lumen [14]. To form this epithelial barrier the adjacent epithelial cells are connected via junctional complexes, including tight junctions (TJ), adherens junctions (AJ), desmosomes (DE), and gap junctions (GJ) (Figure 3.2) [15]. Tight junctions, adherens junctions and desmosomes form the apical junctional complex (AJC). The main task of the AJC is to control epithelial cell-cell adherence and barrier function, but also to regulate the actin cytoskeleton, intracellular signalling pathways, and regulate transcription [16].

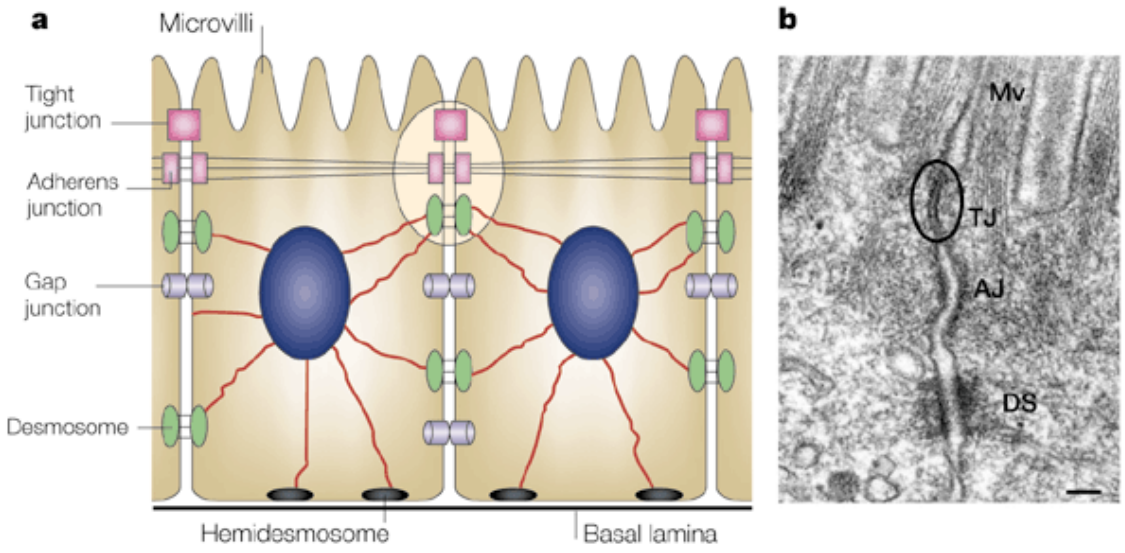

Figure 3.2: Overview of intestinal epithelial tight junctions.
(**A)** Drawing of the intestinal junctional complex connecting adjacent epithelial cells to form an epithelia layer. The permeability is mostly regulated via tight junctions (TJ), consisting of claudins and occludins and the anchor to the epithelial cells the zonula occludens 1-3 (ZO1-3), and adherens junction (AJ), such as E-cadherin. Desmosomes (DS), located underneath the apical junctional complex, are formed via the regulation of desmoglein, desmocolli, desmoplakin and keratin filaments. (**B**) A micrograph of two intestinal epithelial cells connected via junctional complexes. (adapted from [17])

Tight junctions are the limiting factor in the flux of nutrients and water from the lumen through the paracellular pathway into the lamina propria and typically are more permeable than the transcellular pathway [18]. The multi-protein complex of tight junctions is composed of transmembrane proteins, peripheral membrane proteins and regulatory molecules, such as kinases [19]. The most prominent transmembrane proteins in the intestinal epithelial are the 26 members of the claudin family, showing a diverse and heterologous expression pattern in terms of the different epithelial cells they are expressed in [20, 21]. Occludins are also critical to the establishment of tight junctions. However, their precise role remains unclear [22, 23]. Claudin and occludin are anchored through the peripheral membrane proteins zonula occludens 1-3 (ZO1-3) to the intestinal epithelial cell [24].

The adherens junctions consist of a large group of cell-cell adhesion proteins, namely cadherin proteins, such as the epithelial cadherin protein (E-cadherin or Cadherin-1). Absence of adherens junctions leads to loss of cell-cell contact, ineffective differentiation and apoptosis [25]. Desmosomes also connect adjacent epithelial cells, and are formed via the regulation of multiple protein subunits and the attachment to keratin filaments in the plasma membrane [26].

3.2 The intestinal Immune system

As previously discussed, the interface of the gastrointestinal tract harbours a large amount of resident microbiota, estimated to contain 10^{14} bacteria, in addition to viral and fungal species. Furthermore, despite being continuously exposed to dietary and other ingested foreign antigens, pathogens preferentially invade the host through the gastrointestinal tract. Because of the unique exposure to bacteria and pathogens the immune system in the gastrointestinal tract has established into a complex and highly specialized network of immune cells [3].

The vast network of non-lymphoid and secondary lymphoid tissue in the gastrointestinal tract comprises numerous populations of leukocytes. In more detail, these immune cells reside in the intestinal epithelium and lamina propria (LP), which is defined as the gut associated lymphoid tissue (GALT). The GALT also contains the secondary lymphoid structures, i.e. the mesenteric lymph nodes (mLNs) and the Peyers's Patches (PP) in the small intestine (SI) as well as the isolated lymphoid follicles and cryptopatches throughout the intestine [27].

In general, the immune response in the gut can be distinguished into the innate and adaptive immune system. The innate immune system is the first line of defence in removing infectious agents and acts to activate the adaptive immune response. Once pathogens invade the gastrointestinal tract, they can be recognized by the innate immune system via their pathogen-associated molecule patterns (PAMPs) by pathogen recognition receptors (PRRs), such as Toll-like receptors (TLRs) or the nucleotide-binding oligomerization domain- (NOD) like receptors (NLRs), thus inducing either phagocytosis or an antigen specific immune response of the adaptive immunity [28]. Mononuclear phagocytes (MPs) such as macrophages and dendritic cells (DCs) as well as natural killer cells and mast cells are part of the effector cells of the innate immune system. However, nonprofessional cells such as endothelial and epithelial cells and fibroblasts also contribute to innate immunity [28-30]. The adaptive immunity is responsible for controlling pathogenic infection and eliminating pathogens efficiently via T-lymphocytes or B-lymphocytes which infiltrate into the affected areas [31]. Both the innate and adaptive mucosal immune system are needed to maintain the delicate balance of protection against pathogens and tolerance to non-pathogens [27]. In the following sections, the innate and adaptive mucosal immune system is described in further detail, with a focus on the cell populations relevant for this work.

3.2.1 The innate mucosal immune system

The foremost goal of the innate mucosal immune system is to maintain homeostasis in the gastrointestinal tract. As such, the innate immune system tolerates harmless commensal bacteria or removes harmful pathogens, and activates the adaptive immune system as needed.

Mononuclear phagocytes (MPs), such as macrophages and DCs, fulfil this pivotal role of tolerating non-pathogenic but also effectively inducing antigen-nonspecific immune responses against pathogens. Macrophages are predominantly located near the epithelium throughout the entire gastrointestinal tract. In steady state, tissue resident macrophages have the ability to induce clearance of apoptotic or senescent cells [32]. Given the close contact of macrophages to the epithelial barrier, intestinal macrophages are part of the first line of defence in the intestinal structures, where they fulfil their role of protection against pathogens and foreign substances, tolerance to commensal bacteria and food antigens, and scavenging apoptotic and dead cells in the lamina propria. Hence, intestinal macrophages exhibit the ability of phagocytosis and bactericidal killing. However, compared to resident macrophages of other tissues, intestinal macrophages are highly restricted in their pro-inflammatory phenotype in order to maintain a low-level of inflammation in the intestinal structures [33].

Phenotypically, peripheral macrophages can be classified into the paradigm of classically activated macrophages (M1) and alternatively activated macrophages (M2). Peripheral M1 macrophages are polarized by LPS or the T_h1 cytokine IFNγ and express the major histocompatibility complex class II (MHCII), whereas M2 macrophages are polarized by T_h2 cytokine IL-4 and release high amounts of IL-10 [34]. Interestingly, intestinal macrophages display characteristics of both, an expression of high MHCII and TNFα typical of classically activated macrophages (M1) and secretion of IL-10 typical for the alternative activated macrophages (M2) [34-36]. Furthermore, intestinal macrophages express CX3CR1, CD64 and CD11b and moderate amounts of CD11c [35]. Intestinal macrophages also express a variety of pattern recognition receptors, such as TLRs 3-9. In addition to limiting the exposure of the immune system to gut bacteria, these recognition receptors also present another mechanism by which macrophages balance immune responses. Thus, TLRs recognize pathogen motifs including lipopolysaccharide (LPS) and lipoteichoic acid on the surface of gram-negative and gram-positive bacteria and bacteria flagellins [33].

The innate immune system activates the adaptive immune response, which is achieved with the help of DCs, provide the link between the innate and the adaptive immune systems including $CD4^+$ and $CD8^+$ T cells. DCs not only prime $CD4^+$ T cells to

differentiate into effector T cells, but also stimulate the expansion of T_{regs} [37, 38]. Although intestinal macrophages are not thought to initiate the differentiation of naïve T cells, the expression of MHCII leads to a secondary immune expansion of T_{regs} [39]. However, lamina propria macrophages were shown to supress the differentiation of T_h1 and IL-17-producing T helper cells (T_h17 cells), thereby counteracting the T_h17 differentiation promoted by lamina propria DCs [39]. Taken together, macrophages and DCs show a close functional interaction in activation of the adaptive immune system.

3.2.1.1 Phagocytosis and killing of macrophages

As afore mentioned, intestinal macrophages exhibit a distinct defence pattern compared to macrophages of other tissues. Intestinal macrophages are in constant contact with the vast number of bacteria in the intestine, and are needed to tolerate harmless bacteria [40]. The defence of intestinal macrophages begins with the rapid phagocytosis of harmful materials. Following phagocytosis, an immune response is induced. The cytokine release of macrophages, such as IL-6 and TNFα, induced by ligation of toll-like receptors (TLRs) or nucleotide-binding oligomerisation (NOD)-like receptors (NLRs) is altered in intestinal macrophages as they do not release increased amounts of IL-6 and TNFα [41, 42]. Nevertheless, intestinal macrophages do not completely lack an immune response against antigens, as they produce substantial amounts of IL-10 and low levels of TNFα [35].

The process of phagocytosis describes the complex uptake of large particles (>0.5 µm) into cells. Given a diverse range of particles to be phagocytosed, the internalization of particles can be triggered by a variety of receptors. However, all phagocytic processes show the same general procedure. First pathogens, foreign substances or apoptotic cells are recognized by a variety of receptors, e.g. Fc receptor, GTPases or scavenger receptors, such as SR-AI and SR-AII. This recognition leads to actin polymerization and remodelling at the site of ingestion and around the phagocytic cup. Finally, the particle is internalized and the process of degradation or killing in the phagosome is initiated by subsequent acidification of the phagosomes [43, 44].

In addition to phagocytosis, the killing of bacteria in phagosomes is complex and remains poorly elucidated. However, the respiratory burst of macrophages is understood to be involved in the killing of internalized bacteria [44]. Once bacteria are internalized into phagosomes and the pH of the phagosomes has been lowered, these phagosomes mature into phagolysosomes by vesicle-mediated delivery of antimicrobial effectors including proteases, antimicrobial peptides and lysozymes. The respiratory burst is then generated by the NADPH-dependent phagocytic oxidase, and inducible

nitric oxide synthase (iNOS) pathways. NADPH phagocyte oxidase generates superoxide (O_2^-), which modifies organic molecules and is known as reactive oxygen species (ROS). iNOS, which is mainly regulated at the transcriptional level, generates nitric oxide (NO) radicals, which are referred to as reactive nitrogen species (RNS) [45]. Both O_2^- as well as NO can result in the spontaneous formation of different products, e.g. nitrogen dioxide (NO_2), peroxynitrite ($ONOO^-$), hydrogen peroxide (H_2O_2) or dinitrogen trioxide (N_2O_3), with different reactivity, stability and biological activity. Furthermore, ROS and RNS can interact with different targets in a microbial cell, including thiols, metal centres, protein tyrosines, nucleotide bases and lipids. The different targeting strategies, accompanied through ROS and RNS show the complexity of these antimicrobial effectors in the degradation and killing of the phagocytosed bacteria in intestinal macrophages [44, 45]. In order to stimulate an antigen-specific immune response, peptide antigens from the phagosome are preserved for presentation, followed by loading and presenting these peptides via the major histocompatibility complex (MHC) class I or II to cells of the adaptive immune response [46].

3.2.2 The adaptive mucosal immune system

The adaptive mucosal immune system is heavily influenced by the presence or absence of the microbiota, as seen in in the absence of T cell subsets in germ-free mice [4]. The innate immune system is unable to initiate an antigen-specific immune response against invading pathogens. The adaptive immune system makes up for this, and achieves specific immune responses due to the constant somatic recombination of genes for antigen specific receptors. Additionally, the adaptive immune system effectively “remembers” previous infections of the host due to the immunological memory, and thus secondary infections are diminished as invading pathogens are eliminated more efficiently [47, 48].

Innate immune cells, like macrophages and DCs, present foreign or pathogenic antigens to the cells of the adaptive immune system, thereby activating the adaptive immune response [33]. Depending on the cytokine milieu and antigens presented by the innate immune system, either a protective, tolerogenic, or inflammatory immune response is initiated by the leukocytes in the intra- and sub-epithelial compartment of the intestinal structures [49]. Antigens presented by DCs and macrophages via MHCI or MHCII engage the T cell receptor (TCR) to prime naïve T cells into the final T cell subtype. In general, T cells are differentiated into two subsets, the $CD4^+$ T helper (T_h) cells and the $CD8^+$ cytotoxic T cells. Furthermore, $CD4^+$ T cells are divided into subsets

depending on their cytokine release and gene expression due to different roles in modulation of the immune response (see Figure 3.3).

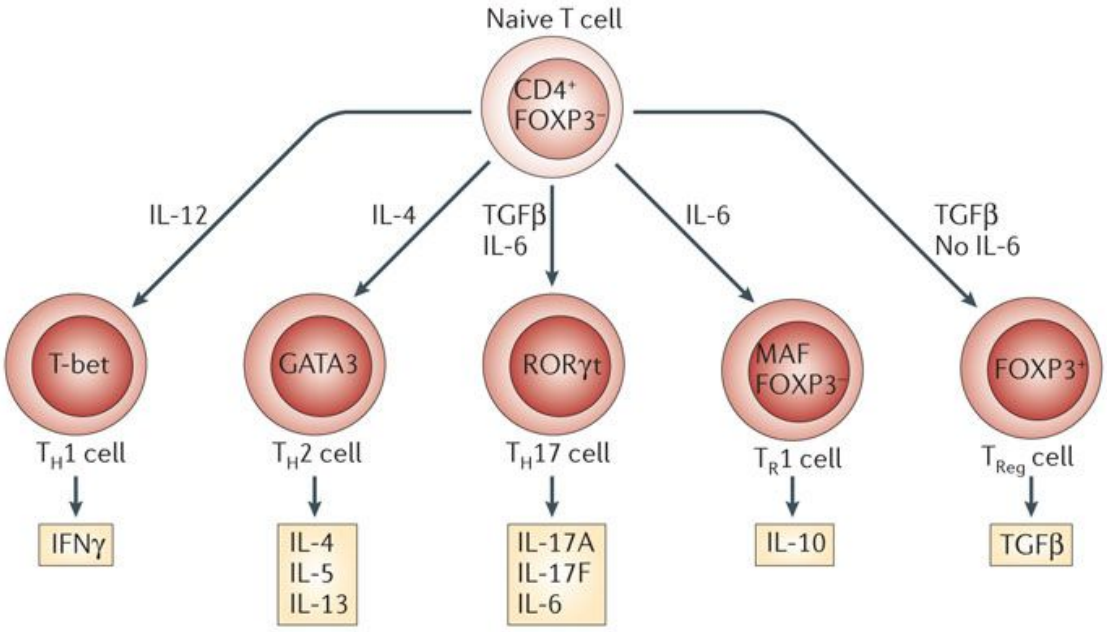

Figure 3.3: Overview of the gene expression and cytokine release of CD4⁺ T cells subsets.
The priming of the CD4⁺ T cell subsets depends on the cytokine milieu as well as on the expression of transcription factors. T_h1 cells are activated by the cytokine IL-12, express the transcription factor T-bet and release the cytokine IFNγ. T_h2 cells express the transcription factor GATA3, are activated by the cytokine IL-4 and produce the cytokines IL-4, IL-5 and IL-13. T_h17 cells release the cytokines IL-17A, IL-17F and IL-6, while they express the transcription factor RORγt and are activated by both, TGFβ and IL-6. The two subsets of regulatory T cells, T_R1 and T_{reg} cells are distinguished by the expression of FoxP3 (Forkhead-box 3). T_R1 cells are also activated by the cytokine IL-6, express MAF and produce IL-10. For T_{regs} TGFβ is needed for both activation and cytokine release (adapted from [4]).

In the gastrointestinal tract T_h1, T_h2 and T_h17 as well as their regulatory counterpart, the regulatory T cells (T_{regs}), are of particular interest [50]. Both T_h1 and T_h17 were shown to be pivotal in the gastrointestinal tract, as the cytokine milieu in the mucosa is primarily driven by IFNγ (T_h1 cytokine), IL-17A and IL-17F (T_h17 cytokines) (see Figure 3.3). The main task of T_h1 cells is to regulate local immune responses against invading pathogens [51]. T_h1 cells are the major source of IFNγ, which thereby activate macrophages. Macrophages themselves begin the cytokine release of IL-12, inducing a positive feedback on the activation of T_h1 cells (see Figure 3.3) [52]. T_h2 cells are known to enhance the clearance of parasites. Both parasites and T_h2 cells are abundant in the mucosa of healthy humans in developed countries [53]. The role of T_h17 cells is a point of debate, as cytokines released by T_h17 are known to have both pro-inflammatory and protective effects [54]. The cytokines IL-17A and IL-17F released by T_h17 cells contribute to neutrophil infiltration, where neutrophils can fulfil the pivotal role of defence against microbial exposure. However, IL-17 was also found to increase intestinal epithelial permeability [55]. T_{regs} fulfil the indispensable role of maintaining the

immune response of T_h1, T_h2 and T_h17 in the gastrointestinal tract. The main task of T_{regs} consist of keeping up self-tolerance against harmless pathogens, inhibition of autoimmune reaction and the reduction of tissue damage during infection [56].
Combining the diverse and counterbalancing roles of adaptive immune cells, the intestinal immune system is highly adapted to the unique environment of the gastrointestinal tract, which includes the presence of a large number of bacteria. The final result is a balanced and rather protective than pro-inflammatory immune response [57].

3.3 Inflammatory bowel disease

Inflammatory bowel diseases (IBD) are chronic relapsing inflammatory disorders affecting the gastrointestinal tract, characterised by the repeated cycles of relapse and remission [58]. Two major types contribute to IBD, namely Crohn's disease and ulcerative colitis. Although neither form of IBD is lethal, affected patients suffer a variety of symptoms including abdominal pain, fever, vomiting, diarrhoea, rectal bleeding, anaemia, and weight loss [59, 60]. Treatment focuses on symptom management through anti-inflammatory steroids and immunosuppressant to reduce inflammation, dietary changes, and in severe cases surgery [59]. The high prevalence (Europe: ulcerative colitis 505 and Crohn's disease 322 per 100,000 persons) and incidence (Europe: ulcerative colitis 24.3 and Crohn's disease 12.7 per 100,000 person/year) as well as the increased risk of ulcerative colitis patients to establish colorectal cancer brought IBD to the forefront of investigation [61, 62].
Although Crohn's disease and ulcerative colitis share similar clinical features, the two diseases can be distinguished with respect to disease localization, histopathology, and endoscopic features [59]. In Crohn's disease patients the entire gastrointestinal tract, from mouth to anus, can be affected with patchy discontinuous inflammation [63]. In terms of histopathology, Crohn's disease is accompanied by transmural inflammation of the entire bowel wall [64]. In contrast, patients suffering from ulcerative colitis show continuous inflammation in the colon, which is restricted to the mucosal layers [65].
The aetiology of IBD remains largely unknown, but genetics, environmental or microbial factors as well as the immune responses are known to play an important role in the establishment of IBD [66].

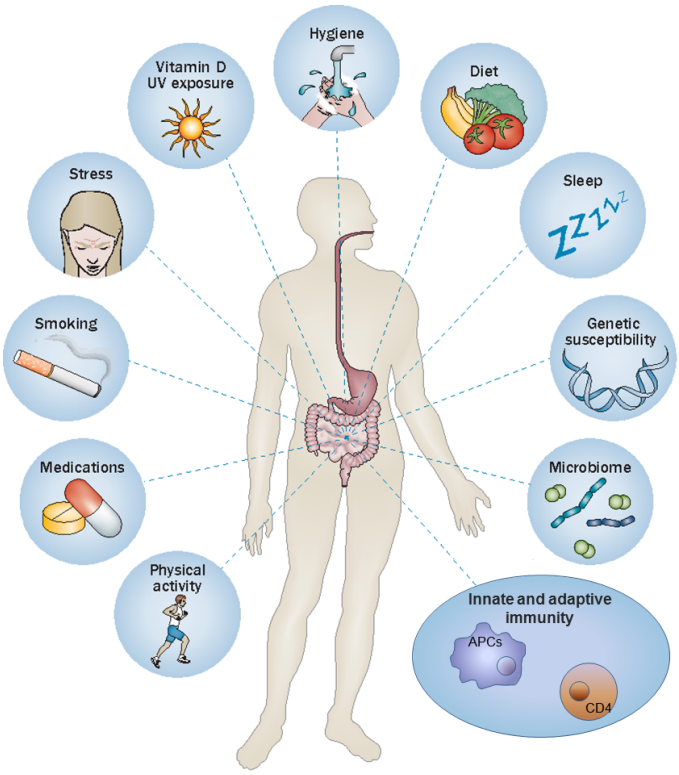

Figure 3.4: Overview of risk factors for the development of IBD.
Imbalance of environmental factors, e.g. physical activity, medications, smoking, stress, UV exposure, hygiene, diet and sleep as well as genetic risk factors and the microbiome, but also an dysfunctional immunity (e.g. antigen presenting cells (APCs) and $CD4^+$ T cells) contribute to the aetiology of inflammatory bowel disease (IBD) (adapted from [67]).

Potential environmental factors range from exposure to stressors in the early childhood to adulthood. Stressors can be as diverse as dietary fibre (particularly fruits and vegetables) [68], stress [69], medications (as NSAIDs) [70], impaired sleep [71] and smoking [72, 73] (see Figure 3.4).

Beyond the expanse of environmental factors, correlation between genetics and IBD also exists. Not only family history [74] but a total of 163 distinct risk loci, 30 % of which are shared in both ulcerative colitis and Crohn's disease, can contribute to the pathogenesis of IBD [75]. Interestingly, the risk genes and loci involved in IBD also contribute to several other pathways including microbial defence, integrity of the barrier function, innate immune regulation, adaptive immunity, reactive oxygen species (ROS) generation as well as autophagy [76].

The intestinal barrier function is a key factor in the development of intestinal inflammation [77]. Indeed, in IBD patients as well as in *in vitro* studies increased permeability correlates with the elevated expression of the tight junction protein claudin-2, allowing the migration of bacteria and macromolecules into the lamina propria [78].

As previously described, under homeostasis in the lamina propria both, innate and adaptive immune cells are present, providing a tolerogenic effect against the commensal microflora, albeit allowing protection from pathogens (see chapter 3.2.). IBD patients showed increased infiltration of leukocytes into the lamina propria, including neutrophils, macrophages, DCs, NK-cells as well as B and T cells [79]. However, $CD4^+$ effector T cells are known to play a particularly important role in the pathology of IBD [3, 80, 81]. Recently, the diverse role of T_h17 in IBD pathogenesis was described, as patients showed increased expression of T_h17-cytokines, such as IL-17A, IL-17F, IL-21, and IL-22 in colonic tissue [82]. Despite this description of a pro-inflammatory phenotype, the exact role of T_h17 cells in IBD continues to be under debate [83].

In terms of microbial defence, the altered interaction between host and pathogenic or commensal bacteria are also implicated in the development of IBD [84, 85]. In previous studies, this unique interaction could be shown in germ-free mice, which do not develop intestinal inflammation when compared to wildtype littermates [86-88]. Another study showed that antibiotic treatment reduced not only the concentration of bacteria present in the gut lumen but also successfully diminished inflammation in an experimental animal model [89]. Furthermore, the microbial composition was shown to be markedly altered in patients suffering from IBD [90]. Alterations of the microbial composition by antibiotic treatment ameliorate IBD [91]. By contrast, some bacteria, such as *Clostridium* spp., *Bifidobacterium* spp. and *Bacteroides fragilis*, were shown to be protective [92-94], while some groups speculate about the contribution to the pathogenesis of several enteropathogens, such as *Mycobacterium avium* subspecies *paratuberculosis*, *Yersinia* spp., *Listeria monocytogenes*, *Salmonella* spp., *Campylobacter concisus* [95, 96].

Collectively, IBD is a multifunctional disease of the gastrointestinal tract with many factors contributing to its aetiology. In order to provide appropriate treatment for patients and to understand the aetiology of IBD, it is critical to gain deeper insights by studying IBD.

3.4 Mouse models of inflammatory bowel disease

As stated afore, the aetiology of IBD remains unclear and thus makes it necessary to understand the mechanism, development, and procession of the disease to achieve successful treatment. To study this, numerous mouse models are used, in which either chemical, bacterial, genetic or adoptive cell transfer methods are used to induce IBD-like conditions in mice [97, 98]. Although none of these models are completely

effective in mimicking human IBD, each model targets different aims, making it possible to study the epithelial intestinal barrier (e.g. by DSS induced colitis, the Muc1$^{-/-}$and Muc2$^{-/-}$ mouse models and N-Cadherin DN tg), the innate immunity (e.g. TRUC), the excessive T effector cell immunity (e,g, Oxazolon, TCRα$^{-/-}$, TNBS and TNF$^{\Delta ARE}$), and regulatory immune response (e.g. CD45RB^{high} into SCID or RAG$^{-/-}$, Gai2$^{-/-}$, IL2$^{-/-}$ and IL10$^{-/-}$) with regards to Crohn's disease and ulcerative colitis (summarized in reference [98]). In this study, the bacterial induced colitis model of *Citrobacter rodentium* was used, to gain insights into host pathogen interactions in the gastrointestinal tract.

3.4.1 Bacterial induced colitis models

Beyond chemically- and genetically-induced colitis, two well established bacterial induced colitis models are used to study stable infection and colonisation of the gastrointestinal tract in mice, namely *Salmonella typhimurium* or *Citrobacter rodentium* (*C. rodentium*) [99]. Differences between the two models are the locally restricted infection with *C. rodentium* in the colon, compared to *Salmonella typhimurium*, which induces a strong systemic infection frequently resulting in sepsis. In addition, pre-treatment of mice with antibiotics (e.g. Streptomycin, Kanamycin) is needed to induce a stable *Salmonella typhimurium* infection, whereas one single infection with *C. rodentium* is sufficient to induce stable infection [100]. In this study, the *C. rodentium* induced colitis mouse model was used, as this robust model provides the opportunity to study the unique interaction of host and pathogen as well as inflammation and healing processes on the mucosal surface.

C. rodentium was first described in 1964 as a gram-negative, non-invasive mouse pathogen, belonging to the gut pathogen family of *Escherichia* (*E.*) *coli* [101]. Genetically, *C. rodentium* shares 67 % homology to the family member's enteropathogenic *E.coli* (EPEC) and enterohemorrhagic *E. coli* (EHEC) [102]. The well-studied ability of *C. rodentium* to regulate epithelial barrier integrity, mucosal healing, inflammation, and composition of commensal microbiota, makes *C. rodentium* a robust model to study human intestinal disorders including inflammatory bowel disease, dysbiosis, and tumorigenesis [103-105]. Infection of mice through the faecal-oral route induces an acute intestinal inflammation with the hallmark of transmissible murine crypt hyperplasia (TMCH) [106]. *C. rodentium* first colonizes the lymph node structure in the caecum before passing straight to the gastrointestinal tract, in which the pathogen uses attaching and effacing (A/E) lesions to colonize the gastrointestinal structures [107]. Attaching und effacing lesions lead to the attachment of the pathogen to the epithelia of the host, followed by the reorganisation of the actin cytoskeleton of the host cell (the

effacing) resulting in actin pedestal formation through which the *C. rodentium* then colonizes intestinal epithelial cells [108].

Once the bacteria have successfully invaded the colon, *C. rodentium* massively proliferates and colonizes the colon. During this acute phase of colonization, *C. rodentium* leads to minor body weight loss due to diarrhoea. Infection of mice with *C. rodentium* can range from self-limiting inflammation of the colon to fatal infection, depending on the genetic disposition of mice [109]. Bacteria can be first detected 1-3 days post infection in the colon, with the maximum amount reached around 7-10 days post infection [99, 107]. *C. rodentium* concentrations then reach 1-3 % of the total intestine microbiota with 10^9 colony forming units (CFU) per gram tissue in the colon [107]. Besides the characteristic crypt hyperplasia (TMCH), a decrease in goblet cells (goblet cell depletion) and increased cell infiltration into the caecum and colon can be detected [110]. Infection severity can also be detected macroscopically by measuring the colon weight and length, as crypt lengthening and thickening of the mucosa also initiates the shortening of the colon. Within 5 days post infection increased colon weight to length ratios can be measured with the maximum being reached two weeks post infection. Within three to four weeks mice are able to clear the bacteria [111]. Once infection is cleared, the colon weight to length ratio declines to normal levels and the mice become resistant to a second infection [112].

Various factors including the composition of the intestinal microbiota, the colonization capacity of *C. rodentium* in the mouse large intestine, and the intestinal mucosal immune response to infection can contribute to resistance to *C. rodentium* colonization [104]. For example, alterations of the intestinal microbiota composition, like antibiotic treatment, increase the susceptibility of mice to *C. rodentium* infection [113].

Once *C. rodentium* successfully attached to the epithelial cells, it is recognized by the myeloid differentiation primary-response protein 88 (MYD88) Toll-like receptor (TLR2 and TLR4) complex [114], which subsequently leads to the activation of transcription factors such as NFκB. NFκB then regulates the release of cytokines and chemokines, such as IL-6, IFNγ, and TNFα which eventually leads to the recruitment of macrophages and neutrophils [115]. In MYD88-deficient mice, infection with *C. rodentium* leads to a lethal infection, associated with overwhelming bacterial burden [114]. In TLR2-deficient mice accelerated mortality is also observed, accompanied with rapid weight loss and severe colonic pathology [116]. Infection of TLR4-deficient mice however, leads to a delayed spread of bacteria. The duration of infection was not affected; indicating that TLR4-mediated responses are not host-protective [117]. Infection of mice with *C. rodentium* also initiates a defect in the intestinal permeability, which thereby induces translocation of the bacteria into the lamina propria. In the

lamina propria *C. rodentium* is recognized by the innate immune system, which goes on to activates the adaptive immune response [118].

Both, the innate and adaptive immune systems are critical for the control of *C. rodentium* infection, and thus the complex interplay between innate and adaptive immunity has been studied extensively over the last decades in this model [119]. Activated macrophages and neutrophils begin to release cytokines to attract adaptive immune cells to induce resistance to *C. rodentium* [120]. As shown in a variety of studies, the adaptive immune response is indispensable, in particular B cells and T_h1- and T_h17-polarized $CD4^+$ T cells as well as IL-22 producing type 3 innate lymphoid cells (ILC3) are critical for containing and eradicating the infection [112, 119, 121, 122]. Increased cytokine release, such as IFNγ, TNFα and IL-12, revealed a predominantly T_h1 immune response, supported by the increased susceptibility of mice lacking either IFNγ or IL-12 [123]. T_h17 cells are known to be essential for the clearance of *C. rodentium*, as they attract innate cells, including macrophages and neutrophils to the site of infection by the production of pro-inflammatory cytokines, such as IL-17A and IL-22. Deficiency of IL-6, the recruiting cytokine of T_h17 cells, leads to failed eradiation of *C. rodentium* infection [121, 124, 125]. Additional to T_h17 cells, the new subset of IL-17 producing innate lymphoid cells (ILC3) were also shown to be implicated in the immune response against *C. rodentium* infection [126].

Collectively, *C. rodentium* is an appropriate murine model to study not only host-pathogen interaction but also inflammation, healing processes on the mucosal surface, and regulation mechanisms of the commensal microbiota.

3.5 Acid sphingomyelinase (ASM) and acid ceramidase (AC)

In 1972, Singer and Nicolson first described the nature of biological membranes with the “fluid mosaic model” postulating a coincidental organization of lipids and free moving proteins within the membrane [127]. 25 years later, this “fluid mosaic model“ has been replaced by the liquid-ordered model, wherein lipids interact with each other due to their hydrophilic and hydrophobic properties, leading to formation of small, structured lipid domains termed “lipid rafts” [128, 129].

Three main classes of lipids are found in the biological membrane, namely glycolipids, sterols, and of particular interest in this study sphingolipids (Figure 3.5) [130].

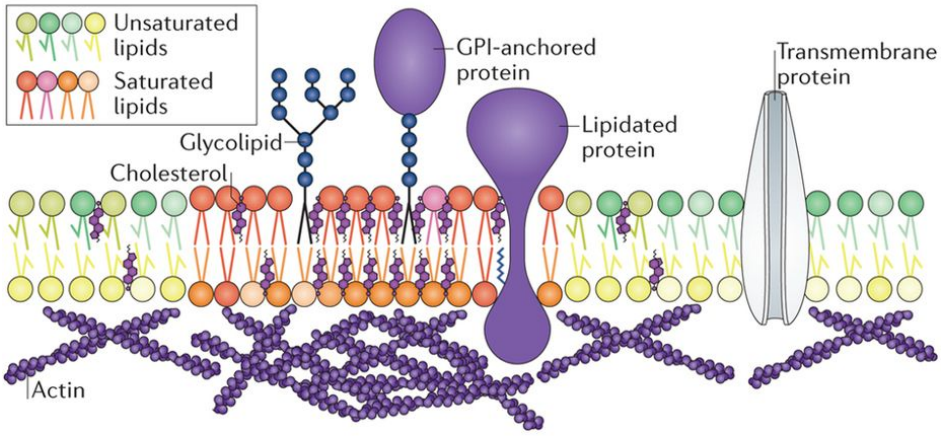

Figure 3.5: Overview of biological membrane and lipid raft domains.
The biological membrane composes of asymmetrical distributed unsaturated and saturated lipids in the inner and outer leaflets of the membrane. However, lipid rafts domains are enriched in saturated phospholipids, sphingolipids, glycolipids, cholesterol, lapidated proteins and glycosylphosphatidylinsitol (GPI)-anchored proteins, leading to increased lipid packing and order, as well as decreased fluidity. The membrane components are further maintained and remodelled by the cortical actin (adapted from [131]).

Sphingolipids contain one of five sphingoid bases as a backbone, in which the amino group of the sphingosine backbone is linked to a fatty acid via an amide bond. Due to their chemical structure, sphingolipids are amphipathic molecules possessing both hydrophobic and hydrophilic properties [132]. Variability in sphingolipids is achieved either by different chain length and saturation status in the hydrophobic tail, or by addition of hydroxyl-groups, phosphates and/or sugars to the hydrophilic head [132, 133]. Sphingomyelin is the most prevalent cellular sphingolipid, which is synthesised on the luminal side of the Golgi apparatus [134]. Due to its amphipathic properties, sphingomyelin forms very small, tightly packed sphingomyelin- and cholesterol-enriched membrane rafts [135]. Following stress stimuli, further transformation of these sphingomyelin-cholesterol rafts into ceramide-enriched domains is induced. To achieve this transformation the acid sphingomyelinase (ASM) is required to hydrolyse sphingomyelin into ceramide [136]. The pivotal role of ASM in this process can be demonstrated by the lysosomal storage disorder Niemann Pick disease type A and B, in which lack of ASM leads to the accumulation of sphingomyelin in the lysosomes [137].

3.5.1 Ceramide synthesis and metabolism

The synthesis of ceramide can occur via several distinct biochemical pathways including the sphingomyelin hydrolysis pathway, the *de novo* pathway, or the salvage pathway [138].

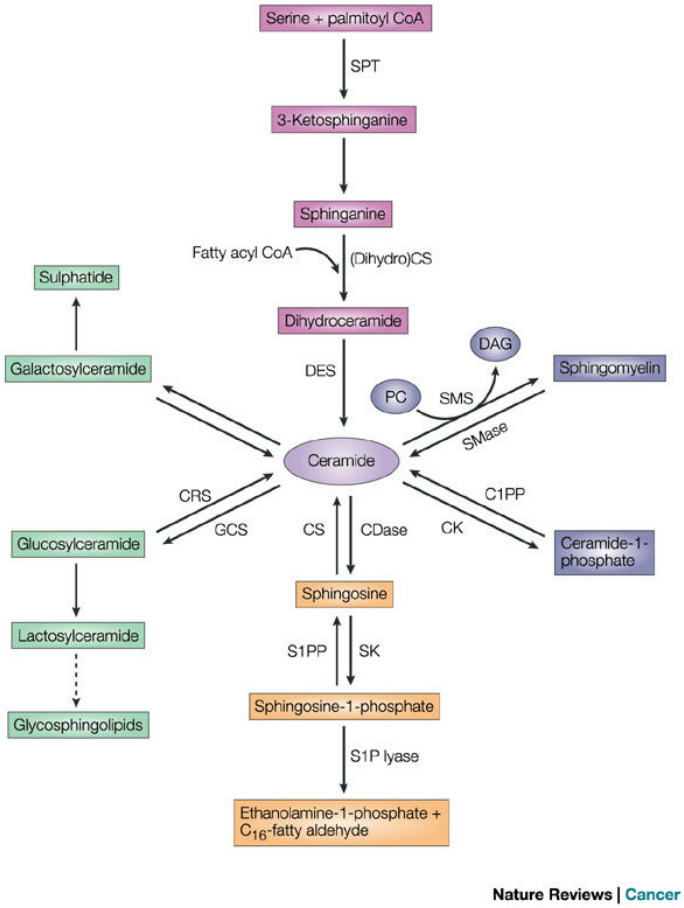

Figure 3.6: Schematic overview of the generation and degradation of ceramide.
Ceramide can be generated by distinct pathways, either by hydrolysation through cerebroside (green) or sphingomyelinase (blue), the *de novo* pathway (pink) or the salvage pathway (orange). Ceramide can be hydrolysed from glucosylceramide by cerebrosidase (CRS) or degrade back into glucosylceramide by glucosylceramide synthase (GCS) (green). Further, ceramide is generated by the condensation of serine and palmitoyl CoA by the consecutive action of transferase (SPT: serine palmitoyl transferase), synthases (CS: ceramide synthases) and desaturases (DES: dihydroceramide desaturase) within the *de novo* pathway (pink). In the salvage pathway (orange), ceramide is formed via sphingosine and sphingosine-1-phosphate and the S1P phosphatase (S1PP) and ceramide synthases (CS). The other way around ceramide can be metabolized by ceramidases (CDases) to yield sphingosine. Sphingosine is then further phosphorylated by sphingosine kinases (SKs) to generate sphingosine-1-phosphate (S1P), which in turn can be cleaved by the S1P lyase into ethanolamine-1 phosphate and a C_{16}-fatty-aldehyde. Also ceramide can be hydrolyzed either from sphingomyelin and ceramide-1-phosphatase with sphingomyelinases (SMase) or ceramide-1-phosphate phosphatase (C1PP) (blue). In return, ceramide is degraded to yield sphingomyelin or ceramide-1-phosphate by the sphingomyelin synthase (SMS) or the ceramide kinase (CK) [139].

In the sphingomyelinase pathway (Figure 3.6), sphingomyelin can be hydrolysed by acid, neutral, or alkaline sphingomyelinases (ASM, NSM and Alk-SM) into ceramide [140]. The ability of ASM in regulating the concentration of the bioactive sphingolipid ceramide and the resulting reorganization of the plasma membranes is what makes ASM of particular scientific interest [141, 142]. ASM can be activated by a wide range of stress stimuli [138] (see Table 3.1), which then results in the translocation of ASM by the secretory lysosome to the cell membrane, where the lysosome and the cell membrane subsequently fuse. This fusion exposes ASM to the outer leaflet of the cell

membrane and induces a reorganization of the plasma membrane (chapter 3.5.4) by hydrolysing sphingomyelin into ceramide [141, 142]. As indicated, ASM preferentially hydrolyses sphingomyelin to ceramide at an optimum acidic pH (~ 4.5-5.0) [136, 143]. However, other lipids in the membrane crucially influence the Michaelis-Menten constant (Km) of the enzyme, permitting ASM activity at a higher pH [144, 145].

Table 3.1: ASM-activating stimuli.
Overview of several stimuli inducing ASM and/or ceramide-enriched platform formation (Adapted from [146]).

Stimuli	
Autoimmunity	*Listeria monocytogenes*
	Measles virus
	Mycobacterium avium
	Neisseria gonorrhoea
	Pseudomonas aeruginosa
	Rhinoviruses
	Salmonella typhimurium
	Sindbis virus
	Staphylococcus aureus
Clustering of differentiation molecules	CD5
	CD14
	CD20
	CD28
	CD32 (FCγR Ⅱ)
	CD38
	CD40
	CD95
	CD95-DISC
	CD253 (TRAIL)
	IL-1 receptor
Drugs	Cisplatin
	Cu^{2+}-treatment
	Doxorubicin
	Heat damage
	Ischemia-reperfusion injury
	Oxidative stress
	Oxygen radicals
	UV-light
	γ-irradiation
	Steatohepatitis
Soluble molecules	Platelet Activating Factor
	Tumor necrosis factor
	Visfatin

Ceramide can not only be generated by hydrolysing sphingomyelin, but also by three other pathways. One major mode is the hydrolysis of glucosylceramide by cerebrosides into ceramide (see Figure 3.6, green pathway) [139]. However, ceramide can also be formed by the *de novo* pathway, in which serine and palmitoyl CoA are condensed by the serine palmitoyl transferase. After 3-ketosphinganine is condensed, ceramide is formed by the consecutive action of 3-ketodihydrosphingosine reductase, dihydroceramide synthases, and dihydroceramide desaturase. This process can be induced by the metabolic loading with either serine or palmitate (see Figure 3.6, pink pathway) [147], chemotherapeutic agents [148], heat stress [149, 150], oxidized LDL [150] as well as cannabinoids [151]. Synthesis of ceramide can also occur via the salvage pathway from sphingosine-1-phosphate and sphingosine catalysed by the S1P phosphatase and the ceramide synthases (see Figure 3.6, orange pathway).
This process is reversible, as ceramide serves as a substrate to yield ceramide-1-phosphate, sphingomyelin or glycolipids [152]. In another pathway, ceramide can also be metabolized by ceramidases to yield sphingosine. Currently, five known ceramidases have been identified which are, distinguished by their different pH optimal activity, analogous to the distinction between sphingomyelinases. The five ceramidases, acid ceramidase (AC), neutral ceramidase (NC), alkaline ceramidase 1 (ACER1), alkaline ceramidase 2 (ACER2), and alkaline ceramidase 3 (ACER3), have been shown to be involved in distinct diseases and/or possess distinct properties [153]. Deficiency of acid ceramidase leads to the lipid storage disorder Faber's disease, characterized by the massive accumulation of ceramide in lysosomes [154]. The neutral ceramidase has shown protective capacity against inflammatory cytokines, [155] and the alkaline ceramidases seem to play a critical role in mediating cell differentiation by controlling the generation of SPH and S1P as well as in cell proliferation and survival [156, 157]. Sphingosine can then be further phosphorylated by sphingosine kinase 1 and 2 into sphingosine-1-phosphate (S1P), which is known to be a critical regulator of many physiological and pathophysiological processes [reviewed in 158, 159]. All in all, sphingolipids and the variable process around synthesizing and metabolizing ceramide play an important role in homeostasis but also in the establishment and progression of a number of different diseases.

3.5.2 Structure, maturation and activation of acid sphingomyelinase

Acid sphingomyelinase is encoded by the 5-6 kb *SMPD1* gene (sphingomyelin (SM) phosphodiesterase 1; OMIM: 607608; human *SMPD1*, murine *Smpd1*) located at chromosome 11 p15.1-p15.4 and consisting of six exons and five introns. In total

SMPD1 yields 7 isoforms, of which only the type 1 transcript gives rise to a functional enzyme (human ASM, murine Asm; Enzyme Commission Classification number 3.1.4.12) [160-162]. The *SMPD1* transcript is then translated into the immature precursor protein ASM (pre-pro ASM). ASM is targeted to the endoplasmic reticulum via its NH_2-terminal endoplasmic reticulum signalling sequence, where it is further cleaved into pro-ASM [161, 163]. The pro-ASM then gives rise to two distinct forms of ASM depending on their cellular trafficking and subsequently cellular activity: a high-mannose-type oligosaccharide lysosomal ASM (L-ASM) and a complex-type *N*-linked oligosaccharide secretory ASM (S-ASM) [146, 164]. Either form of Asm, once activated, hydrolyses sphingomyelin into ceramide. Deficiency of acid sphingomyelinase leads to accumulation of sphingomyelin and the lysosomal storage disorder Niemann-Pick disease [165-167].

3.5.3 Structure, maturation and activation of acid ceramidase

Acid ceramidase ((AC) N-acylsphingosine amidohydrolase, EC 3.5.1.23) is encoded by the 30 kb *ASAH1* gene (OMIM 613468) located on chromosome 8p21.3-p22 and is comprised of 14 exons and 13 introns [168]. The *ASAH1* transcript is translated into the nascent AC polypeptide, followed by several modification and maturation steps between the endoplasmic reticulum to the Golgi, resulting in the 55 kDa inactive precursor polypeptide [169]. The inactive precursor is further glycosylated and transported via the mannose-6-phosphate receptor pathway to the endosomal/lysosomal compartments [169]. By autocleavage of the internal bond at the Cys-143 residue, the inactive proenzyme is activated, resulting in the α subunit (14kDa) and β subunit (40kDa) [154]. Only the precursor form and the β subunit are essential for full enzymatic activity as both possess the critical 5 putative N-linked glycosylation sites required for proper proteolytic processing of the protein [169, 170]. In addition, saposin D, a sphingomyelinase activator, is also required for optimal protein activity of the acid ceramidase [171]. Once activated, ceramidase metabolizes ceramide into sphingosine, and plays an integral role in cellular physiology. Deficiency of acid ceramidase leads to accumulation of ceramide and the lipid storage disorder Faber's disease [154].

3.5.4 Signalling through ceramide-enriched platforms

As previously discussed, there are three main classes of lipids found in biological membranes, of which sphingolipids are of particular scientific interest [130]. The unique chemical structure of sphingolipids makes sphingolipids amphipathic molecules as they possess both hydrophobic and hydrophilic properties. Membrane-domains can then emerge, as both parts of sphingolipids interact with each other and with cholesterol in the membrane either by van-der-Waals forces, by hydrophobic interaction between the tails, or by hydrophilic interaction of the polar head group (Figure 3.7) [172].
Cholesterol fulfils the pivotal role of filling in the spaces between the glycosphingolipids, thereby stabilizing lipid rafts, as extraction of cholesterol from rafts destroy them [173].
The amphipathic properties of sphingomyelin lead to the formation of very small, tightly packed sphingomyelin- and cholesterol-enriched membrane rafts [135]. Upon stress stimuli (see Table 3.1) these rafts are further transformed into ceramide-enriched domains, once ceramide is hydrolysed by ASM from sphingomyelin [174, 175].

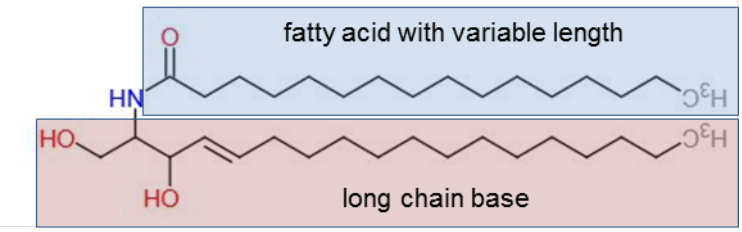

Figure 3.7: Chemical structure of ceramide.
As an example for sphingolipids the chemical structure of ceramide with its fatty acid (blue box) and long chain base (pink box). Variability is achieved by different chain length and saturation of status in the hydrophobic tail. (adapted [134]).

These ceramide-enriched microdomains then spontaneously fuse to larger membrane domains, referred to as ceramide-enriched platforms (see Figure 3.8, A), thereby clustering proteins on the cell surface as well as providing a mechanism for reorganizing receptors and signalling molecules in the cell membrane [176]. Structural differences in proteins can thereby lead to recruitment to or exclusion from platforms. Not only the protein's transmembrane structure but also the receptor-ligand interaction can result in protein reorganization, as platforms may stabilize the receptor-ligand interaction by increasing receptor affinity to the ligand [177]. The reorganization of receptors and signalling molecules in ceramide-enriched platforms enhances clustering of receptors within the small area of ceramide-enriched platforms leading to a high density of receptors [178, 179]. In addition to the clustering effects, the reorganization of receptors also results in the spatial association of activated receptors with intracellular molecules, exclusion of inhibitory molecules and/or the transactivation of

other enzymes leading to strong, local signalling [177, 180]. Taken together, the unique and complex interaction of ceramide and its substrates support the pivotal role of ceramide as a signalling molecule in the regulation of several cellular processes in the context of many diseases and conditions spanning from internal medicine, to psychiatry as well as oncology [181-185].

3.5.5 Functional inhibitors of ASM

Other than the various physiological ASM-inhibitory mechanisms, such as by splice variants of ASM [186], inhibition of the ASM-mediated signalling by inositol-phosphates [187] and by inhibiting the translocation of lysosomal (L-) ASM by nitric oxide [188], ASM translocation can also be further inhibited by a number of functional inhibitors of ASM (FIASMAs).

Since the early 1970s it has been known that ASM can also be chemically inhibited by a number of weak bases which induce the detachment of ASM from inner lysosomal membranes, and subsequently lead to the inactivation of ASM. Collectively, the weak basicity and high lipophilicity yielded by the structure of the functional inhibitors of ASM, are the key characteristics required for effective ASM inhibition [189, 190].

Weak bases are able to passively diffuse across membranes in their neutral state (see Figure 3.8, B). However, once they enter the acid compartment of the lysosomes they become protonated, thereby losing their ability to traverse the membrane and become trapped within the lysosomes [191, 192]. The high lipophilicity is also integral to ASM inhibition. The lipophilicity of effective ASM inhibitors initiates the binding to the inner membrane of the lysosomes, which competes with the binding of electrostatically bound L-ASM to the membrane. L-ASM then loses contact to its membrane-bound substrate sphingomyelin, and thus becomes a target for lysosomal proteases. Therefore, effective functional inhibitors of ASM lead to the abrogation of ASM activity, followed by the proteolytic degradation of the enzyme [193]. Recently, the identified structure of ASM gave rise to another possible mechanism, wherein inhibitory drugs may also bind to the hydrophobic surface of the saposin domain in ASM, thereby inhibiting the saposine-substrate interaction [194].

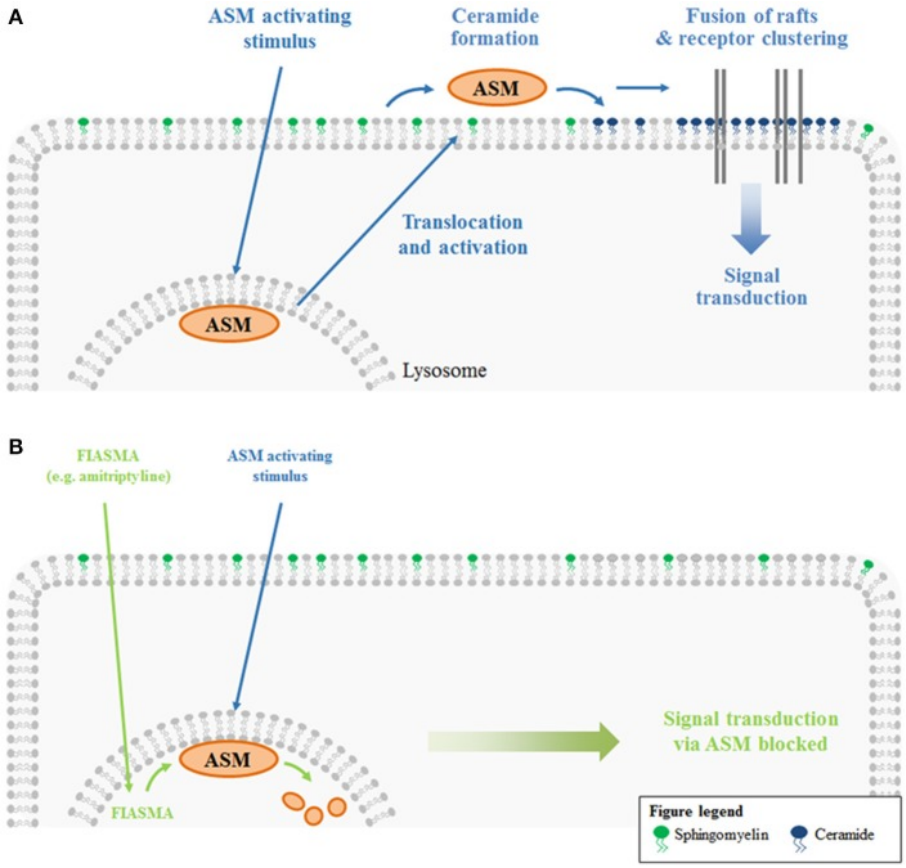

Figure 3.8: Schematic overview of ASM-mediated platform formation and functional inhibition of ASM by FIASMAs.
(**A**) Under steady-state ASM is bound via electrostatic forces to the inner lysosomal membrane. Once ASM translocation is induced by several activating stimuli, ASM is translocated to the outer leaflet of the plasma membrane. In contact with its substrate, ASM hydrolyses sphingomyelin into ceramide, which forms ceramide–enriched microdomains. Subsequently, these microdomains fuse to large, ceramide-enriched platforms. Due to lipid-protein interactions, platform formation also results in lateral sorting of proteins, where clustering but also exclusion of specific receptors serves to facilitate and/or amplify signalling processes. (**B**) Functional inhibitors of acid sphingomyelinase (FIASMAs) interfere with the binding of ASM to the lysosomal membrane, thereby permitting the lysosomal degradation of ASM. Consequently, ASM activating stimuli are not able to induce a translocation of ASM to the plasma membrane and the entire signalling cascade downstream of ASM is lost [146].

Numerous functional inhibitors have been identified, of which most are already in clinical use including the tricyclic antidepressants amitriptyline, desipramine and imipramine [190, 195]. Collectively, these tricyclic antidepressants showed favourable properties, good absorption (all are orally active), effective distribution (extensive tissue binding, most can also cross the blood-brain barrier), metabolism and excretion, no habituation, activity across different cell types, reversible inhibition, and no rebound effects [196]. Regarding specificity, the inhibitory effect of functional inhibitors for ASM is limited to the acid compartment of the lysosomes due to FIASMAs structures. Thus, neutral and alkaline sphingomyelinase are not affected by the treatment with FIASMAs. Furthermore, no general inhibitory effect on other lysosomal hydrolases could be

detected. However, acid ceramidase, lysosomal acid lipase, and phospholipase A and C have been reported to be co-inhibited by cationic amphiphilic drugs [196, 197].

The tricyclic antidepressant used in this study was amitriptyline, which was introduced by Merck in 1961 in order to treat major depressive disorders [198]. To this day, treatment of depression is the only FDA (Food and Drug Administration)-approved indication, although the use of amitriptyline has expanded to numerous types of pain and other symptoms, such as fibromyalgia [199], migraine prophylaxis [200], neuropathic pain orders [201], nocturnal enuresis [202] and irritable bowel syndrome [203]. Beyond the treatment of the symptoms, anti-inflammatory and anti-microbial properties of the drug have been reported as well [204, 205].

Following oral administration, amitriptyline is metabolized mainly by cytochrome P450 (CYP450) into its secondary amine Nortriptyline [206]. Before the secretion into the urine, further metabolism takes place resulting in the inactivation of amitriptyline [207].

Initially, the effect of amitriptyline as an antidepressant was reported to be due to its activity as a serotonin-norepinephrine re-uptake inhibitor, which has a strong effect on serotonin transporters [208]. Owens *et al.* also reported amitriptyline to be a receptor-antagonist for a number of histamine and muscarinic acetylcholine receptors, giving amitriptyline also antihistaminic and anticholinergic properties [209].

Of particular interest is the functional inhibition of acid sphingomyelinase of antidepressant drugs like amitriptyline, so called FIASMAs. Due to their structure FIASMAs are trapped in the acid compartment of the lysosomes and bind to the membrane. However, the attachment of FIASMAs interfere with the attachment of ASM to the membrane. Thereby, FIASMAs display and inactivate ASM (see chapter 3.5.5 for details) [197, 210-213].

The importance of amitriptyline can also be shown in the phase II clinical trial study in cystic fibrosis (CF) patients, in which ceramide accumulation is targeted with the treatment of amitriptyline [214], as ceramide showed to mediate inflammation, cell death and infectious susceptibility in CF [215]. Currently, amitriptyline is under investigation in a phase III clinical trial with CF-patients.

3.5.6 ASM in disease

Originally, ASM was identified as the main source for the lysosomal storage disorder Niemann-Pick disease, in which the loss of activity of ASM leads to a drastic accumulation of sphingomyelin in liver, spleen, lymph nodes, adrenal cortex, lung airways, and bone marrow [216, 217]. Beyond its role in Niemann-Pick disease, the ASM/ceramide system has been shown to play a role in a number of various diseases, including cardiovascular-, metabolic-, hepatic-, inflammatory- and infectious disease. ASM also seems to play a central role in cancer and tumour metastases (more details Table 3.2).

Table 3.2: Acid sphingomyelinase/ceramide-system-related disease.
Overview of diseases, which were shown to be affected by the ASM/ceramide signalling system (Adapted from [218]).

Autoimmunity	Kawasaki disease
	Multiple sclerosis
	Systemic sclerosis
Cancer	Chemotherapeutics
	Irradiation and radiotherapy
	Metastasis
Cardiovascular diseases	Atherosclerosis
	Cardiomyocyte apoptosis (cardioplegia/reperfusion)
	Thrombus formation
Genetic disorders	Cystic fibrosis
	Niemann-Pick disease type A and B
	Sickle-cell disease
	Wilson disease/liver cirrhosis
Infectious Diseases	Bacterial infections
	L. monocytogenes
	M. avium
	N. gonorrhoeae
	P. aeruginosa
	S. typhimurium
	S. aureus
	Endotoxic shock syndrome
	Malaria/plasmodia
	Virus infections
	Measles virus
	Rhinovirus
	Sindbis virus
	Graft-versus-host-disease

Inflammatory disease	Hemophagocytic lymphohistiocytosis Hepatic fibrosis Inflammatory bowel disease Mast cell function/allergies
Metabolic Disease	Diabetes Diabetic retinopathy Obesity-induced kidney damage Steatohepatitis
Neurological disorders	Alzheimer disease Major depression Parkinson's disease
Skin conditions	Atopic dermatitis

More recently, ASM is brought to the centre of interest in depression, as a number of long-standing antidepressant drugs were shown to be actually ASM inhibitors (see chapter 3.5.5). These tricyclic antidepressants do not, as first thought, inhibit the monoamine uptake, but instead inhibit ASM activity [219], thereby reducing hippocampal ceramide concentrations in addition to increasing neuronal proliferation, maturation, and survival [220-222].

The importance of ASM and sphingolipids in diseases can be further illustrated by the use of sphingolipid inhibitors in clinical trials, for various diseases including targeting cystic fibrosis (see chapter 3.5.5).

3.5.6.1 Inflammatory bowel disease

As previously discussed, inflammatory bowel disease is a multifactorial disease, which affects the gastrointestinal tract. Recently, the sphingolipid metabolism was attributed to play a role in colitis. Interestingly, several groups found a pivotal function of the sphingomyelin-ceramide-sphingosine axis (for details see Figure 3.6) within intestinal inflammation using a chemical induced colitis model (dextran sodium sulphate, DSS). DSS is a chemical colitogen which is administered via drinking water and the pathology induced by DSS treatment strongly resembles human ulcerative colitis [223]. In general, DSS destroys the intestinal epithelial monolayer, thereby exposing the underlying tissue to the pro-inflammatory content of the lumen [224].

Interestingly, the role of sphingolipids is discussed controversially. On the one hand, it was shown that the accumulation of sphingomyelin by oral administration of sphingomyelin initiated cathepsin-D induced apoptosis via ceramide accumulation in intestinal epithelial cells. This increased apoptosis of intestinal epithelial cells then enhanced inflammation in the chemical induced colitis model using DSS [225].

On the other hand, some stated a beneficial role of ceramide. The results found by Ohnishi *et al.* showed that accumulation of ceramide via inhibition of sphingomyelin synthase 2 ameliorates DSS induced colitis. In this study the deficiency of sphingomyelin synthase 2 enhanced the ceramide levels during the DSS treatment, while decreased sphingomyelin levels were detected. This shift in the sphingomyelin and ceramide ratio was accompanied by a decrease in cell proliferation, reduced inflammatory cytokines and chemokines and lower infiltration of immune cells in the colon [226]. Furthermore, alteration of the ceramidase synthase 2 was shown to aggravate DSS induced colitis. Deficiency of ceramidase synthase 2 decreased the very long chain ceramide levels. Alongside the loss of the very long chain ceramide, increased colon pathology, disruption of the epithelial barrier integrity and a dysregulation of immune cell infiltration into colonic tissue were detected in ceramide synthase 2 deficient mice [227]. The importance of the sphingolipid metabolism was further displayed by the use of a S1P agonist in clinical studies to ameliorate remission of ulcerative colitis patients [228]. However, the effect of sphingolipids on the development of IBD is incomplete understood and needs to be further elucidated.

3.6 Aim of this study

IBD are chronic relapsing inflammatory disorders affecting the gastrointestinal tract. Although a high prevalence of the disease, the aetiology of IBD is still incompletely understood. Genetic, environmental and microbial factors as well as a dysregulated immune response are known to contribute to the establishment of IBD. However, a deeper understanding of the pathogenesis of IBD is essential to establish specific therapeutic strategies for the treatment of IBD. Sphingolipids are important components of all cell membranes, and are certainly also known to have a fundamental role in numerous diseases, such as inflammatory bowel disease. Recent studies demonstrated a protective as well as a harmful function of sphingomyelin and ceramide in autoimmune mediated intestinal inflammation. However, the impact of the sphingolipid pathways is not analysed in the context of a pathogen driven intestinal inflammation. Therefore, the aim of the present study was to analyse the influence of the Asm and Ac metabolism in the context of bacterial induced colitis using the *C. rodentium* infection mouse model.

Asm KO and Ac cKO mice were infected with *C. rodentium* and the course of infection was carefully analysed regarding the intestinal barrier and the innate and adaptive immunity. In addition, the use of a pharmacological inhibitor of Asm and Ac was included into the experiments to allow the time point specific modulation of the Asm and Ac activity. The results obtained in the present study will provide information about the relevance of the sphingolipid pathway for the control of pathogen driven intestinal inflammation.

Materials and Methods

4.1 Materials

4.1.1 Consumables

Table 4.1: Consumables

Consumables	Manufacturer
Ceramic sphere ¼"	MP Biomedicine, Illkirch, France
Culture plates (6-, 12-, 24-, 48- and 96-well)	Greiner BioOne, Frickenhausen, Germany
Disposable syringe (2 ml, 10 ml)	BD Biosciences, Heidelberg, Germany
MacConkey selection plates	Oxoid, Wesel, Germany
Micro tubes (0.6 ml)	Biozyme Scientific GmbH, Oldendorf, Germany
Micro tubes (1.5 and 2 ml)	Sarstedt, Nümbrecht, Germany
Micro tubes (2 ml)	Sarstedt, Nümbrecht, Germany
Micro tubes (2 ml) with ceramic beads	MP Biomedicals, California, USA
Petri dish, 92 x 16 mm, w/o carms	Sarstedt, Nümbrecht, Germany
Pipettes tips	Thermo Scientific, Sarstedt, Biozyme
Thin layer chromatography (TLC)	Merck KGaA, Darmstadt, Germany
Tubes (15 and 50 ml)	Greiner BioOne, Frickenhausen, Germany
Round bottom plates (96-well)	Greiner BioOne, Frickenhausen, Germany
Cell strainer (40, 50, 70 and 100 µm)	Falcon, Durham, USA

4.1.2 Chemicals

Table 4.2: Chemicals

Chemicals	Manufacturer
LE Agarose	Biozyme Scientific GmbH, Oldendorf, Germany
Amitriptyline hydrochloride	Sigma-Aldrich, St. Louis, USA
AutoMACS Pro Washing Solution	Miltenyi Biotec, Bergisch Gladbach, Germany
AutoMACS Running Buffer	Miltenyi Biotec, Bergisch Gladbach, Germany
BODIPY-sphingomyelin	Thermo Fisher Scientific, Waltham, USA
Boric acid	Carl Roth GmbH & Co. KG, Karlsruhe, Germany
Bradford Protein assay	Biorad Laboratories GmbH, München, Germany
Brefeldin A (BFA)	Sigma-Aldrich, St. Louis, USA
Chloroform	AppliChem GmbH, Darmstadt, Germany
Collagenase Type IV	Sigma-Aldrich, St. Louis, USA
Corn oil	Sigma-Aldrich, St. Louis, USA

Desoxynukleosid Triphosphate	Invitrogen, Karlsruhe, Germany
Deoxyribonuclease I (DNase)-Type II	Sigma-Aldrich, St. Louis, USA
Ethidium bromide 1 %	Carl Roth GmbH & Co. KG, Karlsruhe, Germany
Ethylenediaminetetraacetic acid (EDTA)	Carl Roth GmbH & Co. KG, Karlsruhe, Germany
Ethylene glycol tetraacetic acid (EGTA)	Carl Roth GmbH & Co. KG, Karlsruhe, Germany
Ethanol, absolute and denatured	Carl Roth GmbH & Co. KG, Karlsruhe, Germany
Fetal calf serum (FCS)	Biochrom GmbH, Berlin, Germany
FACS Flow Sheath Fluid	BD Biosciences, Heidelberg, Germany
FACS Clean Solution	BD Biosciences, Heidelberg, Germany
FACS Rinse Solution	BD Biosciences, Heidelberg, Germany
Fluorescein isothiocyanate (FITC)-dextran	Sigma-Aldrich, St. Louis, USA
Glycerin	Carl Roth GmbH & Co. KG, Karlsruhe, Germany
IGEPAL® CA-630 (NP-40)	Sigma-Aldrich, St. Louis, USA
Ionomycin Calcium Salt	Sigma-Aldrich, St. Louis, USA
Ki-67 (clone SP6)	Thermo Fisher Scientific, Waltham, USA
Lipopolysaccharide (LPS)	InvivoGen, San Diego, USA
Magnesium chloride [$MgCl_2$]	Carl Roth GmbH & Co. KG, Karlsruhe, Germany
Methanol (≥ 99 % p.a.)	Diagonal GmbH & Co. KG, Münster, Germany
Monensin (1000x)	eBioscience, San Diego, USA
NBD-ceramide	Thermo Fisher Scientific, Waltham, USA
Paraformaldehyde (PFA)	Carl Roth GmbH & Co. KG, Karlsruhe, Germany
Phorbol 12-myristate 13-acetate (PMA)	Sigma-Aldrich, St. Louis, USA
Penicillin	Sigma-Aldrich, St. Louis, USA
Streptomycin	Sigma-Aldrich, St. Louis, USA
StremPro® Accutase®	Life Technologies, Grand Island, USA
Tissue-Tek® C.C.T. ™ Compound	Sakura Finetek, Alphen aan den Rijn, Netherlands
Trypan blue	Sigma-Aldrich, St. Louis, USA
Tamoxifen	Sigma-Aldrich, St. Louis, USA

4.1.3 Kits, panels and enzymes

Table 4.3: Kits, panels and enzymes

Kits	Manufacturer
$CD4^+$ T cell Isolation Kit	Miltenyi Biotec, Bergisch Gladbach, Germany
FoxP3 staining Kit	eBioscience, San Diego, USA
Gene ruler 100bp ladder Plus	Thermo Fisher Scientific, St. Leon-Tor, Germany
Go Taq Hot Start Polymerase	Promega, Mannheim, Germany
M-MLV Reverse Transcriptase	Promega, Mannheim, Germany
NucleoSpin® RNA XS	Macherey-Nagel, Düren, Germany
pHrodo™ Green *E.* coli BioParticles® Conjugates	Thermo Fisher Scientific, Braunschweig, Germany
RNase Tissue Mini Kit	Qiagen, Hilden, Germany
SYBR Green	Thermo Fisher Scientific, St. Leon-Tor, Germany

4.1.4 Media and buffer

Table 4.4: Media and buffer

Media and Buffer	Concentration	
Ac/Asm assay buffer	250 mM	Sodium acetate
	0.1 %	NP-40
		pH = 4.5 (Ac) or pH = 5.0 (Asm)
Ac lysis buffer	250 mM	Sodium acetate
	1 %	NP-40
		pH = 4.5
Asm assay buffer	250 mM	Sodium acetate
	0.1 %	NP-40
		pH = 4.5 (Ac) or pH = 5.0 (Asm)
Asm substrate solution	0.5 µl	BIODIPY-sphingomyelin
	1 ml	Asm assay buffer

Erythrocyte-Lysis Buffer	8.29 g/l	Ammonium chloride
(ACK-Buffer, pH 7.2-7.4)	1 g/l	Monopotassium phosphate
	0.1 mM	EDTA
		In demineralized water
FACS-Buffer		PBS-Buffer
	2 %	FCS
	2 mM	EDTA
IMDM complete medium		IMDM with GlutaMax™ I and 25 mM HEPES
	10 %	FCS
	100 µg/ml	Streptomycin
	100 U/ml	Penicillin
	25 µM	ß-Mercaptoethanol
LB-Medium	20 g/l	LB-Broth-Base
	4.5 g/l	NaCl
		pH = 7.5
		In demineralized water
LB-Agar		LB-Medium mixed with
	15 g/l	Agar
Macrophages medium		DMEM
	15 %	L-929 supernatant (mouse fibroblast cell line producing macrophage colony stimulating-factor (MCSF))
	10 %	FCS
	1 %	Penicillin/Streptomycin
	50 mM	ß-Mercapthoethanol
PBS-Buffer	8 g/l	Sodium chloride
	2 g/l	Potassium chloride
	1.44 g/l	Disodium phosphate
	0.2 g/l	Potassium phosphate
		In demineralized water

PBS/EDTA		PBS-Buffer
	3 mM	EDTA
RPMI 1640 complete		RPMI with GlutaMax™ I and 25 mM HEPES
medium	10 %	FCS
	100 µg/ml	Streptomycin
	100 U/ml	Penicillin
	2 mM	L-Glutamine
RPMI/FCS		RPMI with GlutaMax™ I and 25 mM HEPES
	20 %	FCS
RPMI/FCS/EGTA/$MgCl_2$		RPMI with GlutaMax™ I and 25 mM HEPES
	1 %	FCS
	1 mM	EGTA
	1.5 mM	$MgCl_2$
TBE-Buffer	89 mM	Tris
	89 mM	Boric acid
	2 mM	EDTA
		In demineralized water
TE-Buffer	10 mM	Tris/HCL (pH 8.0)
	1 mM	EDTA
		In demineralized water

4.1.5 Equipment

Table 4.5: Equipment

Equipment	Manufacturer
7500 Fast Real-Time PCR System	Thermo Scientific, Darmstadt, Germany
autoMACS® Pro Separator	Miltenyi Biotec, Bergisch Gladbach, Germany
Binokular Axiovert Z1	Carl Zeiss Microscopy GmbH, Jena, Germany
Centrifuge MULTIFUGE 3SR+	Thermo Fisher Scientific, Waltham, USA
Centrifuge 5417R	Eppendorf AG, Hamburg, Germany
Flow cytometer BD LSRII	BD Biosciences, Heidelberg, Germany
Fas Prep®-24	MP Biomedicals, California, USA
GelDoc station	INTAS®, Göttingen, Germany
Electrophoresis Apparatus Horizon 11.14	Analytik Jena, Jena, Germany
Heracell 150i CO_2-Incubator	Thermo Scientific, Darmstadt, Germany
Heraeus Multifuge 3SR+	Thermo Scientific, Darmstadt, Germany
Luminex Technology AtheNA Multy-Lyte	Progen, Heidelberg, Germany
Magnetic stirrer Variomag	Thermo Scientific, Darmstadt, Germany
Nanodrop Photometer	peqLab, Erlangen, Germany
Neubauer counting chamber (0.0025 mm^2)	Superior, Marienfeld, Germany
SpeedVac	Thermo Fisher Scientific, Waltham, USA
TriStar2 Microplate reader	Berthold Technologies GmbH & Co. KG, Bad Wildbad, Germany
Typhoon FLA 9500	GE healthcare Europe GmbH, Freiburg, Germany
Work Bench Msc Advantage	Thermo Scientific, Darmstadt, Germany
Vortexer D-6013	Neo Lab, Heidelberg, Germany
Water bath	GFL, Burgwedel, Germany

4.1.6 Software

Table 4.6: Software

Software	Manufacturer
BD FACSDIVA™ Software	BD Biosciences, Heidelberg, Germany
Graph Pad Prism 7.03	GraphPad Software, La Jolla, USA
ImageQuant	GE Healthcare Europe GmbH, Freiburg, Germany
MikroWin, Version 5.18	Mikrotek, Laborsystem GmbH, Overath, Germany

4.2 Methods

4.2.1 Experimental animals and husbandry

In this project different mouse strains were used to analyse the effect of acid sphingomyelinase and acid ceramidase during bacterial induced colitis. An overview of the mouse strains used in this study is given below. C57BL/6 mice were purchased from ENVIGO, Netherlands. Acid sphingomyelinase-deficient (*Smpd1*) mice as well as acid ceramidase-deficient (*Asah1*) mice were bred at the laboratory animal facility of the University Hospital Essen. The animals used in this study were 8 to 12 weeks old male or female mice kept in the animal experimental unit of the University Hospital Essen in individually ventilated cages and pathogen free conditions. Animals were housed under a 12:12-hour light:dark cycle and were provided food and water *ad libitum*. Experiments were performed in accordance with federal and state guidelines (AZ84-02.04.2014.A124 and AZ84-02.04.2017.A366).

4.2.1.1 Acid sphingomyelinase-deficient mice

Asm-deficient (*Smpd1*$^{-/-}$) mice [229] do not express the sphingomyelin phosphodiesterase 1, which encodes a lysosomal acid sphingomyelinase that hydrolyses sphingomyelin to ceramide (see chapter 3.5.1). Heterozygous mice were mated to generate wildtype (WT), heterozygous (HET) and homozygous knockout (KO) animals. In this study both, male and female, Asm WT and Asm KO mice were used up to a maximum of 10-12 weeks to avoid accumulation of sphingomyelin, as this accumulation leads to the lysosomal storage disorder Niemann-Pick disease type A and B [216].

4.2.1.2 Acid ceramidase-deficient mice

Acid ceramidase 1 (*Asah1*$^{fl/fl}$, kindly provided by Prof. Dr. Karl Lang) mice express the N-acylsphingosine amidohydrolase flanked by two loxP sites. N-acylsphingosine amidohydrolase encodes for the acid ceramidase. In order to generate the depletion of acid ceramidase under the control of Tamoxifen in all organs, Asah$^{fl/fl}$ mice were crossed to CreER mice [230]. Breeding generated *Asah1*$^{fl/fl}$ x CreER$^{+/+}$ as wild type (Ac WT), and *Asah1*$^{fl/fl}$ x CreER$^{ki/ki}$ as acid ceramidase conditional knockout mice (Ac cKO), when Tamoxifen is injected intraperitoneal on day 8, 6 and 4 before

infection. Acid ceramidase activity deletion can exceeds 30 %, for example seen in the ovaries [231].

4.2.1.3 Genotyping of transgenic mice

The genotyping of transgenic mice was done by polymerase chain reaction (PCR), applying the following protocols. Primers were ordered from MWG-Biotech (Ebersberg, Germany).

Table 4.7: Primers for genotyping.

transgene	sequence (forward, reverse)	annealing temperature (T^a)
Smpd1$^{-/-}$	5'- GGC TAC CCG TGA TAT TGC TG -3' 5'- AGC CGT GTC CTC TTC CTT AC -3'	58°C
Asah1$^{fl/fl}$	5'- ACAACTGTGTAGGATTCACGCATTCTCC -3' 5'- TCGATCTATGAAATGTCGCTGTCGG -3'	58°C
CreEr$^{+/-}$	5'- TCCAATTTACTGACCGTACACCAA -3' 5'- CCTGATCCTGGCAATTTCGGCTA -3'	62°C

Table 4.8: Mastermix for genotyping

1x	Reaction buffer
1.5 mM	$MgCL_2$
1 mM	dNTPs
5µM	Forward primer
5µM	Backward primer
0.5 U	GoTaq Hot Start polymerase
ad 20 µl	MilliQ H_2O

Table 4.9: PCR program for genotyping.

		10 cycles			27 cycles		
Temperature	95°C	95°C	T_a	72°C	95°C	T_a	72°C
Time (mm:ss)	10:00	00:30	1:30	1:30	00:15	00:45	00:45

Following PCR, the amplification products were analysed by electrophoresis on 1 % agarose gel stained with ethidium bromide in TBE buffer.

4.2.2 Animal procedures

4.2.2.1 Amitriptyline treatment of C57BL/6 mice for Asm inhibition

To inhibit the translocation of acid sphingomyelinase amitriptyline (chapter 3.5.5) was administered to C57BL/6 mice at 180 mg/l via drinking water for 14 days prior to bacterial challenge [232]. The amitriptyline containing water was changed every third day and replaced by freshly diluted amitriptyline.

4.2.2.2 C. rodentium infection

The *C. rodentium* used in this study was the ICC169 strain, obtained from PD. Dr. Christian Riedel (University Ulm) [106]. The ICC169 strain is a derivate of the ICC168 strain, which possesses spontaneous Naladixin resistance (unpublished data).
Female C57BL/6 mice, female and male Asm KO and Asm WT or Ac WT and AC cKO littermates were orally infected with 2-5 x 10^9 colony forming units (CFU) of *C. rodentium*. Prior to infection the *C. rodentium* bacteria were cultured in 200 ml LB medium overnight at 38°C constantly shaking at 180 rpm. After approximately 12-16 hours, the optical density (OD) was determined at a wavelength of 600 nm. Bacterial suspensions of an OD between 0.67-0.74 were used for the oral infection of mice. For each mouse 3ml of the bacterial suspension was centrifuged at 4000 rpm for 10 minutes and resuspended in 100 µl sterile PBS. The suspension was then gavaged to mice, without anaesthesia. CFU of the gavage suspension was determined as described in chapter 4.2.2.3.
Following infection, bodyweight and CFU in faeces were assessed 3, 5 and 7 days post infection. Colony forming units in faeces were determined as described in chapter 4.2.2.3. Mice were sacrificed by CO_2 asphyxiation 5 or 10 days post infection. Serum samples were obtained by puncturing the heart with a 10 ml syringe and centrifuging the whole blood at 10000 g for 15 minutes. Subsequently, serum was analysed for cytokine levels via Luminex (chapter 4.2.3.3). The liver, spleen, mesenteric lymph nodes (mLNs) and colon were excised and processed as described in the following sections.

4.2.2.3 Determination of CFU

In order to determine both the severity and extent of systemic infection, colony forming units (CFU) of *C. rodentium* in the gavage suspension, faeces, spleen and liver were determined. In order to determine the CFU of the *C. rodentium* gavage suspension, the gavage suspension was first diluted 1:10, then in a serial dilution series up to 1 x 10^{-11}. Dilutions from 1 x 10^{-6} up to 1 x 10^{-11} were then plated on the gram-negative selective and differential culture medium MacConkey. Colonies were allowed to grow overnight at 38°C, 5 % CO_2 before counting CFU. The CFU of *C. rodentium* administered per mouse was calculated as a mean of the CFU per 100 µl. CFU in faeces were assessed by first determining the weight of the faeces pellet. Subsequently, the pellet was soaked in sterile PBS to allow for improved homogenisation. With a 200 µl tip the faeces pellet was mechanically homogenized, and further resuspended by vortexing for 5 seconds. As before, faeces samples were diluted 1:10 in a dilution series from 1 x 10^{-2} up to 1 x 10^{-6} and plated on MacConkey plates over night at 38°C, 5 % CO_2. Again, CFU were counted and CFU/g faeces were calculated as the mean of the dilutions depending on the dry faeces weight. Similar to faeces, first the weight of liver and spleen were determined, followed by homogenization of samples in 500 µl sterile PBS with the help of ceramic beads using the FastPrep®-24 at 4 M/s for 25 seconds. Liver and spleen suspensions were then diluted 1:10. The undiluted and the 1 x 10^{-1} diluted sample were then allowed to grow on MacConkey plates overnight (38°C, 5 % CO_2) and the CFU/g liver or spleen was calculated as described before.

4.2.2.4 Colonic biopsies

To begin, colon length and the colon weight were determined. Approximately 20 mg rectal biopsies of the colon were taken before processing with the remainder of the colon for further analysis. Colon biopsies were used for several analyses, to investigate cytokine release by cultivating colon biopsies in 300 µl IMDM complete medium for 6 hours, determining the cytokine release in the supernatant via Luminex following collection, and separation of the colon tissue from the supernatant (14000 g for 10 minutes). Colon biopsies were also analysed for RNA expression of tight junction proteins, inflammatory cytokines, and inflammatory cells (chapter 4.2.5.3). In order to assess the sphingolipid profile and the Asm/Ac activity, approximately 20 mg of the rectal section of the colon were excised, weighed and immediately shock frozen in liquid nitrogen and stored until further analyses (chapter 4.2.4.1).

4.2.2.5 Histology

To determine the inflammation of colonic tissue during the time course of *C. rodentium,* histopathologic analyses were performed. Colons were excised and faeces were flushed out with ice-cold PBS. The colon was placed in tissue cassettes as swiss role and fixed with 4 % buffered formalin. Colon tissues were embedded in paraffin and trimmed to 4 µm sections with a microtome. These tissue sections were then stained with hematoxylin and eosin (H&E) and Ki-67 and analysed at a magnification of 40. The pathology was scored according to the following scale from 0 to 3, with 0 = no pathology and 3 = severe pathology. Furthermore, the colon was divided into an oral, central, and rectal section (sectioning, staining, and scoring of pathology were performed by Robert Klopfleisch, Freie Universität Berlin, Germany).

Table 4.10: Histopathologic parameters of inflammation for the colonic tissue.

scoring	Colonic tissue
0-3	Infiltration of inflammatory cells in the lamina propria and tela submucosa
0-3	Mucous defective
0-3	Neutrophil infiltration
0-3	Hyperplasia
0-3	Crypt abscess

4.2.2.6 Generation of BMDMs

In order to obtain bone marrow derived macrophages (BMDMs), mice were sacrificed, followed by peeling off the skin from the top of each leg down over the foot. The leg was cut off at the hip joint, leaving the femur intact. Muscles were removed from the bone with a wipe. Bones were then washed in 70 % ethanol, followed by washing the bone in PBS. Leg bones were carefully opened proximal to each joint and the bone marrow was flushed from the cavity with a 26G needle containing FACS solution. The bone marrow was resuspended and the resulting cell suspension was washed with FACS buffer. Following further centrifugation, erythrocytes were lysed with 2 ml ACK buffer. After further washing, the cells were resuspended in 10 ml of macrophage complete medium in each petri dish (92 x 16 mm) and incubated at 37°C, 5 % CO_2 for 6 to 7 days. On day 3, 5 ml of fresh macrophage complete medium was added to the cells [233].

4.2.3 Cell biology methods

4.2.3.1 Preparation of single cell suspension

To analyse lymphocyte cells from the relevant organs different protocols were applied. Spleens were homogenised and filtered through a 70 µm nylon cell strainer containing 10 ml erythrocyte lysis buffer, centrifuged at 300 g for 10 minutes, and finally resuspended in IMDM complete medium.
Mesenteric lymph nodes were passed through a 70 µm cell strainer in FACS buffer, centrifuged at 300 g for 10 minutes, and resuspended in IMDM complete medium.
Lymphocytes from the lamina propria of the colon were isolated as previously described [234]. Colons were flushed with ice-cold PBS and cut into small pieces. By washing the colon pieces twice for 10 minutes in 40 ml PBS supplemented with EDTA at 37°C under constant stirring, the epithelium was effectively removed. Subsequently, samples were incubated twice for 15 minutes with 20 ml RPMI media supplemented with FCS, EGTA and $MgCl_2$ at 37°C under constant stirring. Tissues were then subject to digestion in media containing collagenase IV (100 U/ml) of *Clostridium histolyticum* and 20 % FCS for 60 minutes at 37°C. By passing the suspension through a 70 µm cell strainer a single-cell suspension was obtained. Finally, cells were washed with FACS, centrifuged at 300 g for 10 minutes, filtered again through a 30µm filter and resuspended in IMDM complete medium.

4.2.3.2 Flow cytometric analysis

Antibodies for staining are listed in Table 4.11. The antibodies were titrated to determine the optimal concentration of use. Flow cytometric analysis was performed on a LSRII using FACS DIVA software (Version 8.0.1).

Table 4.11: Antibodies used for flow cytometric analysis.

Epitope	Fluorophore	Clone	Manufacturer
CD4	APC Pacific Blue	RM4-5	BD Biosciences
CD11b	APC	M1/70	eBioscience
CD25	PE	PC61	BD Biosciences
F4/80	PE	BM8	eBioscience
FoxP3	FITC	FJK-16s	eBioscience
IFNγ	FITC	XMG1.2	BD Biosciences

IL-17	PE	TC11-18H10.1	BD Biosciences
MHCII	BV510	M5/114.15.2	BioLegend
TLR4	PE-Cy7	SA 15-21	BioLegend

Staining of surface proteins

To analyse the expression of surface proteins, fluorochrome-conjugated antibodies were used. Cells were transferred into a 96-well round bottom plate and centrifuged for 5 minutes at 300 g. Subsequently, surface proteins were stained with antibodies at optimal concentrations in FACS buffer for 10 minutes at 4°C in the dark. Alongside staining of the surface proteins, cells were also dyed with the fixable viability dye eFlour780 to separate living and dead cells. Afterwards, cells were washed with FACS buffer and resuspended in 150 µl FACS buffer for subsequent analysis by flow cytometery.

Intracellular staining of IL-17, IFNγ, or Foxp3

IL-17 and IFNγ levels were analysed by incubating cells in the presence of 1 µg/ml ionomycin, 10 ng/ml phorbol 12-myristate 13 acetate (PMA), 1 µg/ml monensin and 5 µg/ml brefeldin A for 4 hours at 37°C. After washing the cells with FACS buffer surface proteins were stained. This was followed by fixation of the surface proteins on the cells with 2 % buffered formalin for 15 minutes at 4°C. The cells were then washed with PBS and the membrane was permeabilised with 0.1 % NP-40 for 4 minutes in the dark at room temperature. After another washing with FACS buffer, cells were stained with fluorochrome-conjugated antibodies against IL-17 or IFNγ for 30 minutes at 4°C in the dark. For staining of Foxp3 first surface staining was performed as previously described, followed by a washing step with PBS. Subsequently, cells were fixed for 60 minutes at room temperature in the dark using the Invitrogen fixation and permeabilization kit. Cells were washed with 1x permeabilization buffer and stained for Foxp3 in 1x permeabilization buffer for 60 minutes at room temperature in the dark. After the intracellular staining, cells were washed with FACS buffer and resuspended in 150 µl FACS followed by analysing the cells by flow cytometry.

4.2.3.3 Detection of cytokines by Luminex

Cytokines of serum samples or supernatants of colonic biopsies were quantified using a Procarta Cytokine assay kit (Kit Cataloge number: 7-Plex: LXSAMS-07, 9-Plex: LXSAMS-9) according to the manufacturer's guidelines. The assay was run and quantified with a Luminex 200 system using Luminex IS software.

4.2.3.4 Phagocytosis assay of BMDMs

To determine the phagocytic capacity of BMDMs, pHrodo™ green *E.coli* BioParticles®-Conjugates were used according to manufacturer's guidelines. Short BMDMs were isolated and cultured as previously described (chapter 4.2.2.6). 1 x 10^5 BMDMs cells were plated on a dark 96-well plate and allowed to settle and adhere for at least 1 hour at 37°C, 5 % CO_2. Old IMDM complete medium containing non-adherent cells was removed and replaced by IMDM complete medium containing 10 µg pHrodo beads for 15, 30, 45, 60 and 90 minutes (in triplicates). After indicated time points IMDM complete medium containing pHrodo beads was removed and replaced with fresh medium. Subsequently, phagocytosis of the BMDMs was analysed with a fluorescence reader at Excitation wavelength of 485 nm and Emission wavelength of 535 nm.

4.2.3.5 Killing assay of BMDMs

As described earlier, BMDMs were isolated and cultured for 5-7days. Approximately 1 x 10^5 BMDMs were plated in a 96-well plate. To allow BMDMs to adhere, cells were incubated for 1 hour at 37°C, 5 % CO_2 in RPMI antibiotic-free medium. Approximately 1 x 10^6 living *C. rodentium* bacteria were added to the BMDMs and incubated for the indicated time points (15, 30, 45, 60 and 90 minutes). Subsequently, BMDMs were washed, and incubated with RPMI containing antibiotics for another hour at 37°C, 5 % CO_2. The BMDMs were then washed three times with PBS, followed by permeabilization with 1 % Triton X for 5 minutes at room temperature. As described earlier, the supernatant, containing the BMDMs content, were then plated in different dilutions on MacConkey plates. Killing was then calculated by counting CFU the following day after incubation at 37°C, 5 % CO_2.

4.2.3.6 Differentiation of T_h1 and T_h17 cells in vitro

In order to address the differentiation capacity of T_h1 and T_h17 cells, first splenic $CD4^+$ T cells were isolated by magnetic cell separation (MACS) using a $CD4^+$ T cell Isolation Kit. Cells were then stained for the surface marker CD4 and CD25 for 10 minutes at 4°C. $CD4^+$ $CD25^-$ cells were then sorted using a BD FACS Aria II cell sorter (purity achieved ≥95 %). 0.5 x 10^6 $CD4^+$ $CD25^-$ cells were cultivated in an 48 well plate which was pre-coated with 5 µg/ml αCD3 for at least 2 hours at 37°C. In order to initiate differentiation, cells were cultured for 6 days in T_h1/T_h17 differentiation media (see Table 4.12). The control cells (T_h0) received only 1 µg/ml αCD-28. For T_h1 differentiation, cells were splitted 1:2 3 days after incubation; on day 5 500 µl media was replaced with fresh media. For T_h17 differentiation, first 500 µl media was replaced with fresh media 3 days after incubation. Cells were splitted on day 5 1:2. T_h1 and T_h17 cells were analysed for the capacity to differentiate into T_h1 and T_h17 cells 6 days post incubation using the intracellular staining for T_h1/T_h17 cells (see chapter 4.2.3.2).

Table 4.12: Supplements of in vitro differentiation medium for T_h1 and T_h17.

		Concentration	Manufacturer
T_h1	α-CD28	1 µg/ml	BD Biosciences, Heidelberg, Germany
	α-IL-4	200 ng/ml	eBioscience, San Diego, USA
	IL-12	20 ng/ml	R&D systems, Minneapolis, USA
T_h17	α-CD28	1 µg/ml	BD Biosciences, Heidelberg, Germany
	α-IL-2	200 ng/ml	R&D systems, Minneapolis, USA
	α-IL-4	200 ng/ml	eBioscience, San Diego, USA
	α-IFNγ	200 ng/ml	eBioscience, San Diego, USA
	rm-IL-1β	20 ng/,l	eBioscience, San Diego, USA
	rm-IL-6	50 ng/ml	R&D systems, Minneapolis, USA
	rm IL-21	100 ng/ml	R&D systems, Minneapolis, USA
	rm IL-23	20 ng/ml	R&D systems, Minneapolis, USA
	rh-TGFβ	2 ng/ml	R&D systems, Minneapolis, USA

4.2.4 Biochemical methods

4.2.4.1 Ceramide and sphingomyelin quantification

Ceramides and sphingomyelins, were quantified by Dr. Fabian Schuhmacher (University Potsdam) by rapid resolution liquid chromatography/mass spectrometry.

Short lipids were extracted from colon biopsies with C17-ceramide and C16-d31sphingomyelin as internal standards, after homogenization of colonic tissue. Subsequently, samples were analysed by rapid-resolution liquid chromatography-MS/MS using a Q-TOF 6530 mass spectrometer (Agilent Technologies, Waldbronn, Germany) operating in the positive ESI mode. Precursor ions of ceramides [C16-ceramide (m/z 520.508); C17-ceramide (m/z 534.524), C18-ceramide (m/z 548.540), C20-ceramide (m/z 576.571), C22-ceramide (m/z 604.602), C24-ceramide (m/z 632.634), C24:1-ceramide (m/z 630. 618)] were cleaved into the fragment ion m/z 264.270. Similar to ceramide, precursor ions of sphingomyelin (C16-sphingomyelin (m/z 703.575), C16-d31-sphingomyelin (m/z 734.762), C18-sphingoymyelin (m/z 731.606), C20-sphingomyelin (m/z 759.638), C22-sphingomyelin (m/z 787.669), C24-sphingomyelin (m/z 815.700), C24:1-sphingomyelin (m/z 813.684)) were cleaved into the fragment ion m/z 184.074. The subsequent quantification was performed using Mass Hunter Software, and the resulting sphingolipid quantities were normalized to the actual protein content of the homogenate.

4.2.4.2 Ac and Asm activity

The acid ceramidase and acid sphingomyelinase activity were determined with the help of Prof. Dr. med. Dirk M. Hermann and Dr. med. Alexander Carpinteiro. To analyse the Asm and Ac activity in colonic tissue rectal biopsies were snap-frozen and stored at -80°C until further pulverization using a mortar and pestle filled with liquid nitrogen. The tissue powder was then transferred in pre-cooled Asm lysis buffer followed by determination of the protein concentration using the Bradford protein assay. To achieve optimal results the protein concentration varied from 10 µg protein (AC) to 2 µg protein (ASM), which was then transferred into a new tube, followed by adding Ac or Asm lysis buffer to a final volume of 20 µl. 100 pmol/sample NBD-ceramide or 100 pmol/sample BODIPY-sphingomyelin were added to each sample and subsequently incubated for 4 hours (Ac) or for 1 hour (Asm) at 37°C. After incubation time the reaction was terminated by lipid extraction through addition of chloroform:methanol (2:1, v/v), vortexing and centrifugation for 5 minutes at 15000 x g. The lower phase containing lipids was collected and dried in a SpeedVac at 37°C. Again, the dried lipid pellets were resuspended in 20 µl choloroform:methanol (2:1, v/v) and transferred onto a thin layer chromatography (TLC) plate. The running buffer for the TLC run was either with ethyl acetate:acetic acid (100:1, v/v, Ac) or cholorform:methanol (80:20, v/v, Asm). Plates were then imaged using a Typhoon FLA 9500. Spot intensity was quantified with ImageQuant software.

4.2.5 Molecular methods

4.2.5.1 Isolation of RNA and DNA

RNA was isolated from colon tissue using the RNeasy Fibrous Tissue Mini Kit (Qiagen, Hilden, Germany).
According to the manufacturer's instructions, DNA digestion was performed for 15 minutes, followed by washing and collection of the RNA. After isolation, RNA concentration was determined by using a NanoDrop spectrophotometer. 1-2 µg RNA was used for further cDNA synthesis. Any remaining RNA was stored at -80°C until further use.

4.2.5.2 Synthesis of complementary DNA

Isolated RNA was incubated with 0.5 µl Oligo dt and 0.5 µl Random Primer for 10 minutes at 70°C. Samples were cooled down to 42°C for 1 hour to start the reverse transcription into complementary DNA (cDNA) using 1 µl M-MLV (H-) point mutant reverse transcriptase, 4 µl 5x m-MLV RT-Buffer and 1 µl dNTPs (10 mM). By heating up the samples to 95°C for 5 minutes the enzyme was inactivated and samples were stored at -20°C until further use.

4.2.5.3 Quantitative real time PCR

By semi-quantitative PCR the amount of cDNA was determined through the expression of the house-keeping gene ribosomal protein s9 (RPS9) by using the following reaction mix and program prior to qPCR:

Table 4.13: Mastermix for semi-quantitative

1x	Reaction buffer
1.5 mM	$MgCL_2$
1 mM	dNTPs
5 µM	RPS9 forward primer
5 µM	RPS9 backward primer
0.5 U	GoTaq Hot Start polymerase
ad 20 µl	MilliQ H_2O

Table 4.14: Program of semi-quantitative PCR.

		30 cycles			
Temperature	95°C	95°C	58°C	72°C	72°C
Time (mm:ss)	10:00	00:45	00:45	01:00	10:00

Quantitative real-time analysis was performed with a 7500 Real-Time PCR system using the Fast SYBR Green Master Mix and specific primer. For each individual gene mRNA levels were calculated using standard curves, and were normalized to the housekeeping gene RPS9. To determine the relative expression the quotient of the mean of both the target gene and the housekeeping gene RPS9 was calculated.
Below, the reaction mix, qPCR program and primer pairs are listed.

Table 4.15: Mastermix for qPCR.

~20 ng	cDNA template
1x	FAST SYBR Green Master Mix
50-900 nM	Forward primer
50-900 nM	Reverse primer
Ad 20 µl	MilliQ H_2O

Table 4.16: qPCR program.

		40 cycles			melting curve			
Temperature	95°C	95°C	T_a	72°C	95°C	60°C	95°C	60°C
Time (mm:ss)	10:00	00:15	00:30	00:30	00:15	01:00	00:15	00:15

Table 4.17: Sequences of primer pairs for PCR/qPCR.

gene	sequence (forward, reverse)	concentration for qPCR	annealing temperature (T_a)
Claudin	5'- GCG GGA GAT GGG AGC TGG GTT GTA -3'	300 nM	58°C
	5'- GTG GAT CGC GGC GCA GAA TAG AGG -3'	900 nM	
IL-6	5'- ACC ACG GCC TTC CCT ACT TC -3'	300 nM	55°C
	5'- GCC ATT GCA CAA CTC TTT TCT C -3'	300 nM	
Occludin	5'- GCC CTG GCT GAC CTA GAA CTT AC -3'	300 nM	55°C
	5'- AGA CTT AGC CAA AAC TGC CTT AGC -3'	900 nM	
RPS9	5'- CTGGACGAGGGCAAGATGAAGC -3'	900 nM	58°C

	5’- TGACGTTGGCGGATGAGCACA -3’	50nM	
TJ1/Zo-1	5’- TTT TTG ACA GGG GGA GTG G -3’	900 nM	52°C
	5’- TGC TGC AGA GGT CAA AGT TCA AG -3’	300 nM	
TJ2/Zo-2	5’- CTA GAC CCC CAG AGC CCC AGA AA -3’	900 nM	58°C
	5’- TCG CAG GAG TCC ACG CAT ACA AG -3’	900 nM	
TLR4	5’- TGC TGG GGC TCA TTC ACT CAC -3’	300 nM	58°C
	5’- ACA CTC AGA CTC GGC ACT TAG CAC -3’	300nM	
TNFα	5’- CAA TGC ACA GCC TTC CTC ACA G -3’	300 nM	58°C
	5’- CCC GGC CTT CCA AAT AAA TAC AT -3’	50 nM	

4.2.6 Statistical analyses

Statistical analyses were performed using GraphPad Prism software version 7. In order to determine statistical significance, first column statistics were performed using D'Agostino & Pearson normality test and Shapiro-Wilk normality test. Student’s t-test, one-way ANOVA and two-way ANOVA followed by Tukey’s multiple comparisons test, Dunn's multiple comparisons test or Bonferroni's multiple comparisons test were applied. P values were set at a level of $p < 0.05$.

Results

5.1 Role of sphingolipids in bacterial infection models

Sphingolipids are of particular scientific interest, due to their pivotal role in membrane reorganization, and contribution to receptor clustering. Deficiency of sphingolipids leads to life threatening diseases, such as Faber disease or Niemann Pick disease, indicating the importance of sphingolipids in science and health (Table 3.2). In both diseases alterations of the sphingolipid pathway leads to accumulation of ceramide or sphingomyelin in tissue thereby inducing life threatening conditions [154, 167]. Interestingly, several groups show a controversial role of ceramide or sphingomyelin in bacterial induced diseases, such as in *Mycobacterium tuberculosis*, *Staphylococcus aureus* or P*seudomonas aeruginosa* [235, 236]. To gain further insights into the function of ceramide and sphingomyelin within bacterial infection, the impact of acid sphingomyelinase (Asm), hydrolysing sphingomyelin into ceramide, and acid ceramidase (Ac), degrading ceramide into sphingosine-1-phosphate (S1P), during intestinal inflammation was analysed using the *Citrobacter* (*C.*) *rodentium* induced colitis.

5.2 Changes in the sphingolipid profile during *C. rodentium* infection

To investigate the role of sphingolipids in bacterial induced colitis, we infected C57BL/6 mice with 2-5 x 10^9 colony forming units (CFU) of the gram-negative *C. rodentium*. First, sphingomyelin and ceramide concentrations were quantified in the colon during the 10 day infection course. Therefore, rectal colonic tissue was analysed using rapid resolution liquid chromatography/mass spectrometry (Figure 5.1). Sphingomyelin concentrations decrease within 3 to 10 days post *C. rodentium* infection compared to uninfected wild type tissue. Similar results were detected for ceramide; however, ceramide concentrations started to decrease 1 day post *C. rodentium* infection. Further, the Asm activity and Ac activity was analysed in colonic tissue using an enzyme activity assay at day 10 post infection (see chapter 4.2.4.2). Interestingly, the Asm activity was decreased in *C. rodentium* infected C57BL/6 mice 10 days post challenge, albeit, the Ac activity was not affected by *C. rodentium* infection. Taken together, sphingolipids, such as ceramide and sphingomyelin, are influenced by *C. rodentium* infection.

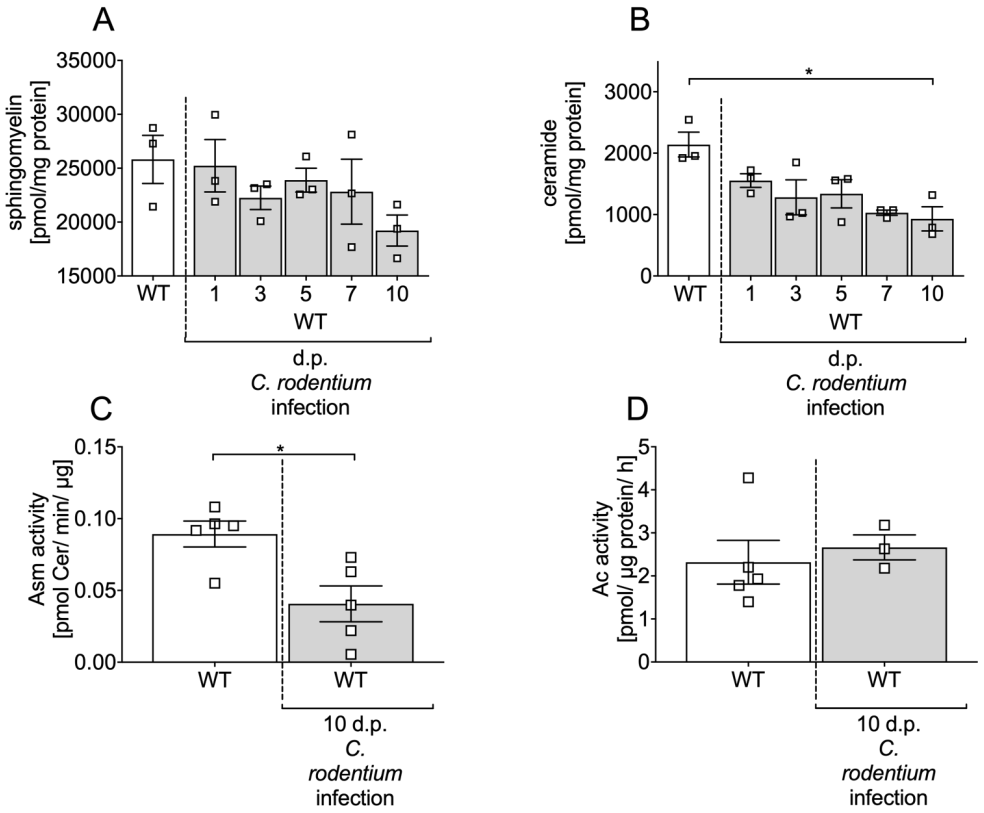

Figure 5.1: Alteration of the sphingolipid profile during *C. rodentium* infection.
(**A-D**) C57BL/6 (WT) mice were orally infected with 2-5 x 10^9 colony forming units (CFU) of *C. rodentium*. At indicated (1, 3, 5, 7 and 10) days post (dp) infection colons were excised. In rectal colonic tissue, the (**A**) sphingomyelin (n = 2-3, parametric one-way ANOVA) and (**B**) ceramide (n = 2-3, non-parametric one-way ANOVA) contents were analysed using rapid resolution liquid chromatography/mass spectrometry. Data are presented as the concentration of ceramide and sphingomyelin in pmol/mg protein. (**C**) Asm activity (n = 5, parametric t-test) and (**D**) Ac activity (n = 3-5, parametric t-test) were quantified in rectal colonic tissue 10 dp infection using BODIPY-sphingomyelin as a substrate. Data were first tested for their normal distribution using D'Agostino & Pearson omnibus normality test. Statistics were performed using the non-parametric Kruskal-Wallis test with Dunn's multiple comparison test, the parametric one-way ANOVA test with Tukey's multiple comparison test or the unpaired t-test. All data are presented as mean ± SEM (*, $p<0.05$).

5.3 The acid sphingomyelinase/ceramidase axis protects from *C. rodentium* infection

Based on the previous data indicating an involvement of sphingomyelin and ceramide during *C. rodentium* infection, the biological effect of the acid sphingomyelinase and acid ceramidase axis was investigated. Therefore, bacterial induced colitis was induced in mice lacking acid sphingomyelinase and/or acid ceramidase. In the first and second part of this work genetically knockout mice, which do not express acid sphingomyelinase or acid ceramidase, were infected with *C. rodentium*. In the third part, the Asm and Ac inhibitor amitriptyline was used [197], which is known to inhibit the transportation of Asm and partially Ac to the outer leaflet of the membrane, thereby stopping the translocation and activation of Asm and Ac (see chapter 3.5.5).

5.3.1 Acid sphingomyelinase protects from *C. rodentium* induced colitis

To address the biological effect of Asm during *C. rodentium* infection, Asm wildtype (Asm WT) or Asm knockout (Asm KO) mice were orally gavaged with PBS or 2-5 x 10^9 colony forming (CFU) units of *C. rodentium.* Infection parameters, sphingomyelin concentration and ceramide concentration were assessed in the early (3 and 5 dp) and/or acute phase (7 and 10 dp) of infection.

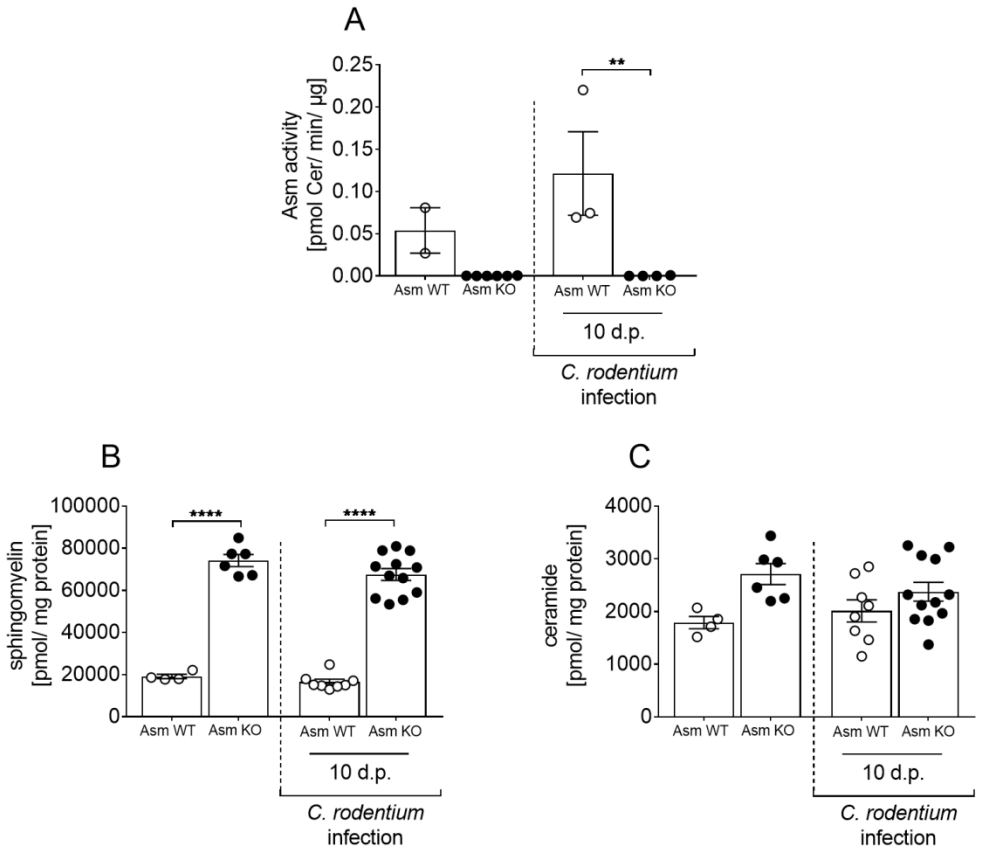

Figure 5.2: Deficiency of acid sphingomyelinase (Asm) in mice alters sphingolipid concentration during *C. rodentium* infection.
(**A-C**) Asm wildtype (Asm WT) and Asm knockout (Asm KO) mice were orally gavaged with PBS or 2-5 x 10^9 colony forming units (CFU) of *C. rodentium*. (**A**) Asm activity [pmol Cer/min/µg] was analysed in rectal colonic tissue (n = 2-6). Colons were excised from uninfected Asm WT and Asm KO mice and 10 dp infection. In rectal colonic tissue, (**B**) sphingomyelin (n = 4-12) and (**C**) ceramide (n = 4-12) concentrations were analysed using rapid resolution liquid chromatography/mass spectrometry. Data are presented as the concentration of ceramide and sphingomyelin in pmol/mg protein. Statistics were performed using the two-way ANOVA test followed by Tukey's multiple comparison. All data are presented as mean ± SEM (**, p<0.01; ****, p <0.0001).

First, the Asm activity was analysed in colonic tissue of Asm WT and Asm KO mice in uninfected or infected mice 10 dp *C. rodentium* infection. Neither in uninfected Asm KO nor in infected Asm KO mice Asm activity was detected. However, Asm activity was enhanced in infected Asm WT mice 10 dp infection compared to uninfected Asm WT mice (Figure 5.2, A). Furthermore, sphingomyelin and ceramide concentrations were

assessed in colonic tissue using rapid resolution liquid chromatography/mass spectrometry in uninfected Asm WT and Asm KO mice, and in the acute phase of infection (Figure 5.2, B-C). Interestingly, sphingomyelin concentrations were elevated in uninfected Asm KO mice compared to uninfected Asm WT littermates as well as upon *C. rodentium* infection. On the contrary, ceramide concentrations were not altered upon infection comparing uninfected Asm WT to infected Asm WT or uninfected Asm KO to infected Asm KO mice (Figure 5.2, B-C).

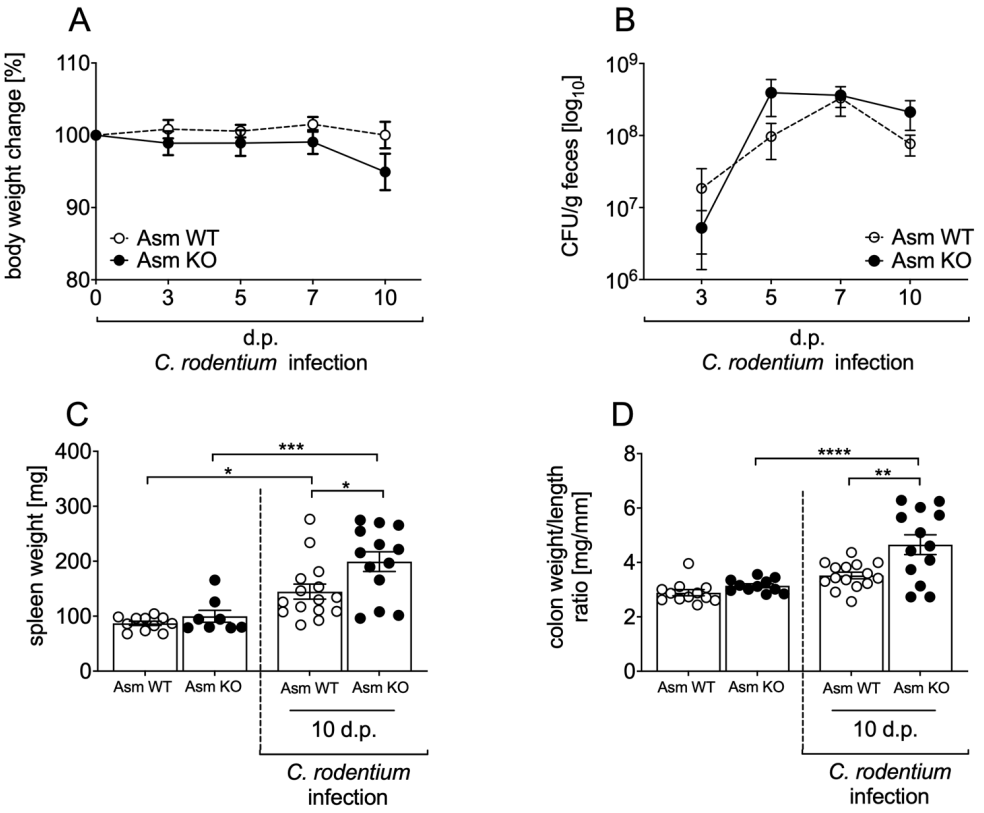

Figure 5.3 Deficiency of acid sphingomyelinase (Asm) in mice increases susceptibility to *C. rodentium* infection.

(**A-D**) Asm wildtype (Asm WT) and Asm knockout (Asm KO) mice were orally gavaged with PBS or 2-5 x 10^9 colony forming units (CFU) of *C. rodentium*. (**A, B**) At indicated time points body weight and CFU in faeces were assessed in Asm WT mice (white dots, n = 16-17) and Asm KO mice (black dots, n = 14-20). Data were first tested for their normal distribution using D'Agostino & Pearson omnibus normality test. Statistics were performed using the non-parametric Mann- Whitney test or the parametric t-test. (**C**) Spleen weight was measured in uninfected Asm WT and Asm KO mice, as well as 10 dp *C. rodentium* infection (n = 8-15). (**D**) Colon weight and length were determined in uninfected Asm WT and Asm KO mice, as well as 10 dp *C. rodentium* infection (n = 11-15). Statistics were performed using the two-way ANOVA test followed by Tukey's multiple comparison test or. All data are presented as mean ± SEM (*, $p<0.05$; **, $p<0.01$; ***, $p<0.001$; ****, $p<0.0001$).

In the acute phase of infection, loss of body weight was stronger in Asm KO mice compared to wildtype littermates (Figure 5.3, A). The peak of infection, detected via the CFU in faeces, was reached as early as 5 dp infection in Asm WT and Asm KO mice, with first signs of declining at 10 dp infection. However, the bacterial burden was elevated in Asm KO mice 5 and 10 dp infection compared to wildtype littermates, giving

first hints of an increased susceptibility of Asm KO mice to *C. rodentium* infection (Figure 5.3, B). Furthermore, the spleen weights were enhanced in Asm deficient mice compared to Asm WT littermates (Figure 5.3, C). In line to the first results, elevated colon weight/length ratios were detected in Asm KO mice 10 dp infection (Figure 5.3, D). The colon weight/length ratio is an indication of the pathology score during *C. rodentium* infection [111].

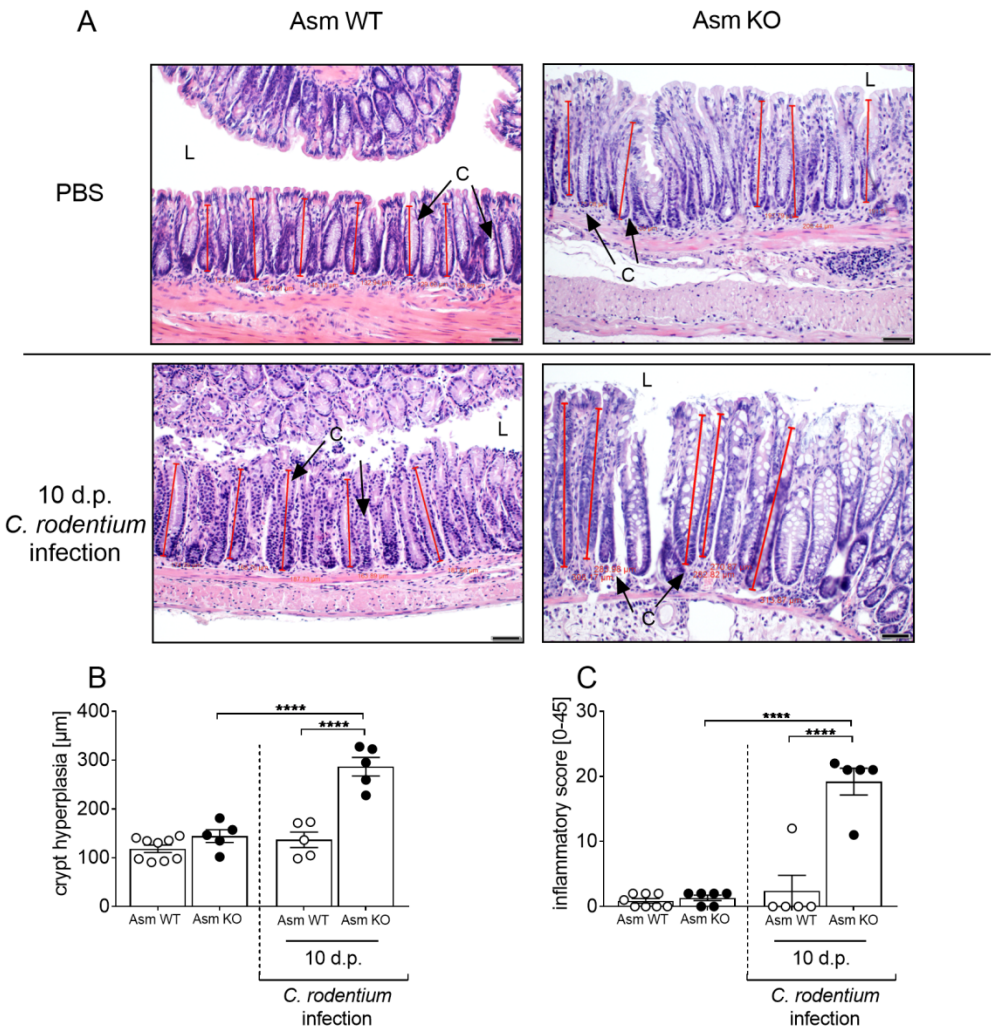

Figure 5.4: Deficiency of acid sphingomyelinase (Asm) in mice increases colon pathology 10 days post *C. rodentium* challenge.
(**A-C**) Asm wildtype (Asm WT) and Asm knockout (Asm KO) mice were orally gavaged with PBS or 2-5 x 10^9 colony forming units (CFU) of *C. rodentium*. Colons were excised from uninfected mice or 10 dp *C. rodentium* infection. (**A**) Representative H&E staining of colon sections from PBS or *C. rodentium* infected Asm WT or Asm KO mice 10 dp infection. (Red bars indicate the crypt length. (L) lumen, (C) crypt. Length of scale bar is 50 µm). (**B**) Measured crypt length in colons of uninfected Asm WT or Asm KO mice, and infected Asm WT and Asm KO 10 dp *C. rodentium* infection (n = 5-9). (**C**) Histopathology score of the colon for inflammatory cell infiltration, mucous defectiveness, neutrophil infiltration, hyperplasia and crypt abscess of uninfected Asm WT and Asm KO mice, and Asm WT and Asm KO mice 10 dp *C. rodentium* infection (n = 5-8). Statistics were performed using the two-way ANOVA test with Tukey's multiple comparison test. All data are presented as mean ± SEM (**** p <0.0001).

To get deeper insights, colonic tissue of Asm WT and Asm KO mice was histologically analysed (Figure 5.4). Colonic tissue was stained with hematoxylin and eosin (H&E), crypt length was measured, and tissue sections were scored for inflammatory cell infiltration, mucous defectiveness, neutrophil infiltration, hyperplasia and crypt abscess. Clearly, the histology reveals elongation of the crypt length in mice lacking Asm 10 dp infection (Figure 5.4, A-B). Also, the inflammatory score of colon tissue was increased in Asm deficient mice 10 dp infection compared to infected wildtype littermates (Figure 5.4, C).

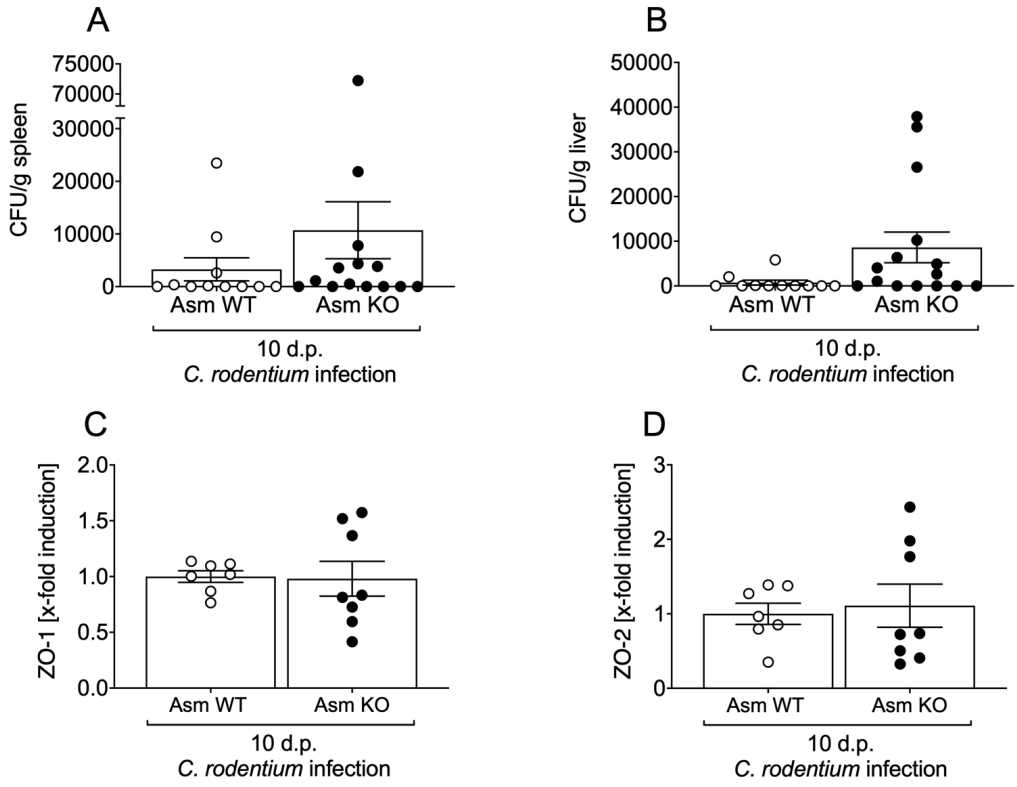

Figure 5.5: Enhanced systemic distribution of *C. rodentium* in acid sphingomyelinase deficient mice.

(**A-D**) Asm wildtype (Asm WT) and Asm knockout (Asm KO) mice were orally infected with 2-5 x 10^9 colony forming units (CFU) of *C. rodentium.* (**A, B**) 10 dp *C. rodentium* infection spleen and liver were isolated and CFU of *C. rodentium* was assessed to determine the systemic distribution of bacteria (n = 11-15, non-parametric t-test). (**C, D**) Rectal colonic tissues were analysed using qPCR for the expression of the tight junction proteins ZO-1 and ZO-2 in Asm WT and Asm KO mice 10 dp *C. rodentium* infection (n = 7-8, parametric t-test). Data were first tested for their normal distribution using D'Agostino & Pearson omnibus normality test. Statistics were performed using the non-parametric Mann Whitney test or the parametric t-test. All data are presented as mean ± SEM.

To investigate the epithelial barrier function, the systemically distribution of the normally non-invasive *C. rodentium* was analysed [101]. Hence, CFU in spleen and liver were assessed 10 dp infection in Asm WT and Asm KO mice, showing increased bacterial burden in Asm KO mice (Figure 5.5, A-B). In addition, the epithelial barrier was analysed for the expression of tight junction proteins, regulating the transfer of materials from the lumen into the lamina propria [18, 24]. However, the expression of

the tight junction protein zonula-1 and zonula-2 (ZO-1 and ZO-2) were not altered in Asm KO mice compared to Asm WT littermates 10 dp infection in rectal colonic tissue (Figure 5.5, C-D).

The cytokine profile gives first insights into the inflammatory response against *C. rodentium*. Therefore, macrophages, T_h1, T_h17 and T_{regs} related cytokines were investigated in serum and supernatant of cultured colonic tissue of Asm WT and Asm KO mice 10 dp infection. Interestingly, cytokines, like IL-17A, IFNγ, IL-10 and TNFα were slightly elevated in Asm deficient mice 10 dp infection (Figure 5.6). Together with the previous findings of the enhanced invasion of *C. rodentium* into the periphery, these data suggest increased susceptibility of Asm deficient mice to *C. rodentium* infection as indicated by increased infection parameters.

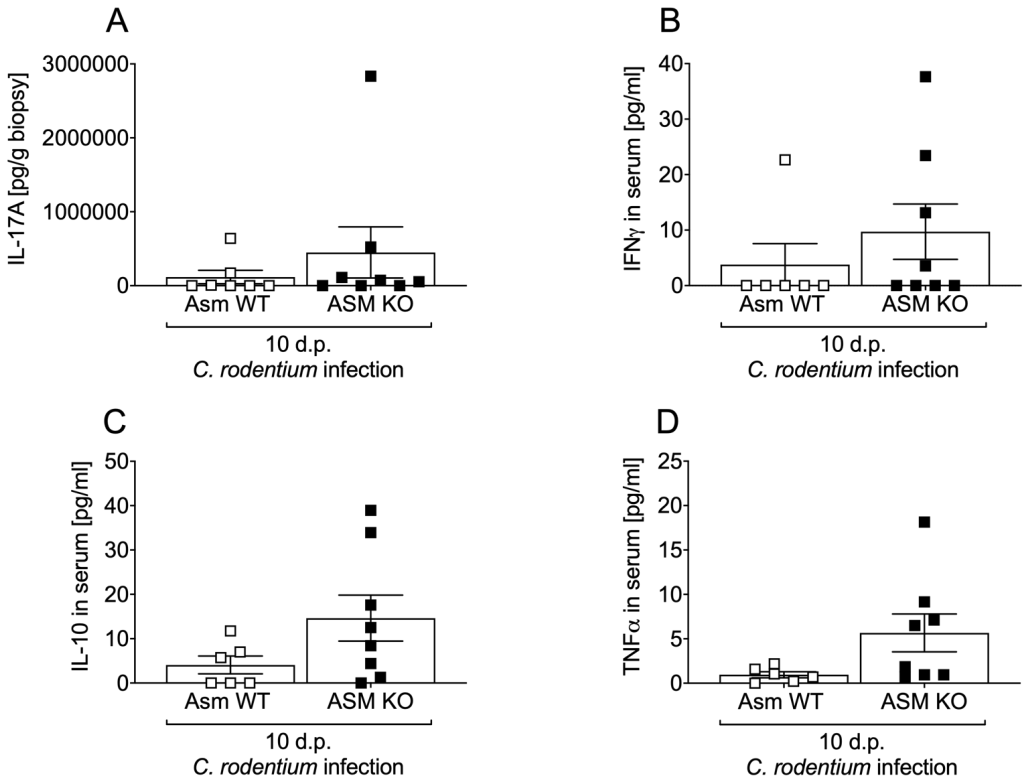

Figure 5.6: Asm deficiency increases the release of cytokines 10 days post *C. rodentium* infection. (**A-D**) Asm wildtype (Asm WT) and Asm knockout (Asm WT) mice were orally infected with 2-5 x 10^9 colony forming units (CFU) of *C. rodentium.* Concentration of the cytokines IL-17A (**A**), IFNγ (**B**), IL-10 (**C**) and TNFα (**D**) in colonic tissue and serum of Asm WT and Asm KO mice 10 days post (dp) *C. rodentium* infection were measured using Luminex technologies (n = 6-8). Data were first tested for their normal distribution using D'Agostino & Pearson omnibus normality test. Statistics were performed using the non-parametric Mann Whitney test or the parametric t-test. All data are presented as mean ± SEM.

5.3.2 Acid ceramidase protects from *C. rodentium* induced colitis

Ceramide, in the centre of the sphingolipid pathway, is known to be involved in the internalization of pathogens, the induction of apoptosis in infected cells, the intracellular activation of signalling pathways, and the release of cytokines [237-239]. As seen in C57BL/6 mice, ceramide concentration decline as soon as 1 day post *C. rodentium* infection (Figure 5.1, A), suggesting an involvement of ceramide during *C. rodentium* infection. Hence, the role of ceramide was investigated using the conditional Asah$^{fl/fl}$ x CreEr$^{+/ki}$ mouse, in which the intraperitoneal (i.p.) injection of Tamoxifen 8, 6 and 4 days before infection induces systemic depletion of acid ceramidase in mice (chapter 4.2.1.2).

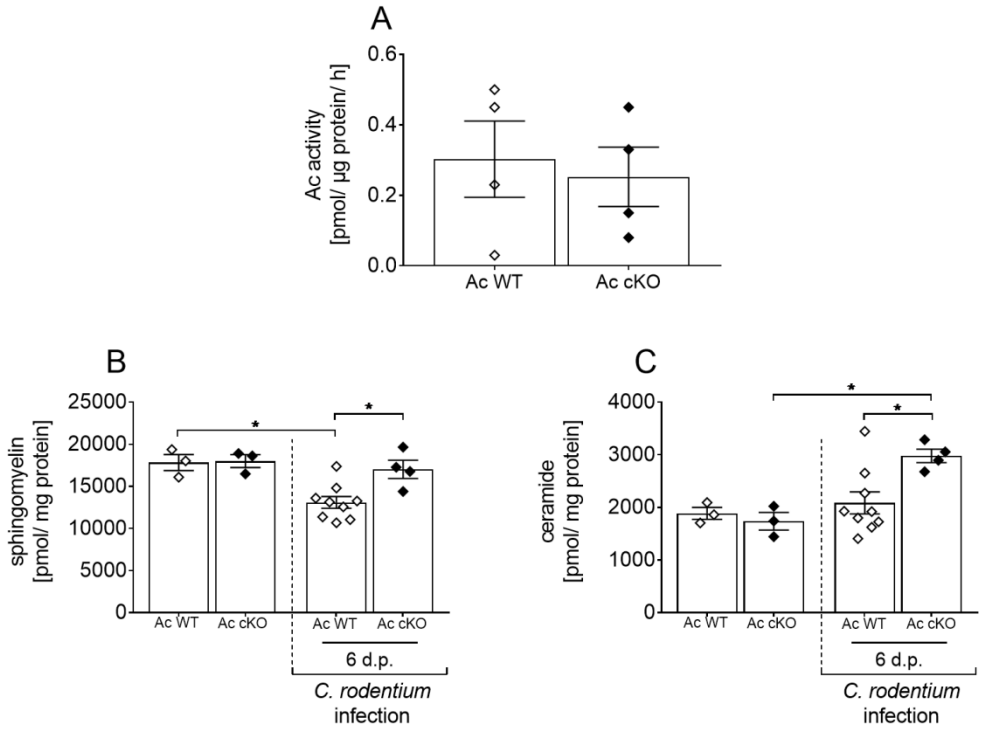

Figure 5.7: Deficiency of acid ceramidase (Ac) in mice alters sphingolipid concentration during *C. rodentium* infection.
(**A-C**) Asah$^{fl/fl}$ x Cre$^{+/+}$ (Ac WT) and Asah$^{fl/fl}$ x Cre$^{ki/ki}$ (Ac cKO) mice were orally gavaged with PBS or 2-5 x 10^9 colony forming units (CFU) of *C. rodentium*. Colons were excised from uninfected Ac WT and Ac cKO mice and 10 dp infection. (**A**) Ac activity [pmol/h/mg] was analysed in rectal colonic tissue (n = 4) of uninfected Ac WT and Ac cKO mice. (**B**) Sphingomyelin (n = 3-9) and (**C**) ceramide (n = 3-9) concentrations were analysed using rapid resolution liquid chromatography/mass spectrometry. Data were first tested for their normal distribution using D'Agostino & Pearson omnibus normality test. Statistics were performed using the parametric t-test or the two-way ANOVA test followed by Tukey's multiple comparison test. All data are presented as mean ± SEM (*, $p<0.05$).

First, the Ac activity in uninfected mice was analysed. In vitro, no changes in the Ac activity were observed comparing colonic tissue of Ac WT and Ac cKO mice (Figure 5.7, A). Next, the sphingomyelin and ceramide concentrations were addressed in uninfected and infected Ac WT and Ac cKO mice. While induction of the conditional

knockout of Ac did not impair the sphingomyelin and ceramide concentration, infection of Ac WT and Ac cKO mice with *C. rodentium* altered sphingomyelin and ceramide concentrations. Infection of Asm WT mice reduced the concentration of sphingomyelin, albeit ceramide concentrations were not impaired. Interestingly, the sphingomyelin concentration was not altered 6 dp infection, although accumulation of ceramide was detected in Ac cKO mice (Figure 5.7, A-B).

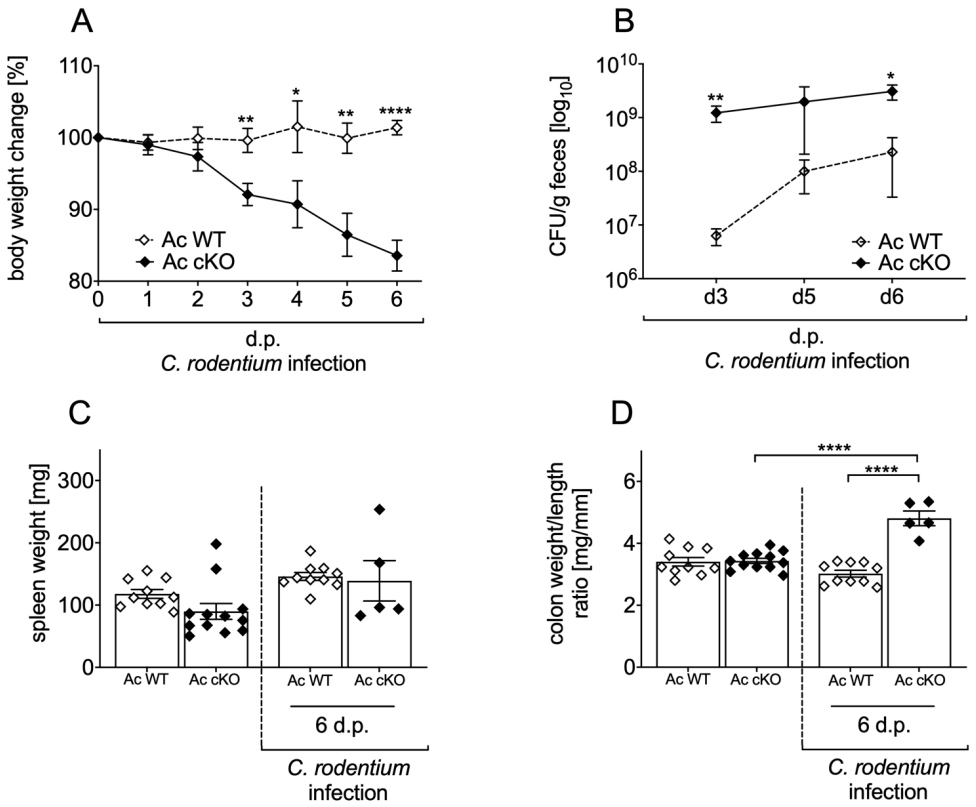

Figure 5.8: Deficiency of acid ceramidase in mice increases susceptibility to *C. rodentium* infection.
(**A-D**) Asah$^{fl/fl}$ x Cre$^{+/+}$ (Ac WT) and Asah$^{fl/fl}$ x Cre$^{ki/ki}$ (Ac cKO) mice were orally gavaged with PBS or 2-5 x 10^9 colony forming units (CFU) of *C. rodentium*. (**A, B**) At indicated time points body weight and CFU in faeces in Ac WT mice (white bar; n = 5-14) and Ac cKO mice (black bar; n = 4-12) were assessed. Data were first tested for their normal distribution using D'Agostino & Pearson omnibus normality test. Statistics were performed using the non-parametric Mann- Whitney test or the parametric t-test. (**C**) Spleen weight was measured in uninfected Ac WT and Ac cKO mice, and 10 dp *C. rodentium* infection (n = 5-10). (**D**) Colon weight and length was determined in uninfected Ac WT and Ac cKO mice, as well as 10 dp *C. rodentium* infection (n = 5-10). Statistics were performed using the two-way ANOVA test followed by Tukey's multiple comparison test. All data are presented as mean ± SEM (*, p<0.05; **, p<0.01; ****, p <0.0001).

To address the biological effect of Ac during *C. rodentium* infection, body weight, CFU in faeces and colon weight/length ratio were assessed in Ac WT and Ac cKO mice in the early phase (3 and 5 dp infection). Ac cKO mice lost 20 % of the initial body weight within 6 days, therefore we had to analyse the mice earlier than 10 dp infection (Figure 5.8, A). Compared to wildtype littermates Ac cKO mice showed not only higher loss of body weight, but also increased bacterial burden in faeces 3 to 6 dp infection (Figure

5.8, B). Although the spleen weight was not affected in both groups, the elevated colon weight/length ratio in Ac cKO mice again indicated a stronger histopathology (Figure 5.8, C-D). Colon crypt length was measured and the colonic tissue was scored for inflammatory cell infiltration, mucous defectiveness, neutrophil infiltration, hyperplasia and crypt abscess. Albeit the crypt length was not elongated 6 dp infection in Ac WT and Ac cKO mice, the inflammatory score was elevated in Ac cKO mice compared to infected Ac WT littermates (Figure 5.9).

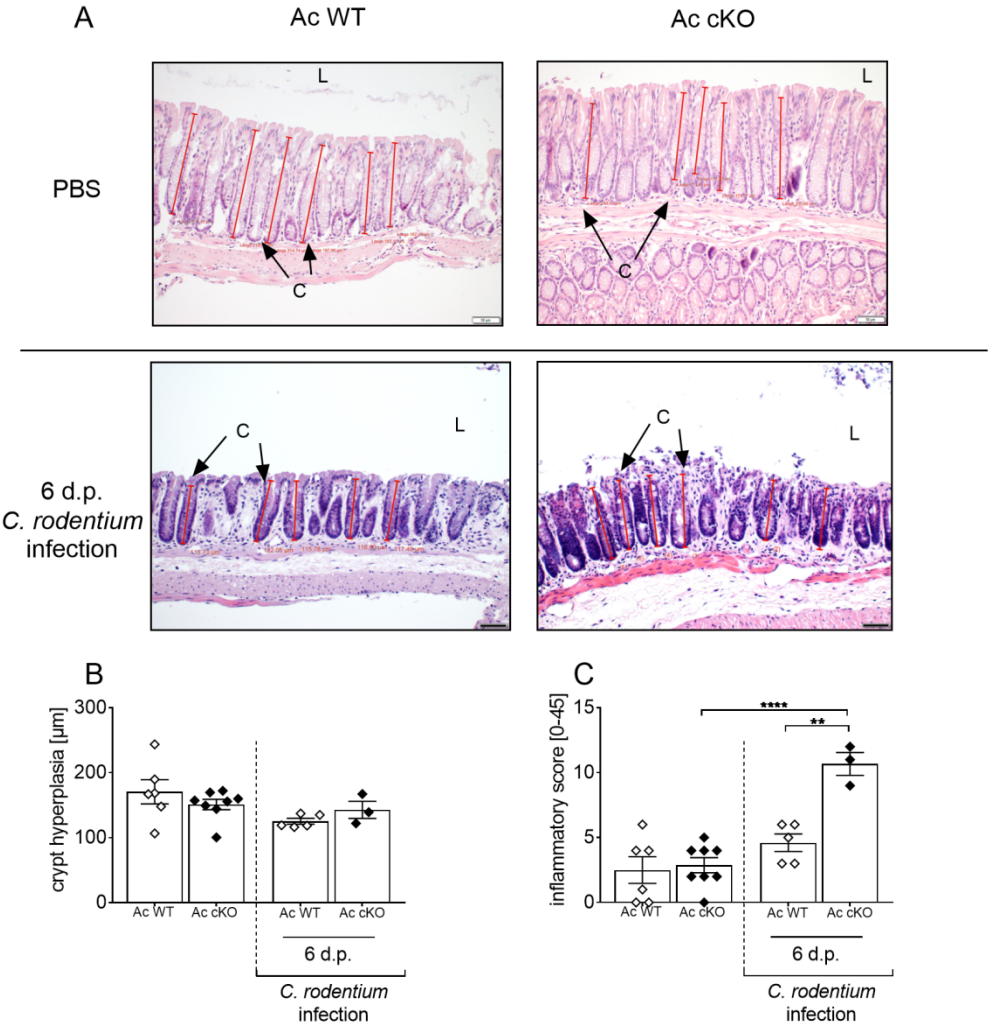

Figure 5.9: Deficiency of acid ceramidase in mice increases pathology in colons 6 days post *C. rodentium* challenge.

(**A-C**) Asah$^{fl/fl}$ x Cre$^{+/+}$ (Ac WT) and Asah$^{fl/fl}$ x Cre$^{ki/ki}$ (Ac cKO) mice were orally gavaged with PBS or 2-5 x 10^9 colony forming units (CFU) of *C. rodentium.* 6 dp *C. rodentium* infection colons were excised. (**A**) Representative H&E staining of colon sections from uninfected Ac WT and Ac cKO mice as well as 6 dp *C. rodentium* infection (Red bars indicate the crypt length. (L) lumen, (C) crypt. Length of scale bar is 50 µm). (**B**) Measured crypt length in colons of uninfected Ac WT and Ac cKO mice, and infected Ac WT and Ac cKO mice 6 dp *C. rodentium* infection (n = 3-8). (**C**) Histopathological score of the colon for inflammatory cell infiltration, mucous defective, neutrophil infiltration, hyperplasia and crypt abscess of uninfected Ac WT and Ac cKO mice, and Ac WT and Ac cKO mice 6 dp *C. rodentium* infection (n = 3-8). Statistics were performed using the two-way ANOVA test with Tukey's multiple comparison test. All data are presented as mean ± SEM (**, p<0.01; ****, p <0.0001).

To get deeper insights into the role of ceramide during *C. rodentium* induced colitis, the epithelial barrier function was investigated. Therefore, the bacterial burden in spleen and liver was analysed for the normally non-invasive *C. rodentium* in Ac WT and Ac cKO mice. Clearly, in both organs the bacterial burden was elevated 6 dp infection in Ac cKO mice compared to wildtype littermates (Figure 5.10 A-B). Despite increased systemic distribution, the expression of tight junction protein ZO-1 and ZO-2 was not altered 6 dp infection in Ac WT and Ac cKO mice (Figure 5.10, C-D).

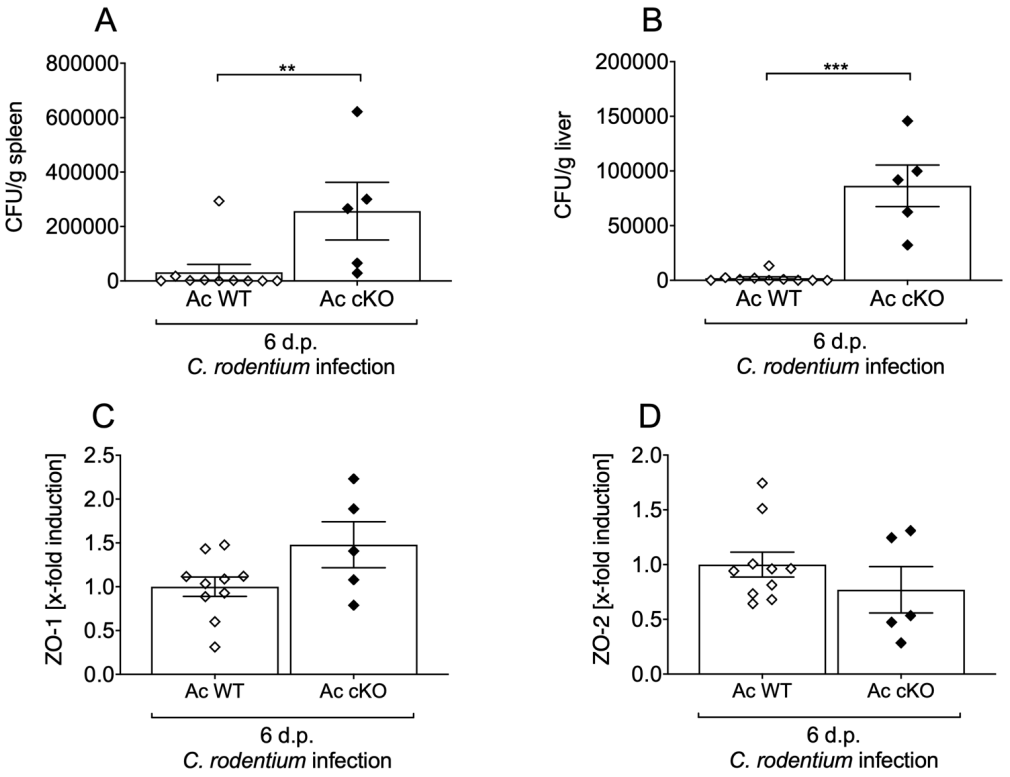

Figure 5.10: Enhanced systemic distribution of C. rodentium in acid ceramidase deficient mice. (**A-D**) Asah$^{fl/fl}$ x Cre$^{+/+}$ (Ac WT) and Asah$^{fl/fl}$ x Cre$^{ki/ki}$ (Ac cKO) mice were orally infected with 2-5 x 10^9 colony forming units (CFU) of *C. rodentium*. (**A, B**) 6 dp *C. rodentium* infection spleen and liver were isolated and CFU of *C. rodentium* were assessed (n = 5-10, non-parametric t-test). (**C, D**) Rectal colonic tissues were analysed using qPCR for the expression of the tight junction proteins ZO-1 and ZO-2 in Ac WT and Ac cKO mice 6 dp *C. rodentium* infection (n = 5-10). Data were first tested for their normal distribution using D'Agostino & Pearson omnibus normality test. Statistics were performed using the non-parametric Mann Whitney test or the parametric t-test. All data are presented as mean ± SEM (**, $p<0.01$; ***, $p<0.001$).

Induction of the conditional knockout is not affecting spleen weight or colon weight/length ratio, although induction of the conditional knockout slightly affects the colon architecture (Figure 5.8 and Figure 5.9). However, the deficiency of Ac increased susceptibility to *C. rodentium* infection. Especially, the higher loss of body weight indicates a strong involvement of Ac in the development of *C. rodentium* colitis.

5.3.3 Amitriptyline treatment enhanced *C. rodentium* induced colitis

As discussed afore, in both genetically knockout mouse strains strong effects on the development and pathology in bacterial induced colitis were detected. In the third part, the effect on the development and pathology of *C. rodentium* induced colitis was analysed in mice lacking both, Asm and partially AC (see chapter 3.5.5). Therefore, mice were administered 180 mg/l amitriptyline in drinking water 2 weeks prior to infection. Amitriptyline accumulates in the acid compartments of the lysosomes and interferes with the translocation of Asm and partially Ac to the outer leaflet of the membrane. Thereby amitriptyline inhibits the activation of Asm and Ac [146].
First, sphingomyelin and ceramide concentrations were analysed in colonic tissue of both, amitriptyline treated mice and untreated mice, as well as 7-10 dp infection, using rapid resolution liquid chromatography/mass spectrometry. While comparable sphingomyelin and ceramide concentrations were detected in uninfected WT and WT/Ami mice, both, sphingomyelin and ceramide concentrations were increased in amitriptyline treated mice compared to untreated mice 7-10 dp *C. rodentium* infection (Figure 5.11, A-B).

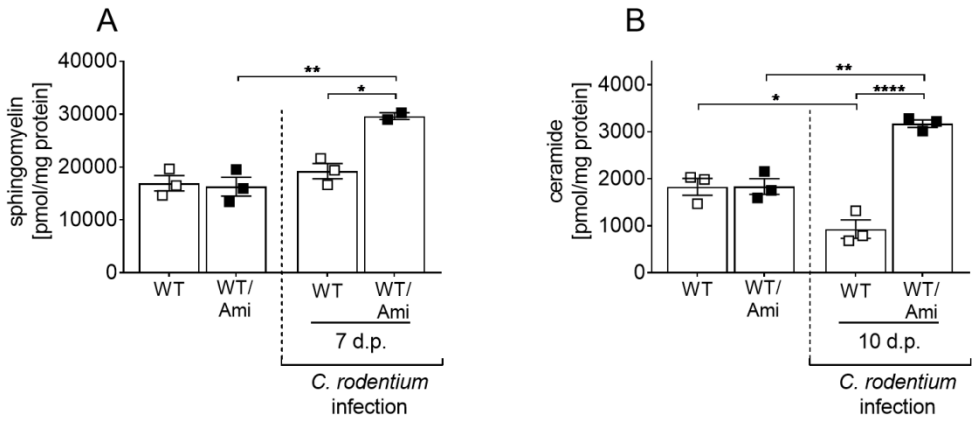

Figure 5.11: Amitriptyline pre-treatment alters sphingolipid concentration during *C. rodentium* infection.
(**A-B**) C57BL/6 mice were either left untreated (WT) or pre-treated with 180 mg/l Amitriptyline in drinking water two weeks prior to infection (WT/Ami). Mice were then orally gavaged with PBS or 2-5 x 10^9 colony forming units (CFU) of *C. rodentium*. In rectal colonic tissue, the (**A**) sphingomyelin (n = 3) and (**B**) ceramide (n = 3) concentrations were analysed using rapid resolution liquid chromatography/mass spectrometry. Statistics were performed using the two-way ANOVA test followed by Tukey's multiple comparison. All data are presented as mean ± SEM (*, p<0.05; **, p<0.01; ****, p <0.0001).

Amitriptyline treatment increased the loss of body weight as soon as 3 dp infection (Figure 5.12, A). The peak of *C. rodentium* was reached 7 dp infection in amitriptyline treated mice and wildtype littermates. However, the bacterial burden was mostly enhanced in amitriptyline treated mice compared to wildtype littermates 5 and 7 dp infection (Figure 5.12, B). Amitriptyline treatment also increased spleen weight 10 dp

infection (Figure 5.12, C). Further, the colon weight/length ratios were elevated in infected mice treated with amitriptyline 10 dp infection compared to untreated littermates (Figure 5.12, D). In line with the results obtained from the knockout mouse models, amitriptyline treatment seems to enhance susceptibility towards *C. rodentium* infection (Figure 5.12, D).

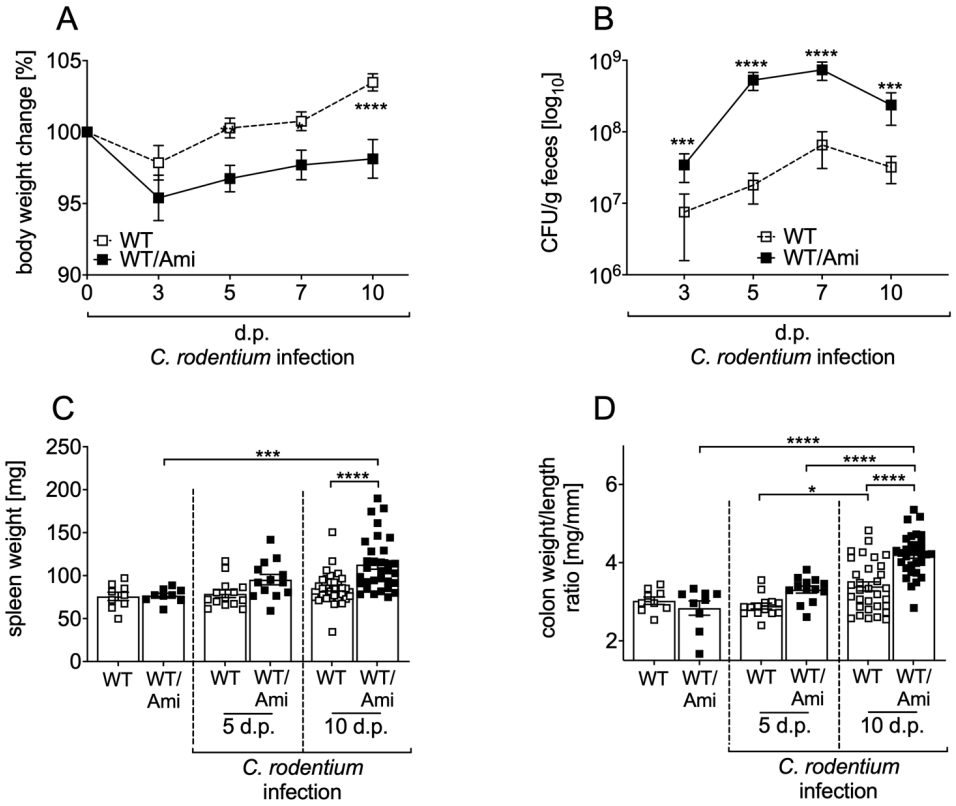

Figure 5.12: Amitriptyline pre-treatment increases susceptibility to *C. rodentium* challenge.
(**A-D**) C57BL/6 mice were either left untreated (WT) or pre-treated with 180 mg/l Amitriptyline in drinking water two weeks prior to infection (WT/Ami). Mice were then orally gavaged with PBS or 2-5 x 10^9 colony forming units (CFU) of *C. rodentium*. (**A, B**) At indicated (3, 5, 7 and 10) dp infection body weight and CFU in faeces in WT mice (white bar; n = 32-33) and WT/Ami mice (black bar; n = 32-35) were assessed. Data were first tested for their normal distribution using D'Agostino & Pearson omnibus normality test. Statistics were performed using the non-parametric Mann Whitney test. (**C**) Spleen weight was measured in uninfected and untreated or Amitriptyline treated mice 5 and 10 dp *C. rodentium* infection (n = 9-32). (**D**) Colon weight and length were determined in uninfected and untreated and uninfected Amitriptyline treated mice 5 and 10 dp *C. rodentium* infection (n = 9-32). Statistics were performed using the two-way ANOVA test followed by Tukey's multiple comparison test. All data are presented as mean ± SEM (*, p<0.05; **, p<0.01; ***, p<0.001; ****, p <0.0001).

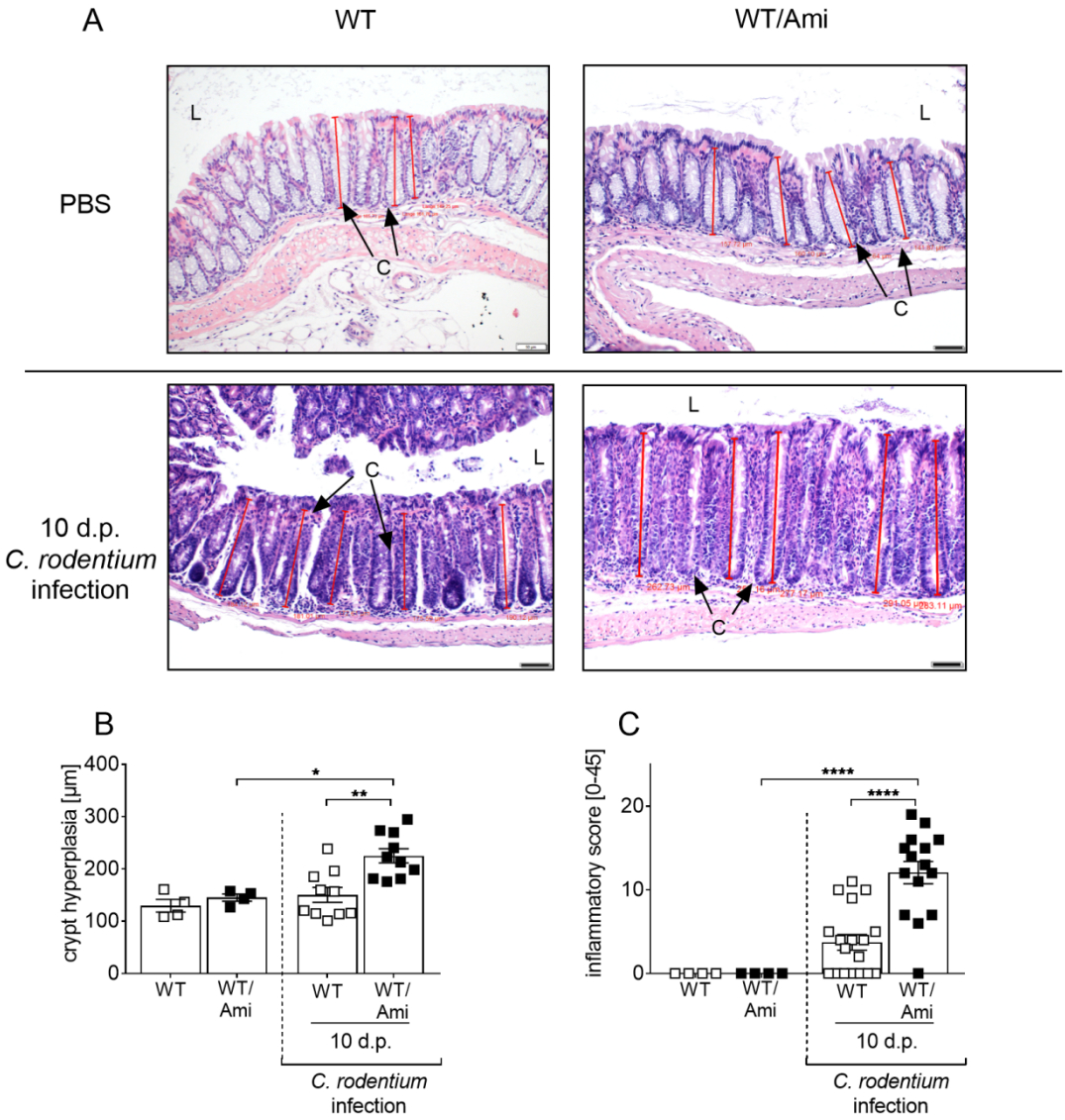

Figure 5.13: Amitriptyline pre-treatment increases pathology in colons 10 days post *C. rodentium* challenge.
(**A-C**) C57BL/6 mice were either left untreated (WT) or pre-treated with 180 mg/l Amitriptyline in drinking water two weeks prior to infection (WT/Ami). Mice were then orally gavaged with PBS or 2-5 x 10^9 colony forming units (CFU) of *C. rodentium*. Colons were excised 10 dp *C. rodentium* infection. (**A**) Representative H&E staining of colon sections from PBS or *C. rodentium* infected WT or WT/Ami mice 10 dp challenge. (Red bars indicate the crypt length. (L) lumen, (C) crypt. Length of scale bar is 50 µm). (**B**) Measured crypt length in colons of uninfected WT or WT/Ami mice, and infected WT and WT/Ami 10 dp *C. rodentium* infection (n = 4-18). (**C**) Histopathology score of the colon for inflammatory cell infiltration, mucous defectiveness, neutrophil infiltration, hyperplasia and crypt abscess of uninfected WT and WT/Ami mice, and WT and WT/Ami mice 10 dp *C. rodentium* infection (n = 4-18). Statistics were performed using the two-way ANOVA test with Tukey's multiple comparison test. All data are presented as mean ± SEM (*, p<0.05; ** p < 0.005; **** p <0.0001).

As indicated by the enhanced infection parameters, next the colon architecture was investigated. Amitriptyline treatment enlarged crypt length 10 dp infection compared to wildtype littermates (Figure 5.13, A-B). In addition, increased inflammatory cell infiltration, mucous defectiveness, neutrophil infiltration, hyperplasia and crypt abscess

were detected in *C. rodentium* infected amitriptyline treated mice compared to infected littermates (Figure 5.13, C). The results gained from the histopathology strongly underline the increased susceptibility of amitriptyline treated mice towards *C. rodentium* infection.

The bacterial burden of *C. rodentium* in spleen and liver was determined. Interestingly, the bacterial burden was not altered in the spleen of amitriptyline treated mice 5 and 10 dp infection. However, 5 and 10 dp infection the CFU of *C. rodentium* was enhanced in the liver of amitriptyline treated mice compared to infected littermates (Figure 5.14 A-B). Tight junction protein claudin and occludin expression were investigated 5 and 10 dp infection. Although the expression of the tight junction protein occludin was decreased in colonic tissue of amitriptyline treated mice, the expression of the claudin did not change within 10 dp infection in amitriptyline treated mice compared to wild type littermates.

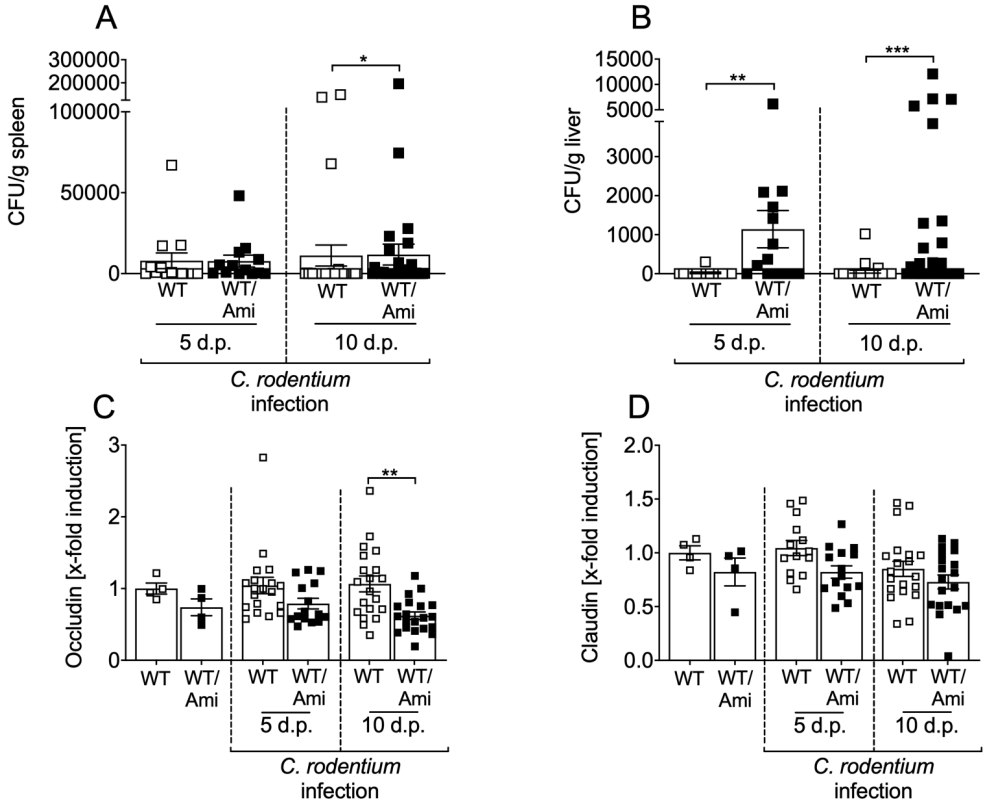

Figure 5.14: Enhanced systemic distribution of *C. rodentium* in mice pre-treated with amitriptyline. (**A-D**) C57BL/6 mice were either left untreated (WT) or pre-treated with 180 mg/l in drinking water two weeks prior to infection (WT/Ami). Mice were then orally gavaged with PBS or 2-5 x 10^9 colony forming units (CFU) of *C. rodentium*. (**A, B**) 5 and 10 dp *C. rodentium* infection spleen and liver were isolated and CFU of *C. rodentium* assessed to determine the systemic distribution of bacteria (n = 13-27). (**C, D**) Rectal colonic tissue were analysed using qPCR for the tight junction expression of claudin and occludin in uninfected WT and WT/Ami mice, as well as 5 and 10 dp *C. rodentium* infection (n = 13-27). Data were first tested for their normal distribution using D'Agostino & Pearson omnibus normality test. Statistics were performed using the parametric Mann Whitney test or the two-way ANOVA test with Tukey's multiple comparison test. All data are presented as mean ± SEM (*, $p<0.05$; ** $p < 0.005$; ***, $p<0.001$).

The characteristic of transmissible murine crypt hyperplasia during *C. rodentium* induced colitis can be further displayed by staining of crypts for the proliferation marker Ki-67 [240, 241]. Therefore, colonic tissues of infected wildtype and amitriptyline treated mice were stained for proliferating cells 10 dp *C. rodentium* infection. In line with the increased crypt hyperplasia in amitriptyline treated mice, the number of Ki-67 positive cells was enlarged in amitriptyline treated mice compared to uninfected littermates (Figure 5.15).

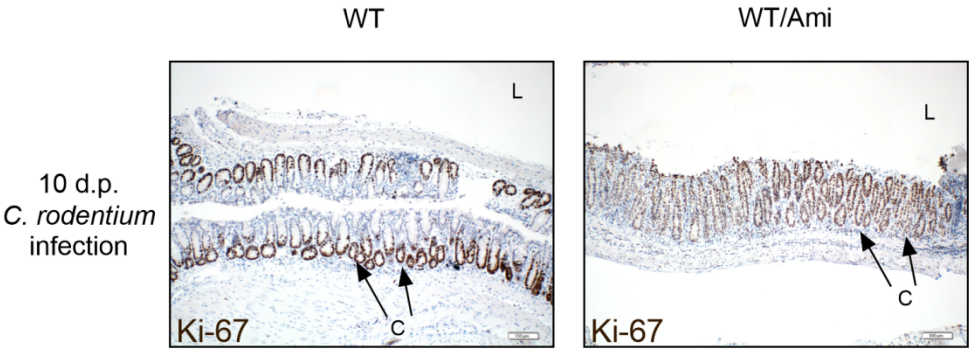

Figure 5.15: Amitriptyline pre-treatment enlarges transmissible murine crypt hyperplasia 10 dp *C. rodentium* infection.
C57BL/6 mice were either left untreated (WT) or pre-treated with 180 mg/l in drinking water two weeks prior to infection (WT/Ami). Mice were then orally gavaged 2-5 x 10^9 colony forming units (CFU) of *C. rodentium*. Colonic tissue was fixed in paraffin and stained for Ki-67 (Red bars indicate the crypt length. (L) lumen, (C) crypt. Length of scale bar is 50 µm).

To gain insights into the immune response against invading pathogens the cytokine profile in the colon of *C. rodentium* infected wildtype and amitriptyline treated mice was determined. Hence, macrophages, T_h1, T_h17 and T_{regs} related cytokines, e.g. IL-6, IL-17A, IL12p70, IFNγ, IL-10 and TNFα, were analysed (Figure 5.16). Interestingly, all cytokines were significantly stronger expressed in amitriptyline treated mice compared to untreated littermates 10 dp infection. Amitriptyline treatment alone was not affecting spleen weight, colon weight/length ratio and colon architecture. However, once amitriptyline treated mice were infected with *C. rodentium*, the pathology was much stronger compared to infected wildtype littermates.
In summary, all three mouse models suggest a strong involvement of Asm and Ac in *C. rodentium* induced colitis, which is indicated by the increased susceptibility of Asm and Ac deficient mice.

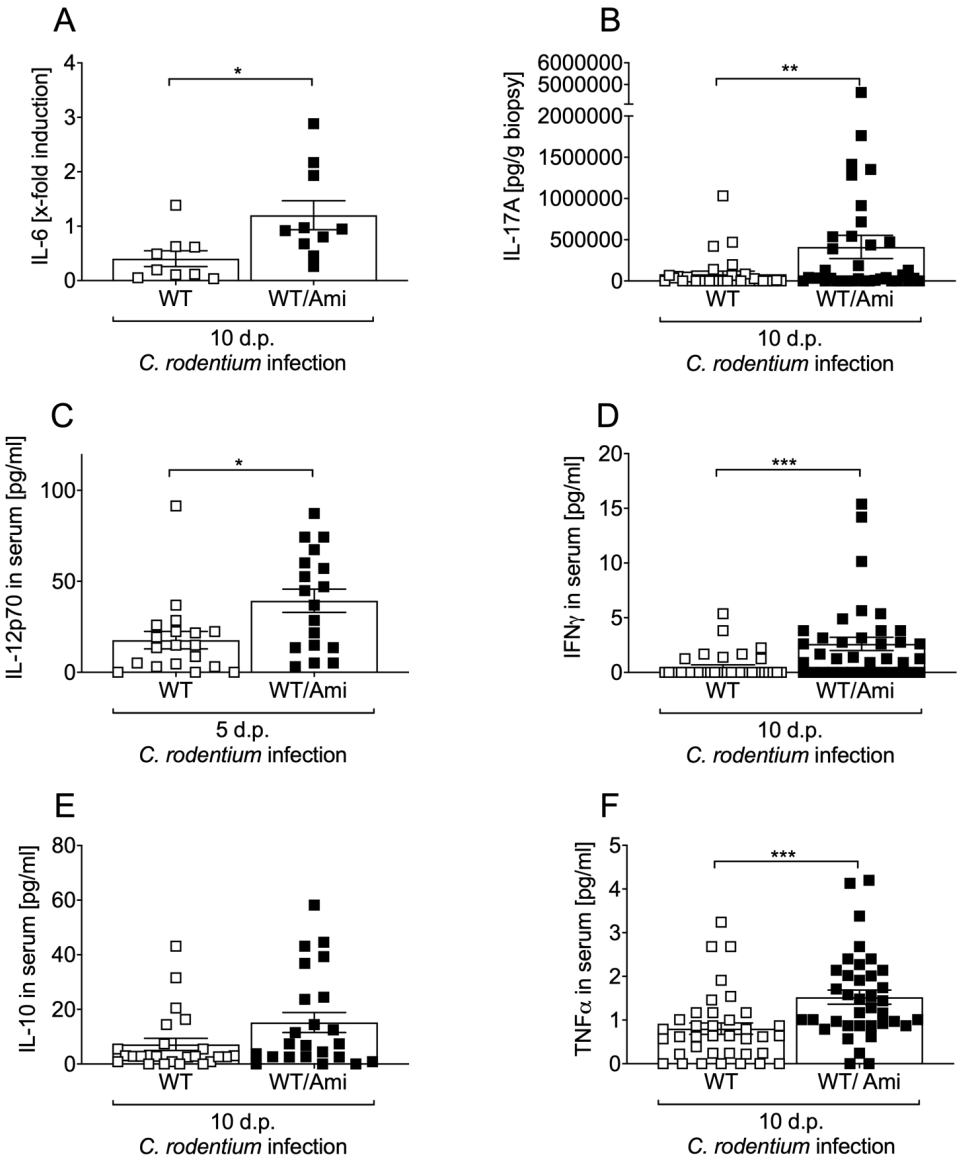

Figure 5.16: Asm and Ac inhibition increases the release of cytokines 10 days post *C. rodentium* infection.

(**A-F**) C57BL/6 mice were either left untreated (WT) or pre-treated with 180 mg/l amitriptyline in drinking water two weeks prior to infection (WT/Ami). Mice were then orally infected with 2-5 x 10^9 colony forming units (CFU) of *C. rodentium*. (**A**) Rectal colonic tissue was analysed using qPCR for the expression of the cytokine IL-6 in Asm WT and Asm KO mice 5/10 dp *C. rodentium* infection (n = 9-10, parametric t-test). (**B-F**) Concentration of the cytokines IL-17A, IL-12p70, IFNγ, IL-10 and TNFα in colonic tissue or serum of Asm WT and Asm KO mice 10 dp *C. rodentium* infection were measured using Luminex technologies (n = 18-37, non-parametric t-test). Data were first tested for their normal distribution using D'Agostino & Pearson omnibus normality test. Statistics were performed using the non-parametric Mann Whitney test or the parametric t-test. All data are presented as mean ± SEM (*, p<0.05; **, p<0.01; ***, p<0.001).

5.4 Impact of amitriptyline treatment on the innate immune system

Given the close contact of macrophages to the epithelial barrier, intestinal macrophages are part of the first line of defence in the intestinal structures, where they fulfil their role of protection against pathogens and foreign substances. Furthermore, macrophages participate in the tolerance to commensal bacteria and food antigens, and scavenging apoptotic and dead cells in the lamina propria [33]. Further, macrophages related cytokines, such as IL-6, IL-12p70 and TNFα were increased in the early and acute phase of *C. rodentium* infection (Figure 5.6, D and Figure 5.16, A, C, F). Hence, the effect of Asm and Ac deficiency on the innate immune system was analysed in the early and the acute phase of *C. rodentium* infection (5 and 10 dp infection).

5.4.1 Macrophages are not impaired after the loss of Asm and Ac during *C. rodentium* infection

As described above, macrophages are part of the first defence line, possessing the ability of phagocytosis and bactericidal killing. Hence, macrophages ($F4/80^+$, $CD11b^+$ and $MHCII^+$, see chapter 4.2.3) were investigated in the spleen, mesenteric lymph nodes (mLNs) and lamina propria (LP) of amitriptyline treated mice and untreated littermates in the early (5 dp infection) and acute phase (10 dp infection) of *C. rodentium* infection using flow cytometry.

Macrophages were gated as depicted in Figure 5.17, A. 5 dp *C. rodentium* infection increased frequencies of macrophages in the spleen, mLNs and LP were detected. First declines in mLNs, and constant levels in the spleen and the LP were observed 10 dp infection. However, no alterations of macrophages frequencies were detected in tissue of wildtype and amitriptyline treated littermates (Figure 5.17, B). In line to the first results, also the MHCII expression peaks 5 dp infection, while decreased levels of MHCII expression in spleens and mLNs and constant levels in the LP were detected 10 dp infection. As afore, no differences concerning MHCII expression on macrophages were detected in WT and WT/Ami mice (Figure 5.17, C).

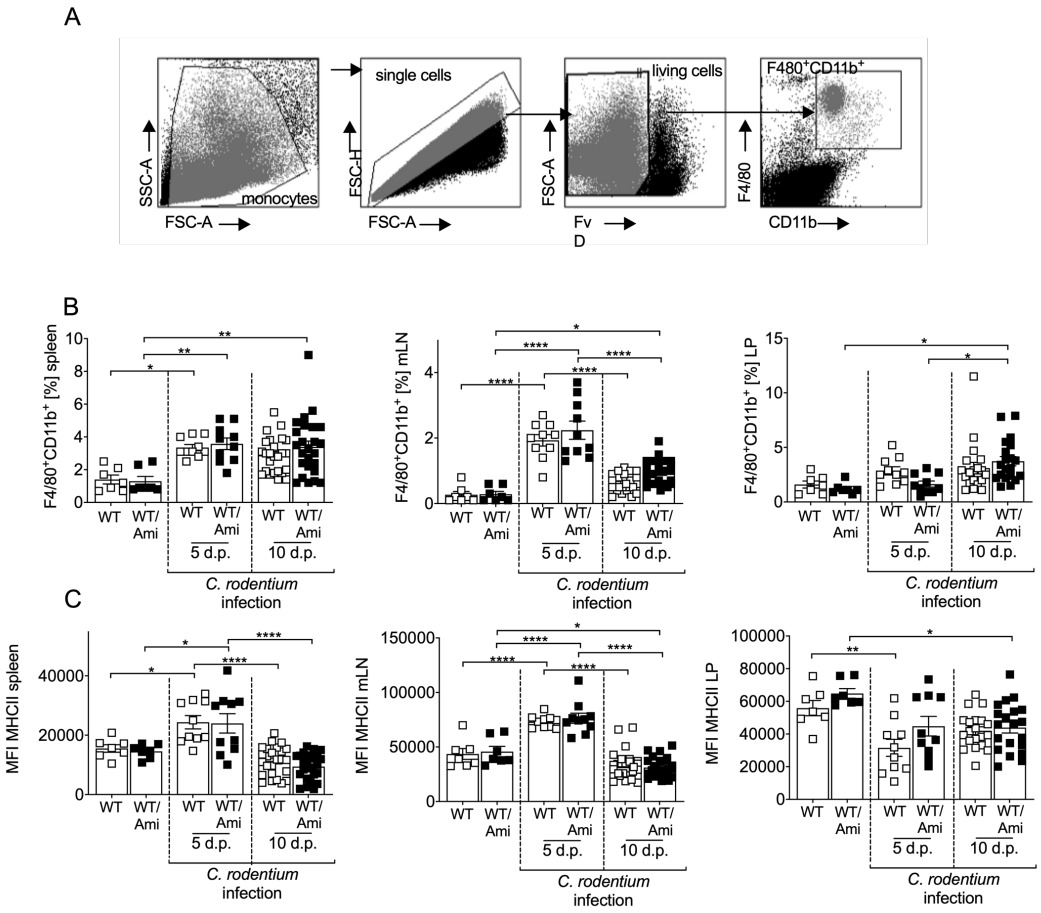

Figure 5.17: Invasion of macrophages into colonic tissue is not altered in amitriptyline pre-treated mice after *C. rodentium* challenge.
(**A-C**) C57BL/6 mice were either left untreated (WT) or pre-treated with 180 mg/l Amitriptyline in drinking water two weeks prior to infection (WT/Ami). Mice were then orally gavaged with PBS or 2-5 x 10^9 colony forming units (CFU) of *C. rodentium*. (**A**) Flow cytometry gating strategy of macrophages ($F4/80^+CD11b^+$) and mean fluorescence intensity (MFI) of MHCII. (**B**-**C**) Cells from the spleen, mesenteric lymph nodes (mLNs) and the lamina propria (LP) were isolated from uninfected WT and WT/Ami mice, 5 and 10 days post *C. rodentium* infection and stained for macrophages. Frequencies of macrophages from living cells are displayed (n = 7-25) (**B**) and MFI of MHCII of macrophages (n = 7-25) (**C**). Statistics were performed using the two-way ANOVA test with Tukey's multiple comparison test. All data are presented as mean ± SEM (*, p<0.05; **, p<0.01; ****, p <0.0001).

As frequencies of macrophages are not altered in mice after loss of Asm and Ac, next the phagocytosis capacity as well as the killing capacity of bone marrow derived macrophages (BMDMs) from Asm WT/KO or Ac WT/c KO mice were investigated. Therefore, phagocytosis capacity of BMDMs was analysed using GFP-fluorescence labelled *Escherichia (E.) coli* beads (GFP-labelled pHrodo™ Green *E. coli* BioParticles®) (Figure 5.18, A). Although increased intensity of GFP was detected over time, no differences between phagocytosis of the GFP labelled beads was detected in BMDMs differentiated from Asm WT and Asm KO or Ac WT and Ac cKO mice (Figure 5.18, B-C). To investigate the killing capacity, BMDMs were incubated with *C. rodentium* (MOI 1:10) for different time spans. Although increased CFU of

C. rodentium were detected over time, again loss of Asm or Ac did not significantly alter the killing capacity of BMDMs (Figure 5.18, D-E).

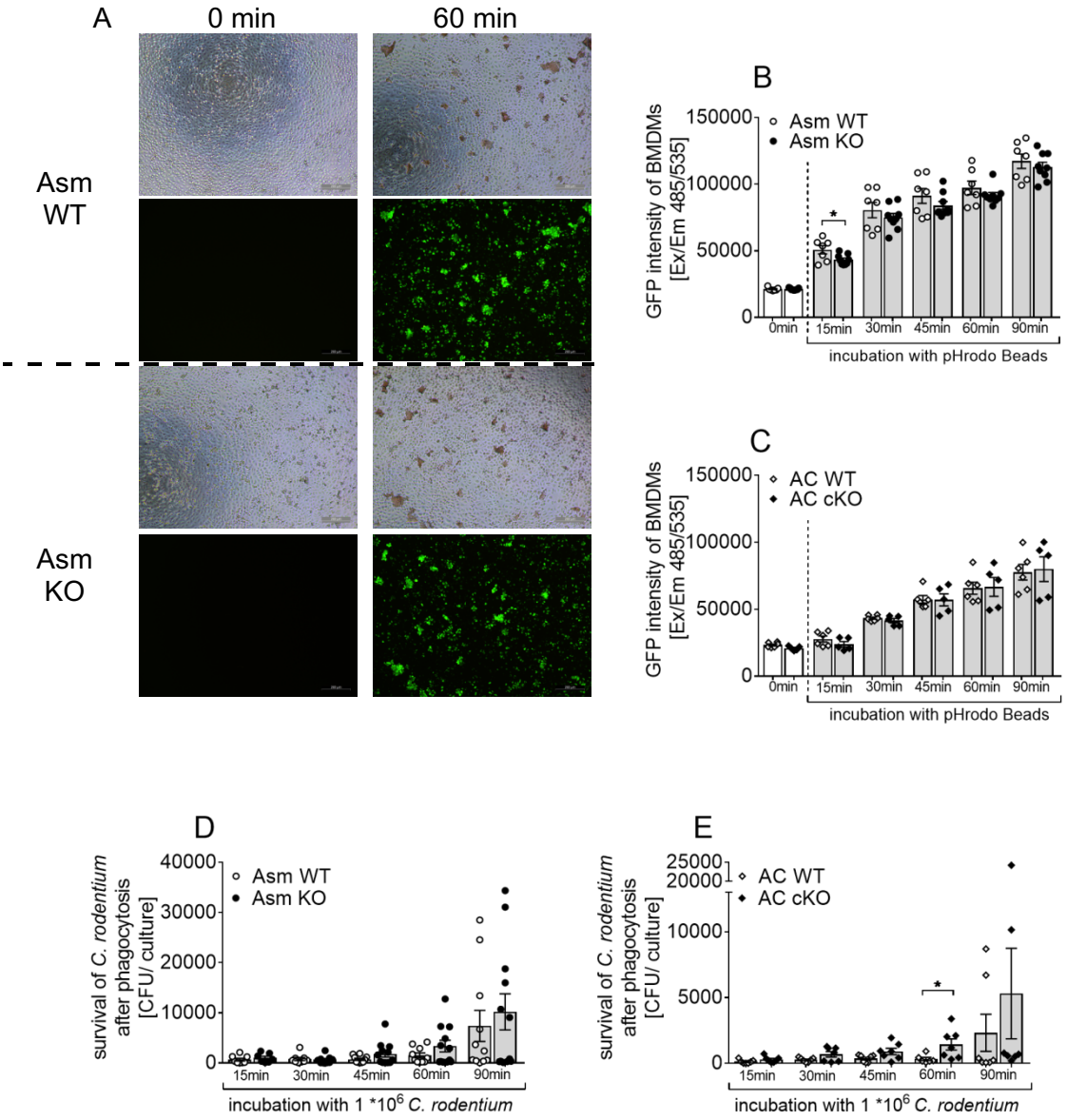

Figure 5.18: Phagocytosis and killing mechanism in bone marrow derived macrophages (BMDMs) is not altered after the loss of Asm or Ac.

(**A-E**) Bone marrow was isolated from Asm wildtype (Asm WT) and Asm knockout (Asm KO) and $Asah^{fl/fl}$ x $Cre^{+/+}$ (Ac WT) and $Asah^{fl/fl}$ x $Cre^{ki/ki}$ (Ac cKO) mice. For 6-7 days bone marrow was cultured under macrophages differentiation conditions to gain bone marrow derived macrophages (BMDMs). 1 x 10^5 BMDMs were plated per well. (**A-C**) 10 µg GFP-labelled pHrodo™ Green *E.* coli BioParticles® were added for indicated time spans to BMDMs. Uptake of GFP-labelled pHrodo™ Green *E.* coli BioParticles® was analysed at Ex/Em 485 nm/535 nm. (**A**) Representative picture of the density of BMDMs and the uptake of GFP-labelled pHrodo beads after 60 minutes of Asm WT and Asm KO mice. Uptake of pHrodo labelled beads by BMDMs from (**B**) Asm WT/KO (n = 7-9) and (**C**) Ac WT/cKO (n = 5-6) within 90 minutes. (**D-E**) Killing capacity of BMDMs isolated from Asm WT/KO (n = 8-12) and Ac WT/cKO (n = 6-7) was analysed by adding 1 x 10^6 colony forming units (CFU) of *C. rodentium* to 1 x 10^5 BMDMs for indicated time points. Colony forming units (CFU) of macrophages was determined in BMDMs. Data were first tested for their normal distribution using D'Agostino & Pearson omnibus normality test. Statistics were performed using the non-parametric Mann Whitney test or the parametric t-test. All data are presented as mean ± SEM (*, $p<0.05$)

5.4.2 The Toll-like-receptor 4 increases susceptibility to *C. rodentium* infection

Macrophages attracted to the site of *C. rodentium* infection are activated via the myeloid differentiation primary-response protein 88 (MyD88) and Toll-like receptor (TLR2 and TLR4) complex. Once *C. rodentium* successfully attached to the epithelial cells, the activation of transcription factors such as NFκB is activated via the MyD88/TLR2/4 complex. NFκB then regulates the release of cytokines and chemokines, such as IL-6, IFNγ, and TNFα which eventually leads to the recruitment of macrophages and neutrophils [114]. Interestingly, TLR4 was shown to act as a ceramide agonist [242]. Furthermore, expression of TLR4 is increased during *C. rodentium* infection in amitriptyline treated mice (Figure 5.19, A). Hence, the impact of the TLR4 receptor was investigated in more detail during *C. rodentium* and amitriptyline treatment.

Therefore, the TLR4 induced release of inflammatory cytokines is inhibited by the injection of the TLR4 inhibitor TAK242 [243]. TAK242 is a small-molecule selectively binding to the intercellular domain of TLR4, thereby interfering with the protein-protein interaction of TLR4 and its adaptor molecules [243].

In our experimental setting, TLR4 inhibitor TAK242 (inh.TLR4) was injected intravenously (i.v.) into mice every other day, starting with the day of *C. rodentium* challenge (Figure 5.19, B). To compare the effect of TLR4 inhibition, with or without amitriptyline, TAK242 was injected into two groups. The first group was left untreated, while the second group was treated with 180 mg/l drinking water 2 weeks prior to the *C. rodentium* infection. After 10 days of *C. rodentium* infection parameters were assessed.

As shown above, amitriptyline treatment increases susceptibility towards *C. rodentium* induced colitis, which is indicated by increased colon weight/length rations and inflammatory scores (Figure 5.19, D, F). However, further injection of the TLR4 inhibitor TAK242 of amitriptyline treated mice did not impair or rescue mice from stronger infection induced by *C. rodentium*. Indeed, comparable levels of spleen weight, colon weight/length ratio, crypt hyperplasia and inflammatory score were detected compared to infected amitriptyline treated mice without TAK242 injection (Figure 5.19, C-F). Intriguingly, inhibition of TLR4 via TAK242 injection in infected *C. rodentium* wildtype mice worsened the infection. While colon weight/length ratio and crypt hyperplasia were slightly increased, highly increased inflammatory score of colonic tissue were detected in wildtype mice in which the TLR4 was inhibited. Interestingly, spleen weight, colon weight/length ratio, crypt hyperplasia and inflammatory score of colonic tissue were comparable to results seen in amitriptyline treated mice (Figure 5.19, C-D).

Finally, inhibition of TLR4 increases susceptibility to *C. rodentium* infection. However, inhibition of TLR4 does not further enhance the impact of amitriptyline.

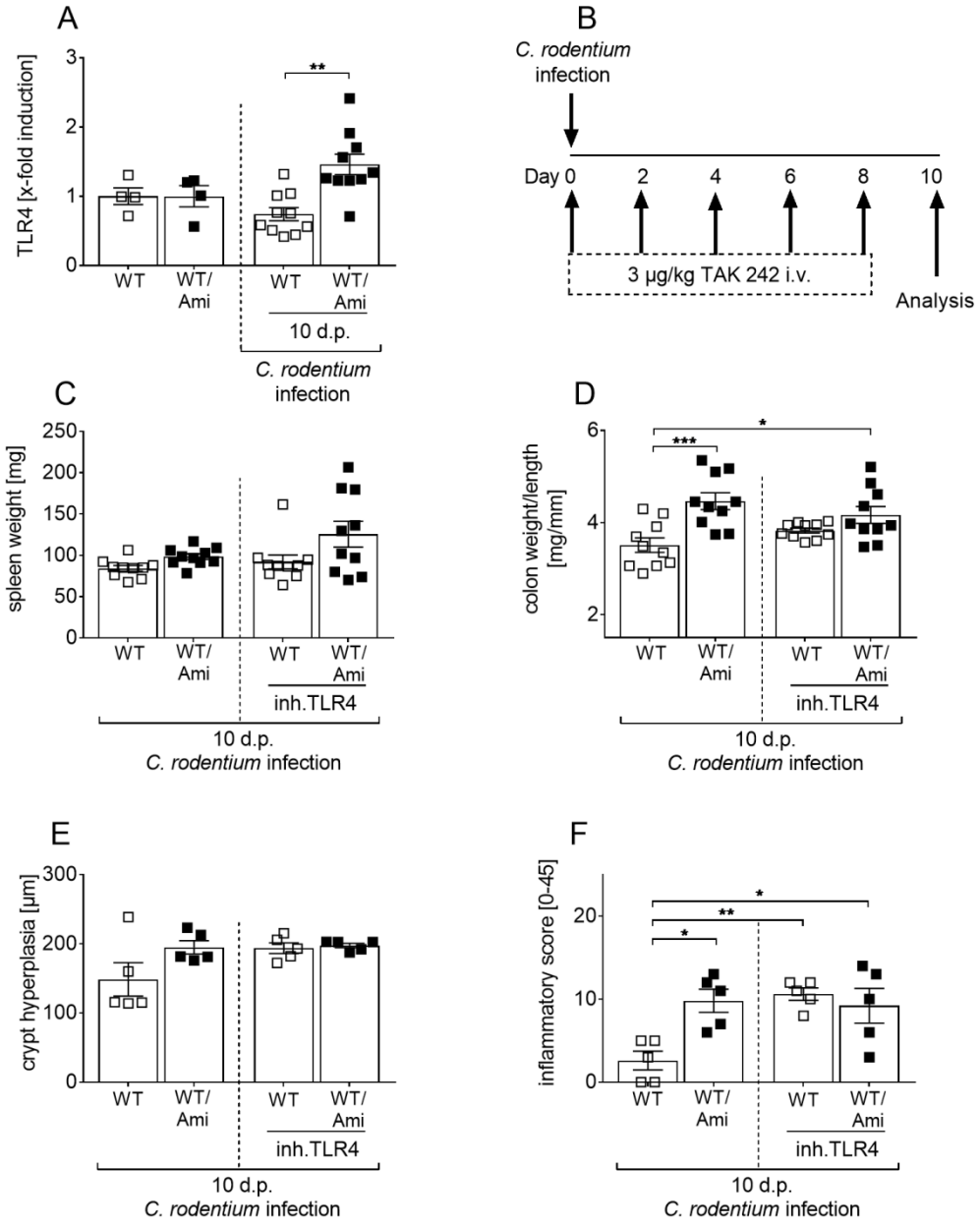

Figure 5.19: Inhibition of TLR4 in amitriptyline treated mice does not alter *C. rodentium* infection. (**A-F**) C57BL/6 mice were either left untreated (WT) or pre-treated with 180 mg/l amitriptyline in drinking water two weeks prior to infection (WT/Ami). Mice were then orally infected with 2-5 x 10^9 colony forming units (CFU) of *C. rodentium*. (**A**) Rectal colonic tissues were analysed using qPCR for the expression of the TLR4 in uninfected and infected WT or WT/Ami mice 10 dp infection (n = 4-10, two-way ANOVA). (**B**) Schematic experimental setup of Experiment. TAK242 (inh.TLR4) was injected intravenously (i.v.) every other day, starting with the day of *C. rodentium* challenge. Infection parameters, such as spleen weight (n= 10, non-parametric one-way ANOVA) (**C**), colon weight/length ratio (n= 10, parametric one-way ANOVA) (**D**), crypt hyperplasia (n = 5, non-parametric one-way ANOVA) (**E**) and inflammatory score of untreated mice or mice treated with amitriptyline and/or TAK242 i.v. injection 10 dp *C. rodentium* infection (n = 5, paramedic one-way ANOVA). Data were first tested for their normal distribution using D'Agostino & Pearson omnibus normality test. Statistics were performed using the non-parametric Kruskal-Wallis test with Dunn's multiple comparison test or the parametric one-way ANOVA test with Tukey's multiple comparison test. All data are presented as mean ± SEM (*, p<0.05; **, p<0.01; ***, p<0.001).

5.5 Impact of amitriptyline treatment on the adaptive immune system

The adaptive immune system in the gastrointestinal tract faces the unique challenge of tolerating commensal microbiota, and at the same time fight invading pathogens [49]. The mouse model used in this work induces strong T_h1 and T_h17 immune responses to fight and eliminate the non-invasive mouse pathogen *C. rodentium* [119, 124]. However, the regulating counterpart consisting of T_{regs} were also shown to be crucial to regulate the immune response [244]. Hence, the adaptive immune system was analysed in C57BL/6 mice and amitriptyline treated littermates in the early and acute phase (5 and 10 dp infection) of *C. rodentium* induced colitis.

5.5.1 The adaptive immune response is altered when Asm and Ac are inhibited during *C. rodentium* infection

T_h1 cells were shown to be crucial to effectively eliminate *C. rodentium* infection [119]. Our previous results already indicate an altered T_h1 immune response, as enhanced concentrations of T_h1 related cytokines, e.g. IL-12p70 and IFNγ, were detected in serum 10 dp infection in Asm KO or amitriptyline treated mice (Figure 5.6, B and Figure 5.16, C-D). Hence, $CD4^+$ T cells producing IFNγ (T_h1) were analysed in amitriptyline treated and untreated littermates in the early (5 dp infection) and acute (10 dp infection) phase of *C. rodentium* infection. Once mice were infected with C*. rodentium*, T_h1 cells were analysed according to Figure 5.20, A.

In the early phase of infection (5 dp infection) T_h1 cells were not altered in amitriptyline treated mice and untreated littermates. In the acute phase of infection (10 dp infection) however, increased invasion of T_h1 cells into colonic tissue was observed in wildtype and amitriptyline treated mice. Intriguingly, significantly enhanced frequency of T_h1 cells in amitriptyline treated mice compared to untreated wildtype littermates 10 dp infection were detected (Figure 5.20, B).

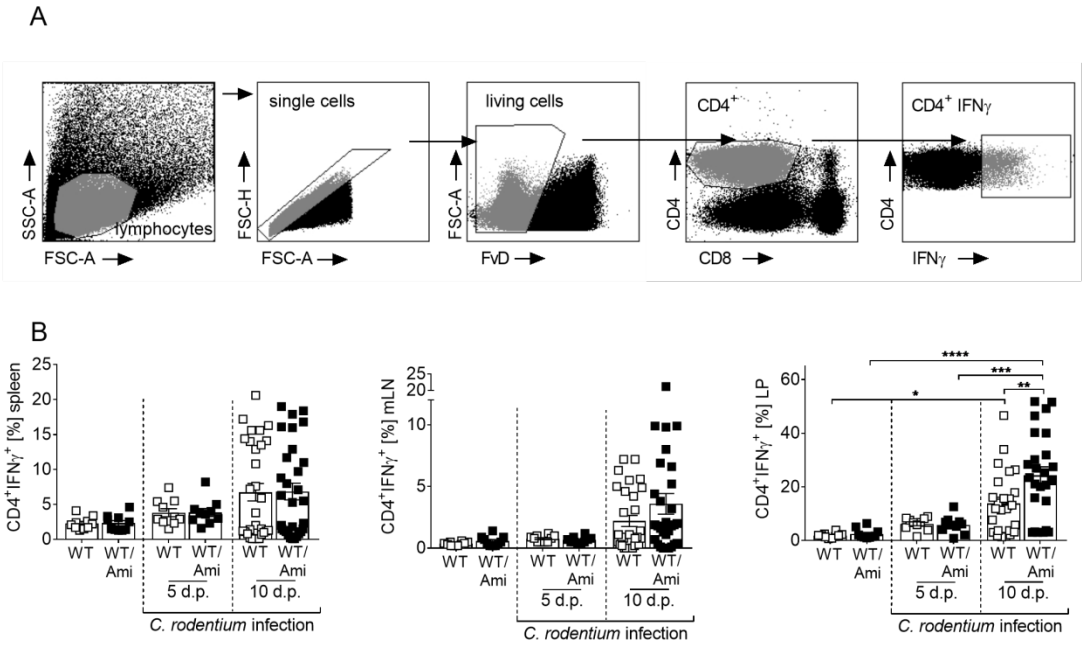

Figure 5.20: Increased invasion of T_h1 cells into colonic tissue in amitriptyline treated mice.
(**A-B**) C57BL/6 mice were either left untreated (WT) or pre-treated with 180 mg/l Amitriptyline in drinking water two weeks prior to infection (WT/Ami). Mice were then orally gavaged with PBS or 2-5 x 10^9 colony forming units (CFU) of *C. rodentium*. (**A**) Flow cytometry gating strategy of T_h1 cells ($CD4^+IFN\gamma^+$). (**B**) Single cells were isolated from spleen, mesenteric lymph nodes (mLNs) and lamina propria (LP) of uninfected WT or WT/Ami mice, or 5 and 10 days post *C. rodentium* infection, and stained for T_h1 cells. Frequencies of $CD4^+IFN\gamma^+$ cells from $CD4^+$ cells are displayed (n = 10-25). Statistics were performed using the two-way ANOVA test with Tukey's multiple comparison test. All data are presented as mean ± SEM (*, p<0.05; **, p<0.01; ***, p<0.001; ****, p <0.0001).

Not only T_h1 cells, but also T_h17 cells were shown to be crucial to fight and eliminate invading *C. rodentium*. Further, T_h17 cells are known to be strongly involved in the pathology during *C. rodentium* infection. Interestingly, increased T_h17 related cytokines were detected in Asm WT and Asm KO mice, as well as in amitriptyline treated mice 10 dp infection (Figure 5.16, A, B). Hence, $CD4^+$ IL-17 producing T cells (T_h17) were investigated in spleen, mLNs and LP of amitriptyline treated mice and untreated littermates in the early (5 dp infection) and acute phase (10 dp infection) of infection using flow cytometry.

After infecting mice with *C. rodentium* T_h17 cells were analysed with the gating strategy showed in Figure 5.21, A in the spleen, mLNs and LPs. Comparable frequencies of T_h17 cells were detected in uninfected mice treated with or without amitriptyline. In the early phase of *C. rodentium* infection (5 dp infection) the frequencies of T_h17 cells was neither increased compared to uninfected littermates nor altered in infected amitriptyline treated mice compared to infected littermates. However, in the acute phase of infection (10 dp infection) increased frequencies of T_h17 cells were detected

in the spleen, mLNs and the LP of mice treated with amitriptyline compared to untreated littermates (Figure 5.21, B).

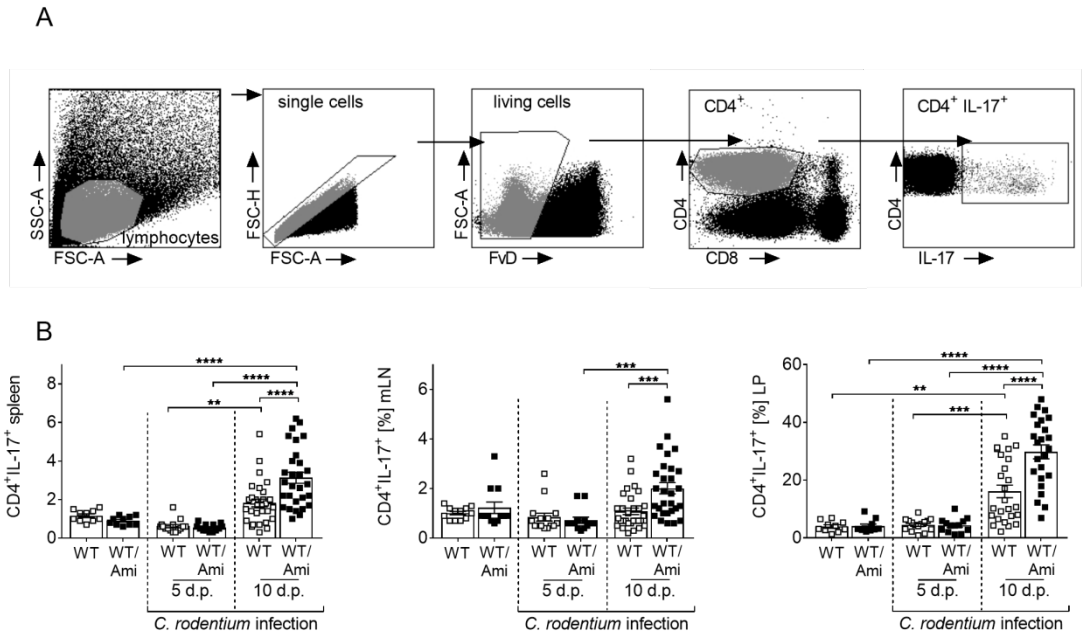

Figure 5.21: Increased invasion of T_h17 cells into colonic tissue in amitriptyline treated mice.
(**A-B**) C57BL/6 mice were either left untreated (WT) or pre-treated with 180 mg/l Amitriptyline in drinking water two weeks prior to infection (WT/Ami). Mice were then orally gavaged with PBS or 2-5 x 10^9 colony forming units (CFU) of *C. rodentium*. (**A**) Flow cytometry gating strategy of T_h17 cells ($CD4^+IL\text{-}17^+$) (**B**) Single cells were isoalted from spleen, mesenteric lymph nodes (mLNs) and lamina propria (LP) from uninfected WT or WT/Ami mice, 5 and 10 dp *C. rodentium* infection and stained for T_h17 cells. Frequencies of $CD4^+IL\text{-}17^+$ cells from $CD4^+$ cells are displayed (n = 10-25). Statistics were performed using the two-way ANOVA test with Tukey's multiple comparison test. All data are presented as mean ± SEM (**, p<0.01; ***, p<0.001; ****, <0.0001).

Under homeostatic conditions T_h1 and T_h17 responses are counter regulated by T_{regs} to balance the immune system. Interestingly, it was shown, that deficiency of T_{regs} enhances susceptibility to *C. rodentium* infection [244]. Furthermore, Asm deficiency affects the frequency of T_{regs} [245]. Thus, T_{regs} were analysed in amitriptyline treated and untreated littermates in the acute (10 dp infection) phase of *C. rodentium* infection (Figure 5.22, A).

Frequencies of T_{reg} cells were slightly enhanced in infected mice 10 dp *C. rodentium* infection in spleen and mLNs of mice treated with or without amitriptyline. However no differences were detected in spleen and mLNs in untreated mice compared to amitriptyline treated mice. Strikingly, among cells isolated from the LP decreased percentage of T_{reg} cells were found in amitriptyline treated mice (WT/Ami) compared to untreated littermates (WT) 10 dp *C. rodentium* infection (Figure 5.22, B).

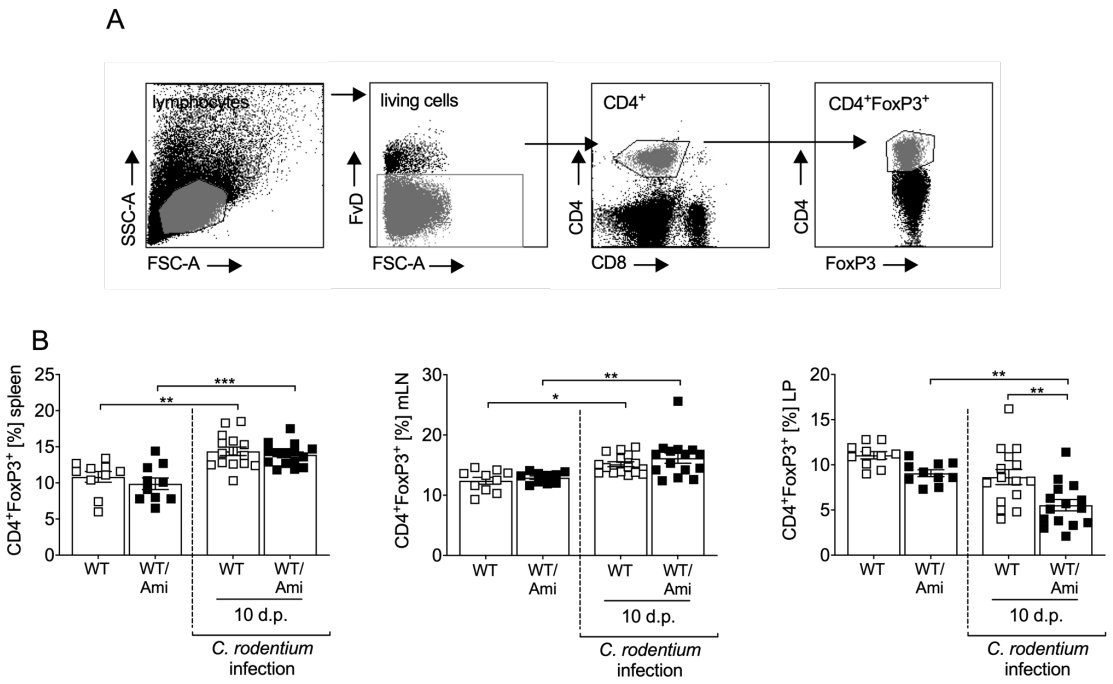

Figure 5.22: Decreased invasion of T_{reg} cells into colonic tissue in amitriptyline treated mice.
(**A-B**) C57BL/6 mice were either left untreated (WT) or pre-treated with 180 mg/l Amitriptyline in drinking water two weeks prior to infection (WT/Ami). Mice were then orally gavaged with PBS or 2-5 x 10^9 colony forming units (CFU) of *C. rodentium*. (**A**) Flow cytometry gating strategy of T_{reg} cells ($CD4^+FoxP3^+$). (**B**) Single cells were isolated from spleen , mesenteric lymph nodes (mLNs) , and lamina propria (LP) from uninfected WT or WT/Ami mice, and 10 dp *C. rodentium* infection and stained for T_{reg} cells. Frequencies of $CD4^+FoxP3^+$ cells of $CD4^+$ cells are displayed (n = 10-15). Statistics were performed using the two-way ANOVA test with Tukey's multiple comparison test. All data are presented as mean ± SEM (*, $p<0.05$; **, $p<0.01$; ***, $p<0.001$).

Inhibition of Asm and Ac enlarged the frequency of T_h1 and T_h17 in the lamina propria in mice 10 dp *C. rodentium* infection compared to wildtype littermates. To investigate if this increase is due to an altered differentiation capacity or due to a higher bacterial burden (Figure 5.5, Figure 5.10 and Figure 5.14), the differentiation capacity of splenic $CD4^+$ $CD25^-$ cells into T_h1 and T_h17 was analysed. Hence, splenic $CD4^+$ $CD25^-$ cells from Asm WT and Asm KO mice were isolated and cultured in T_h0, T_h1 and T_h17 differentiation media and analysed regarding the production of IFNγ ($CD4^+IFN\gamma^+$) or IL-17 ($CD4^+$IL-17^+).

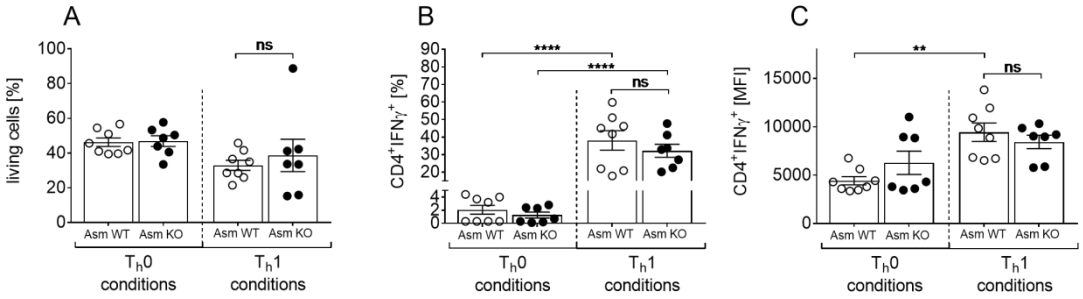

Figure 5.23: Differentiation capacity of T_h1 cells is not altered after the loss of Asm.
(**A-C**) Splenic $CD4^+$ $CD25^-$ cells were isolated from Asm wildtype (Asm WT) and Asm knockout (Asm KO) mice and cultured for 6 days in T_h0 or T_h1 differentiation medium. Harvested cells were then stained for CD4 and IFNγ. (**A**) Frequencies of living cells in Asm WT and Asm KO under T_h0 or T_h1 differentiating conditions (n = 7-8). (**B, C**) Frequencies and mean fluorescence intensity (MFI) of $CD4^+$ $IFN\gamma^+$ cells in Asm WT and Asm KO under T_h0 or T_h1 differentiating conditions (n = 7-8). Graphs show pooled data from 3 independent experiments. Statistics were performed using the two-way ANOVA test with Tukey's multiple comparison test. All data are presented as mean ± SEM (ns, not significant; **, p<0.01; ***, p <0.001).

The percentage of living cells was not altered (Figure 5.23, A) after loss of Asm. In addition, no differences of $CD4^+IFN\gamma^+$ were detected in splenic cells isolated from Asm WT and Asm KO mice (Figure 5.23, B-C). Same results were detected for $CD4^+IL\text{-}17^+$ since no differences of $CD4^+IL\text{-}17^+$ were identified in splenic cells isolated from Asm WT and Asm KO (Figure 5.24).

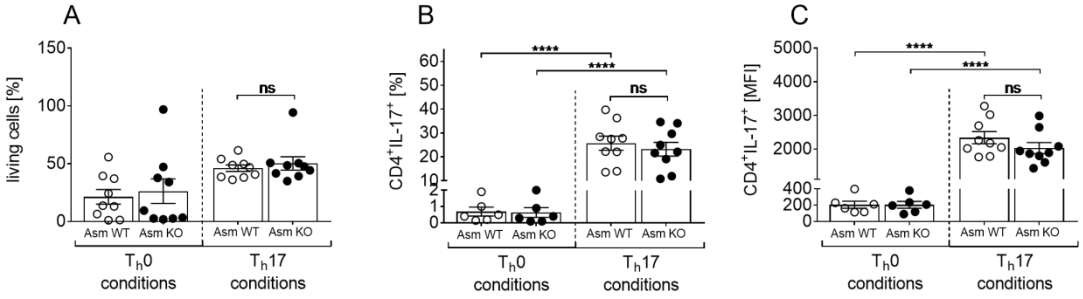

Figure 5.24: Differentiation capacity of T_h17 cells is not altered after loss of Asm.
(**A-C**) Splenic $CD4^+$ $CD25^-$ cells were isolated from Asm wildtype (Asm WT) and Asm knockout (Asm KO) mice and cultured for 6 days in T_h0 or T_h17 differentiation medium. Harvested cells were then stained for CD4 and IL-17. (**A**) Frequencies of living cells in Asm WT and Asm KO under T_h0 or T_h17 differentiating conditions (n = 9). (**B, C**) Frequencies and mean fluorescence intensity (MFI) of $CD4^+$ $IL\text{-}17^+$ cells in Asm WT and Asm KO under T_h0 or T_h17 differentiating conditions (n = 6-9). Graphs show pooled data from 4 independent experiments. Statistics were performed using the two-way ANOVA test with Tukey's multiple comparison test. All data are presented as mean ± SEM (ns, not significant; **, p<0.01; ****, p <0.0001).

In summary, Asm and Ac are protective in the bacterial induced colitis model using *C. rodentium*. Interestingly, neither the barrier function was impaired in the early or acute phase of infection nor macrophages frequencies and antigen presentation, phagocytosis or killing was altered after loss of Asm and/or Ac. Interestingly, increased frequencies of T_h1 and T_h17 were detected, while decreased frequencies of T_{regs} were found in mice lacking Asm and Ac, albeit differentiation capacity was not affected by the loss of Asm.

Discussion

The gastrointestinal tract is the largest mucosal surface in the human body, fulfilling the pivotal role of nutrition and water absorption. Pathogens preferentially invade the host through the gastrointestinal tract forcing it to distinguish between harmless and beneficial bacteria. The gastrointestinal tract adapted to these unique circumstances by limiting direct bacterial contact to the epithelial cell surface, rapid detection and killing of invading bacteria, and minimizing the exposure of commensal bacteria to the immune system [3]. Misbalance of this sensitive and uniquely balanced system can lead to chronic inflammation, resulting in inflammatory bowel disease (IBD), such as Crohn's disease and ulcerative colitis [246]. Among other factors, the composition and misbalance of the gut microbiota is crucially involved in the development of IBD. The mouse pathogen *Citrobacter (C.) rodentium* was used in this study to investigate the effect of misbalanced bacteria [103-105].

Increasing evidence implicates a function of the sphingolipid metabolism in intestinal diseases such as IBD [247-251]. Sphingolipids are essential plasma membrane components of eukaryotic cells and important bioactive cell signalling molecules, which are known to be involved in many diseases [252]. For example, sphingolipids, such as ceramide and sphingomyelin, were repeatedly discussed to be involved in the maintenance of the intestinal integrity [227, 247].

For the first time, we showed that sphingomyelin and ceramide concentrations decrease during the bacterial induced colitis using *C. rodentium* infection (Figure 5.1, A-B). Both, sphingomyelin and ceramide concentration are strongly related to their degrading enzymes, namely acid sphingomyelin (Asm) and acid ceramidase (Ac). Asm is known to degrade sphingomyelin into ceramide, whereas Ac degrades ceramide into sphingosine (Sph) (details see Figure 3.6). Interestingly, Asm activity was decreased during *C. rodentium* infection (Figure 5.1, C), albeit Ac activity was only slightly increased during *C. rodentium* infection. However, the role of Asm and Ac during *C. rodentium* induced colitis is still largely unknown. Hence, in this work the role of these two enzymes was studied during bacterial induced colitis.

To investigate the role of sphingomyelin and ceramide in bacterial colitis, acid sphingomyelin and acid ceramidase were inhibited via systemic (Asm) or conditional knockout (Ac). On the one hand accumulation of sphingomyelin (Figure 5.2, B-C), on the other hand accumulation of ceramide (Figure 5.7, B-C) is achieved in colonic tissue [229]. In a third model, sphingomyelin and ceramide accumulation was induced in colonic tissue using the antidepressant agent amitriptyline (Figure 5.11) [146]. Although the three mouse models target the degrading enzymes differently, mice lacking Asm and/or Ac suffer rigorous from *C. rodentium* induced colitis compared to infected wildtype littermates (Figure 5.3, Figure 5.8 and Figure 5.12).

As mentioned above, the sphingolipid metabolism is noted to be relevant for the development of IBD. However, the role of sphingolipids in this disease is controversially discussed. In some studies ceramide, one of the main sphingolipids, was shown to play a harmful role, while others stated a beneficially role of ceramide in IBD. Indeed, the accumulation of ceramide in intestinal epithelial cells via IL-1 activation *in vitro* was shown to increase the inflammatory response by enhancing survival of intestinal epithelial cells via activation of cyclooxycenase-2 (COX-2) and NFκB [253]. The activation of COX-2 and NFκB eventually results in reduced pro-apoptotic protein expression and increased levels of anti-apoptotic molecules [254].

Furthermore, exogenous sphingomyelinase (SMase) treatment of a colon cancer cell line results in elevation of the matrix metalloproteinase- (MMP) 1 and MMP-10. MMP-1 was shown to damage the colonic mucosa by degrading the extracellular matrix [255]. Moreover, dietary sphingomyelin was shown to be harmful as it augments weight loss, intestinal mucosal inflammation and epithelial damage caused by DSS. The dietary sphingomyelin accumulates ceramide concentrations, which then results in higher cathepsin D activity and intestinal epithelial apoptosis [225].

On the contrary, dietary sphingomyelin was also discussed to have a beneficial effect in IBD. In fact, Furaya *et al.* showed that dietary sphingomyelin reduces inflammation in mice exposed to DSS [256]. Moreover, deficiency of ceramide synthase 2, hydrolysing sphingosine-1 into ceramide, aggravates DSS induced colitis [227]. Furthermore, rectal application of alkaline SMase alleviates DSS induced inflammation and preserves the colonic epithelium [257]. Chen *et al.* demonstrated that mice lacking alkaline SMase suffer stronger from the azoxymethane plus DSS treatment, indicated by higher colon tumour incidence and more aggressive cancer [258]. Recently, pharmacological inhibition of Asm activity using desipramine was shown to ameliorate disease activity index and cytokine release in mice exposed to DSS [259].

Clearly, alteration of the sphingolipid metabolism alleviates DSS induced colitis, which stands in contrast to our results. This study shows a harmful role of ceramide and sphingomyelin in bacterial induced colitis. Intriguingly, deficiency of Asm and/or Ac augments weight loss and systemic distribution of *C. rodentium* in mice (Figure 5.2, Figure 5.5, Figure 5.8, Figure 5.10, Figure 5.12 and Figure 5.14).

Interestingly, the increased systemically distribution of the normally non-invasive bacteria points towards an impaired barrier function. In fact, sphingolipids were shown to effectively weaken the epithelial barrier integrity [247]. Oertel *et al.* revealed that exposure of ceramide synthase 2 deficient mice to DSS disrupts the epithelial barrier integrity stronger due to loss of the tight junction protein zonula-1 (ZO-1) [227]. In contrast to our finding, in which tight junction proteins, such as ZO-1, ZO-2, claudin or

occludin (Figure 5.5, Figure 5.10 and Figure 5.14) were not impaired in the early or acute phase of infection. However, the initial phase of infection using *C. rodentium* induced colitis was not investigated and may reveal an involvement on the epithelial barrier during the development of *C. rodentium* induced colitis. Indeed, exogenous sphingomyelin was shown to enhance the permeability of the human intestinal epithelial cell line Caco-2 within 4 hours *in vitro*, indicating an effect of sphingolipids on the permeability [260].

Once *C. rodentium* attached to the epithelium, it subsequently induces the MyD88/TLR2 and TLR4 signalling, followed by the activation of the transcription factor NFκB [114, 115]. The activation of NFκB then regulates the release of cytokines and chemokines such as IL-6, IFNγ, and TNFα, which eventually leads to the recruitment of macrophages and neutrophils to the site of infection [114]. Interestingly, Fischer *et al.* claimed a role of ceramide as an agonist of TLR4 [242]. In fact, aggravated infection parameters were detected once the TLR4 receptor is blocked via the inhibitor TAK242 (Figure 5.19, D and F) [243]. However, additional injection of the TLR4 inhibitor in mice in which the sphingolipid composition is altered does not impair infection parameters (Figure 5.19, C-F). Although inhibition of TLR4 increases susceptibility of mice towards *C. rodentium* infection, we could not definitely declare a role of the MYD88/TLR4 complex in the context of Asm and Ac. Yet, TLR4 is not exclusively expressed on the epithelial, but also on macrophages to initiate cytokine release. Hence, we cannot rule out that the MYD88/TLR4 complex is somehow altered on macrophages, thereby altering the innate immune system.

Following the attachment and invasion of *C. rodentium* bacteria into the lamina propria (LP) the immune response is activated [119, 120]. As the first line of defence, macrophages infiltrate the site of infection, where harmful materials are phagocytosed, killed and finally presented to cells from the adaptive immune system to activate the adaptive immune response [261]. In fact, during bacterial induced colitis infiltration of macrophages into colonic tissue (LP) started in the early phase of infection, albeit the absence of Asm and Ac did not impair the infiltration of macrophages into colonic tissue (Figure 5.17, B). Sphingolipids were also discussed to have an impact on macrophages. Via the inhibition of the SMase using SMA-7 DSS induced colitis was ameliorated. The group found decreased levels of TNFα, IL-1β and IL-6, reduced ceramide levels in macrophages and NFκB stimulation caused by LPS [262]. In contrast to our data, in which elevated expression of IL-6 in colonic tissue and enhanced levels of TNFα in serum were detected in mice lacking Asm and/or Ac (Figure 5.16, A, F), which was accompanied by increased inflammation parameters in mice lacking Asm and/or Ac.

Phagocytosis is an essential innate immune system mechanism to clear pathogens. Intriguingly, an intact sphingolipid metabolism is needed in order to effectively phagocytose bacteria, such as *Candida albicans* and *Cryptococcus neoformans* [263, 264]. Nonetheless, phagocytosis of pHrodo™ Green *E.* coli BioParticles® Conjugates (pHrodo beads) was unaltered after the loss of Asm or Ac in bone marrow derived macrophages (Figure 5.18, B-C). Although phagocytosis of pHrodo beads is not impaired, we cannot exclude, that phagocytosis of *C. rodentium* bacteria is modified after the loss of Asm or Ac. Furthermore, not only macrophages but also neutrophils are part of the first line of defence against invading pathogens, with the ability to phagocytose [265]. Interestingly, the phagocytic ability of neutrophils was shown to be regulated by ceramide [266]. Hence, we cannot rule out a dysfunctional phagocytic ability of neutrophils leading to an altered elimination of invading bacteria.

After pathogens are phagocytosed and stored in phagosomes of macrophages or neutrophils, pathogens are killed, followed by presentation of fragments to the cells of the adaptive immune system [261]. Interestingly, killing ability of *Cryptococcus neoformans* was impaired after inhibition of the sphingomyelin synthase in neutrophils [267]. Furthermore, McCollister *et al.* showed that lack of Asm activity enhances the intracellular survival of an isogenic *Salmonella* strain [268]. Yet, no such impact on the killing ability of Asm was detected in our results, in which the killing ability was alike in macrophages isolated from bone marrow with or without Asm or Ac (Figure 5.18, D-E). As stated afore, we cannot exclude neutrophils to be essentially affected in their killing ability by the loss of Asm or Ac.

Alongside an impact of the sphingolipid metabolism on bacterial phagocytosis and killing ability, also the antigen presentation of monocytes was shown to be altered in patients with the lipid storage disorder Gaucher diseases. Intriguingly, MHCII was shown to be fundamental impaired in patients suffering from the lysosomal storage disorder, thereby initiating an imbalance of the T cell subsets [269]. During bacterial induced colitis, MHCII expression on macrophages peaks in spleen and mesenteric lymph nodes in the early phase of infection, while antigen presentation via MHCII presented at constant levels in colonic tissue. However, alteration of the sphingolipid metabolism via amitriptyline did not impair antigen presentation via MHCII (Figure 5.17, C). Yet, not only antigen presentation of macrophages is known to be crucial to effectively activate cells from the adaptive immune system but also DCs are known to be an essential link between the innate and adaptive immune system [37, 38]. Eventually, although the first glance on DCs did not reveal changes, we cannot absolutely exclude an effect of sphingolipids on the antigen presentation of DCs during bacterial induced colitis.

MHCII restricted antigen presentation during *C. rodentium* infection induces the activation and differentiation of naïve $CD4^+$ T cells into specific T_h cell subsets, including T_h1 and T_h17 cells. T_h1 and T_h17 cells are indispensable to effectively clear *C. rodentium* infection [119, 121]. Indeed, T_h1 and T_h17 cells infiltrate into colonic tissue (Figure 5.20, B and Figure 5.21, B) in the acute phase of *C. rodentium* infection. Conspicuously, enhanced T_h1 and T_h17 cell infiltration into colonic tissue was detected in the absence of Asm and Ac. The sphingolipid metabolism has been repeatedly reported to be involved in $CD4^+$ T cell activation and also in the modulation of the T cell receptor (TCR) signalling via TNF [270]. Moreover, the activation of $CD4^+$ T cells is crucially related to Asm activity and ceramide production, as pharmacological inhibition of Asm abrogates CD3/CD28 signal cascade, followed by dampened $CD4^+$ T cell activation and proliferation [271]. Furthermore, Bai *et al.* demonstrated that pharmacological inhibition or knockdown of Asm blocks STAT3 signals. This blockage then limits IL-17 production of $CD4^+$ T cells in blood and lamina propria mononuclear lymphocytes isolated from intestinal tissue [272]. Moreover, Asm and ceramide were also reported to affect the differentiation into T cell subsets. Bai *et al.* showed that the pharmacological inhibition of Asm activity using imipramine dampens T_h1 cells differentiation under T_h1 differentiation conditions [271]. Furthermore, isolated $CD4^+$ T cells from the lamina propria of Crohn's disease patients treated with the pharmacological inhibitor imipramine results in decreased T_h17 cells once stimulated in T_h17 differentiation media [272]. Yet, no such impact on the differentiation capacity into T_h1 and T_h17 cell were detected in our experiments (Figure 5.23, B-C and Figure 5.24 B-C). Nevertheless, Asm was not blocked using a pharmacological inhibitor, but via the genetically knockout. Hence, we cannot exclude a pivotal impact of the pharmacological inhibition on Ac, which then can influence the differentiation capacity of $CD4^+$ T cells into T_h1 and T_h17 cells.

In order to regulate the T_h1 and T_h17 driven immune response and to protect against severe pathology, the regulatory T cells (T_{regs}), the counterpart of T_h1 and T_h17 cells, are important. T_{regs} were shown to be essential for regulating immune responses against *C. rodentium* infection [244]. In order to dampen excessive immune responses, T_{regs} are attracted to the site of infection, and release the immunosuppressive interleukin 10 (IL-10) to maintain immune responses [56]. Indeed, elevated levels of IL-10 were detected in serum of *C. rodentium* infected mice in which the sphingolipid metabolism is altered using amitriptyline (Figure 5.6, B and Figure 5.16 E). However, in spleen and mesenteric lymph nodes comparable percentages of T_{regs} were detected, albeit T_{reg} frequencies were decreased in the lamina propria in the acute phase of

infection in mice treated with the pharmacological inhibitor amitriptyline to alter the sphingolipid metabolism (Figure 5.22, B).

Interestingly, the role of T_{regs} was studied in the T_h1 mediated colitis model using Trinitrobenzenesulfonic acid (TNBS). By alteration of the S1P content and migration of lymphocytes using FTY720 [273] colitis symptoms were ameliorated. At the same time, reduced T_h1 related cytokines and upregulated FoxP3 and IL-10 expression were detected, clearly pointing towards a direct effect of sphingolipids on T_{reg} activation [274]. Furthermore, Asm has been noted to be a negative regulator of T_{reg} development, indicated by increased numbers of systemic T_{regs} in Asm deficient mice [275]. No such elevation of systemic T_{regs} were detected in our study, in which comparable frequencies of T_{regs} were found in uninfected amitriptyline treated mice compared to uninfected littermates (Figure 5.22, B). Besides the genetic impact of Asm on T_{regs} also pharmacological inhibition of Asm influences T_{regs} significantly. Certainly, Schneider-Schaulies *et al.* showed enhanced systemic T_{regs} in amitriptyline treated mice. In fact, pharmacological inhibition of Asm in tissue culture of murine or human T cells, as well as in mice induces higher frequencies of T_{reg} cells within a few days [245, 276]. Intriguingly, amitriptyline treatment does not boost T_{regs} development in our study (Figure 5.22, B). However, Schneider-Schaulies *et al.* applied amitriptyline intraperitoneal (i.p.), while we choose the oral route via drinking water. Hence, we cannot eliminate the different systemic distribution of amitriptyline and therefore, the different impact of amitriptyline on the differentiation of T_{regs}.

Intriguingly, the application of the pharmacological inhibitor (e.g. amitriptyline) of Asm and Ac seems to essentially shape the inhibitory ability if applied orally or systemically. Indeed, first results point to an altered effect when amitriptyline is applied systemically during *C. rodentium* induced colitis. Certainly, the difference of systemically or orally applied amitriptyline during the bacterial induced colitis needs to be further elucidated.

Interestingly, sphingolipids were not only reported to impact the innate immune response initiated by bacterial infection but also to strongly shape bacterial infections. Indeed, the acid sphingomyelinase/ceramide system was shown to highly impact the bactericidal ability of mice challenged with pathogens such as *Pseudomonas aeruginosa*, *Listeria monocytogenes, Neisseria ssp.* and *Staphylococcus aureus* [215, 277-279]. In fact, Asm is required for a successful infection with *Neisseria gonorrhoeae* and *Neisseria meningitides*, as the acid sphingomyelinase/ceramide system severely contributes to the internalization of the bacteria [280-282]. Furthermore, Asm deficient mice are highly susceptible to *Pseudomonas aeruginosa, Listeria monocytogenes* and *Staphylococcus* infection, due to altered internalization and dysfunctional macrophage

phagocytosis and killing [277, 279, 283]. Conspicuously, bacterial internalization and bactericidal ability is strongly influenced by sphingolipids.

The gastrointestinal tract is colonized by approximately 10^{14} bacteria with at least 1000 distinct bacteria species, such as Bacteroidetes phylum and Chlorobi phylum [7, 8, 284]. Heaver *et al.* stated the group of Bacteroidetes to be one of the few bacteria to produce sphingolipids independently. The group found members of the Bacteroidetes to produce sphingophospholipids, glycosphingolipids and dihydroceramides autonomously [284]. Additional, overabundant levels of ceramide and sphingomyelin in faeces samples of patients suffering from ulcerative colitis or Crohn's disease were recently found [285]. Conspicuously, alkaline sphingomyelinase was shown to be reduced in patients suffering from colorectal adenocarcinoma [286]. The alkaline sphingomyelinase hydrolyses sphingomyelin with an alkaline pH optimum into ceramide, which subsequently induces apoptosis in the epithelium [287, 288]. Yet, probiotic therapy of patients restored alkaline sphingomyelinase levels, accompanied by ameliorated ulcerative colitis disease activity index [289]. These studies indicate that the gut microbiota may be shaped essentially by the sphingolipid metabolism.

In our study, the inhibitor for Asm and Ac was given via the oral instead of the systemic route. Hence, the inhibition of Asm and Ac may alter the microbiota composition, thereby impairs the healthy gut microbiota and alleviate colonisation of the colon by *C. rodentium.*

In summary, giving the findings of this study, both, Asm as well as Ac, show a protective function during the bacterial induced colitis using the gram negative bacteria *C. rodentium*. Clearly, absence of Asm and Ac shapes the adaptive immune response to a more aggressive and misbalanced immune response. Further studies may reveal an opportunity of a potential therapeutic target in the sphingolipid metabolism to alleviate IBD symptoms.

References

1. Gallo RL, Hooper LV. Epithelial antimicrobial defence of the skin and intestine. Nature reviews Immunology. 2012;12(7):503-16.
2. Peterson LW, Artis D. Intestinal epithelial cells: regulators of barrier function and immune homeostasis. Nature reviews Immunology. 2014;14(3):141-53.
3. Shale M, Schiering C, Powrie F. CD4(+) T-cell subsets in intestinal inflammation. Immunological reviews. 2013;252(1):164-82.
4. Hooper LV, Macpherson AJ. Immune adaptations that maintain homeostasis with the intestinal microbiota. Nature reviews Immunology. 2010;10(3):159-69.
5. Johansson ME, Hansson GC. Mucus and the goblet cell. Digestive diseases (Basel, Switzerland). 2013;31(3-4):305-9.
6. Johansson ME, Phillipson M, Petersson J, Velcich A, Holm L, Hansson GC. The inner of the two Muc2 mucin-dependent mucus layers in colon is devoid of bacteria. Proceedings of the National Academy of Sciences of the United States of America. 2008;105(39):15064-9.
7. Martens EC, Chiang HC, Gordon JI. Mucosal glycan foraging enhances fitness and transmission of a saccharolytic human gut bacterial symbiont. Cell Host Microbe. 2008;4(5):447-57.
8. Sonnenburg JL, Xu J, Leip DD, Chen CH, Westover BP, Weatherford J, et al. Glycan foraging in vivo by an intestine-adapted bacterial symbiont. Science (New York, NY). 2005;307(5717):1955-9.
9. Xu J, Bjursell MK, Himrod J, Deng S, Carmichael LK, Chiang HC, et al. A genomic view of the human-Bacteroides thetaiotaomicron symbiosis. Science (New York, NY). 2003;299(5615):2074-6.
10. Pelaseyed T, Bergstrom JH, Gustafsson JK, Ermund A, Birchenough GM, Schutte A, et al. The mucus and mucins of the goblet cells and enterocytes provide the first defense line of the gastrointestinal tract and interact with the immune system. Immunological reviews. 2014;260(1):8-20.
11. Li H, Limenitakis JP, Fuhrer T, Geuking MB, Lawson MA, Wyss M, et al. The outer mucus layer hosts a distinct intestinal microbial niche. Nature communications. 2015;6:8292.
12. Antoni L, Nuding S, Weller D, Gersemann M, Ott G, Wehkamp J, et al. Human colonic mucus is a reservoir for antimicrobial peptides. Journal of Crohn's & colitis. 2013;7(12):e652-64.
13. Gutzeit C, Magri G, Cerutti A. Intestinal IgA production and its role in host-microbe interaction. Immunological reviews. 2014;260(1):76-85.
14. Barker N, van de Wetering M, Clevers H. The intestinal stem cell. Genes & Development. 2008;22(14):1856-64.
15. Farquhar MG, Palade GE. Junctional complexes in various epithelia. The Journal of cell biology. 1963;17:375-412.
16. Mehta S, Nijhuis A, Kumagai T, Lindsay J, Silver A. Defects in the adherens junction complex (E-cadherin/ beta-catenin) in inflammatory bowel disease. Cell and tissue research. 2015;360(3):749-60.
17. Tsukita S, Furuse M, Itoh M. Multifunctional strands in tight junctions. Nature reviews Molecular cell biology. 2001;2(4):285-93.
18. Turner JR. Intestinal mucosal barrier function in health and disease. Nature reviews Immunology. 2009;9(11):799-809.
19. Harhaj NS, Antonetti DA. Regulation of tight junctions and loss of barrier function in pathophysiology. The international journal of biochemistry & cell biology. 2004;36(7):1206-37.
20. Garcia-Hernandez V, Quiros M, Nusrat A. Intestinal epithelial claudins: expression and regulation in homeostasis and inflammation. Annals of the New York Academy of Sciences. 2017;1397(1):66-79.
21. Mineta K, Yamamoto Y, Yamazaki Y, Tanaka H, Tada Y, Saito K, et al. Predicted expansion of the claudin multigene family. FEBS Lett. 2011;585(4):606-12.

22. Groschwitz KR, Hogan SP. Intestinal barrier function: molecular regulation and disease pathogenesis. The Journal of allergy and clinical immunology. 2009;124(1):3-20; quiz 1-2.
23. Hammer AM, Morris NL, Earley ZM, Choudhry MA. The First Line of Defense: The Effects of Alcohol on Post-Burn Intestinal Barrier, Immune Cells, and Microbiome. Alcohol research : current reviews. 2015;37(2):209-22.
24. Assimakopoulos SF, Papageorgiou I, Charonis A. Enterocytes' tight junctions: From molecules to diseases. World journal of gastrointestinal pathophysiology. 2011;2(6):123-37.
25. Hermiston ML, Gordon JI. In vivo analysis of cadherin function in the mouse intestinal epithelium: essential roles in adhesion, maintenance of differentiation, and regulation of programmed cell death. The Journal of cell biology. 1995;129(2):489-506.
26. Kowalczyk AP, Green KJ. Structure, function, and regulation of desmosomes. Progress in molecular biology and translational science. 2013;116:95-118.
27. Kabat AM, Pott J, Maloy KJ. The Mucosal Immune System and Its Regulation by Autophagy. Frontiers in immunology. 2016;7:240.
28. Takeuchi O, Akira S. Pattern recognition receptors and inflammation. Cell. 2010;140(6):805-20.
29. Hume DA. The mononuclear phagocyte system. Current opinion in immunology. 2006;18(1):49-53.
30. Souza-Fonseca-Guimaraes F, Adib-Conquy M, Cavaillon JM. Natural killer (NK) cells in antibacterial innate immunity: angels or devils? Molecular medicine (Cambridge, Mass). 2012;18:270-85.
31. Maynard CL, Elson CO, Hatton RD, Weaver CT. Reciprocal interactions of the intestinal microbiota and immune system. Nature. 2012;489(7415):231-41.
32. Nagashima R, Maeda K, Imai Y, Takahashi T. Lamina propria macrophages in the human gastrointestinal mucosa: their distribution, immunohistological phenotype, and function. The journal of histochemistry and cytochemistry : official journal of the Histochemistry Society. 1996;44(7):721-31.
33. Smith PD, Smythies LE, Shen R, Greenwell-Wild T, Gliozzi M, Wahl SM. Intestinal macrophages and response to microbial encroachment. Mucosal immunology. 2011;4(1):31-42.
34. Biswas SK, Mantovani A. Macrophage plasticity and interaction with lymphocyte subsets: cancer as a paradigm. Nature immunology. 2010;11(10):889-96.
35. Bain CC, Scott CL, Uronen-Hansson H, Gudjonsson S, Jansson O, Grip O, et al. Resident and pro-inflammatory macrophages in the colon represent alternative context-dependent fates of the same Ly6Chi monocyte precursors. Mucosal immunology. 2013;6(3):498-510.
36. Weber B, Saurer L, Schenk M, Dickgreber N, Mueller C. CX3CR1 defines functionally distinct intestinal mononuclear phagocyte subsets which maintain their respective functions during homeostatic and inflammatory conditions. European journal of immunology. 2011;41(3):773-9.
37. Coombes JL, Siddiqui KR, Arancibia-Carcamo CV, Hall J, Sun CM, Belkaid Y, et al. A functionally specialized population of mucosal CD103+ DCs induces Foxp3+ regulatory T cells via a TGF-beta and retinoic acid-dependent mechanism. J Exp Med. 2007;204(8):1757-64.
38. Uematsu S, Fujimoto K, Jang MH, Yang BG, Jung YJ, Nishiyama M, et al. Regulation of humoral and cellular gut immunity by lamina propria dendritic cells expressing Toll-like receptor 5. Nature immunology. 2008;9(7):769-76.
39. Denning TL, Wang YC, Patel SR, Williams IR, Pulendran B. Lamina propria macrophages and dendritic cells differentially induce regulatory and interleukin 17-producing T cell responses. Nature immunology. 2007;8(10):1086-94.
40. Zigmond E, Jung S. Intestinal macrophages: well educated exceptions from the rule. Trends in immunology. 2013;34(4):162-8.
41. Smythies LE, Sellers M, Clements RH, Mosteller-Barnum M, Meng G, Benjamin WH, et al. Human intestinal macrophages display profound inflammatory anergy

despite avid phagocytic and bacteriocidal activity. The Journal of clinical investigation. 2005;115(1):66-75.
42. Hedl M, Li J, Cho JH, Abraham C. Chronic stimulation of Nod2 mediates tolerance to bacterial products. Proceedings of the National Academy of Sciences of the United States of America. 2007;104(49):19440-5.
43. Aderem A, Underhill DM. Mechanisms of phagocytosis in macrophages. Annual review of immunology. 1999;17:593-623.
44. Slauch JM. How does the oxidative burst of macrophages kill bacteria? Still an open question. Molecular microbiology. 2011;80(3):580-3.
45. Fang FC. Antimicrobial reactive oxygen and nitrogen species: concepts and controversies. Nature reviews Microbiology. 2004;2(10):820-32.
46. Mantegazza AR, Magalhaes JG, Amigorena S, Marks MS. Presentation of phagocytosed antigens by MHC class I and II. Traffic (Copenhagen, Denmark). 2013;14(2):135-52.
47. Sun JC, Ugolini S, Vivier E. Immunological memory within the innate immune system. The EMBO journal. 2014;33(12):1295-303.
48. Nishana M, Raghavan SC. Role of recombination activating genes in the generation of antigen receptor diversity and beyond. Immunology. 2012;137(4):271-81.
49. Biancone L, Monteleone I, Del Vecchio Blanco G, Vavassori P, Pallone F. Resident bacterial flora and immune system. Digestive and liver disease : official journal of the Italian Society of Gastroenterology and the Italian Association for the Study of the Liver. 2002;34 Suppl 2:S37-43.
50. Zenewicz LA, Antov A, Flavell RA. CD4 T-cell differentiation and inflammatory bowel disease. Trends in molecular medicine. 2009;15(5):199-207.
51. Weaver CT, Harrington LE, Mangan PR, Gavrieli M, Murphy KM. Th17: an effector CD4 T cell lineage with regulatory T cell ties. Immunity. 2006;24(6):677-88.
52. Kjerrulf M, Grdic D, Ekman L, Schon K, Vajdy M, Lycke NY. Interferon-gamma receptor-deficient mice exhibit impaired gut mucosal immune responses but intact oral tolerance. Immunology. 1997;92(1):60-8.
53. Artis D, Kane CM, Fiore J, Zaph C, Shapira S, Joyce K, et al. Dendritic cell-intrinsic expression of NF-kappa B1 is required to promote optimal Th2 cell differentiation. Journal of immunology (Baltimore, Md : 1950). 2005;174(11):7154-9.
54. Zenewicz LA, Yancopoulos GD, Valenzuela DM, Murphy AJ, Stevens S, Flavell RA. Innate and adaptive interleukin-22 protects mice from inflammatory bowel disease. Immunity. 2008;29(6):947-57.
55. Maxwell JR, Zhang Y, Brown WA, Smith CL, Byrne FR, Fiorino M, et al. Differential Roles for Interleukin-23 and Interleukin-17 in Intestinal Immunoregulation. Immunity. 2015;43(4):739-50.
56. Sakaguchi S, Yamaguchi T, Nomura T, Ono M. Regulatory T cells and immune tolerance. Cell. 2008;133(5):775-87.
57. Geuking MB, Cahenzli J, Lawson MA, Ng DC, Slack E, Hapfelmeier S, et al. Intestinal bacterial colonization induces mutualistic regulatory T cell responses. Immunity. 2011;34(5):794-806.
58. Lee SH, Kwon JE, Cho ML. Immunological pathogenesis of inflammatory bowel disease. Intestinal research. 2018;16(1):26-42.
59. de Lange KM, Barrett JC. Understanding inflammatory bowel disease via immunogenetics. Journal of autoimmunity. 2015;64:91-100.
60. Neurath MF, Finotto S. The many roads to inflammatory bowel diseases. Immunity. 2006;25(2):189-91.
61. Molodecky NA, Soon IS, Rabi DM, Ghali WA, Ferris M, Chernoff G, et al. Increasing incidence and prevalence of the inflammatory bowel diseases with time, based on systematic review. Gastroenterology. 2012;142(1):46-54.e42; quiz e30.
62. Lakatos PL, Lakatos L. Risk for colorectal cancer in ulcerative colitis: changes, causes and management strategies. World journal of gastroenterology. 2008;14(25):3937-47.

63. Mazal J. Crohn disease: pathophysiology, diagnosis, and treatment. Radiologic technology. 2014;85(3):297-316; quiz 7-20.
64. Baumgart DC, Sandborn WJ. Inflammatory bowel disease: clinical aspects and established and evolving therapies. Lancet (London, England). 2007;369(9573):1641-57.
65. Adams SM, Bornemann PH. Ulcerative colitis. American family physician. 2013;87(10):699-705.
66. Zhang YZ, Li YY. Inflammatory bowel disease: pathogenesis. World journal of gastroenterology. 2014;20(1):91-9.
67. Ananthakrishnan AN. Epidemiology and risk factors for IBD. Nature reviews Gastroenterology & hepatology. 2015;12(4):205-17.
68. Ananthakrishnan AN, Khalili H, Konijeti GG, Higuchi LM, de Silva P, Korzenik JR, et al. A prospective study of long-term intake of dietary fiber and risk of Crohn's disease and ulcerative colitis. Gastroenterology. 2013;145(5):970-7.
69. Bonaz BL, Bernstein CN. Brain-gut interactions in inflammatory bowel disease. Gastroenterology. 2013;144(1):36-49.
70. Ananthakrishnan AN, Higuchi LM, Huang ES, Khalili H, Richter JM, Fuchs CS, et al. Aspirin, nonsteroidal anti-inflammatory drug use, and risk for Crohn disease and ulcerative colitis: a cohort study. Annals of internal medicine. 2012;156(5):350-9.
71. Kinnucan JA, Rubin DT, Ali T. Sleep and inflammatory bowel disease: exploring the relationship between sleep disturbances and inflammation. Gastroenterology & hepatology. 2013;9(11):718-27.
72. Harries AD, Baird A, Rhodes J. Non-smoking: a feature of ulcerative colitis. British medical journal (Clinical research ed). 1982;284(6317):706.
73. Mahid SS, Minor KS, Soto RE, Hornung CA, Galandiuk S. Smoking and inflammatory bowel disease: a meta-analysis. Mayo Clinic proceedings. 2006;81(11):1462-71.
74. Yang H, McElree C, Roth MP, Shanahan F, Targan SR, Rotter JI. Familial empirical risks for inflammatory bowel disease: differences between Jews and non-Jews. Gut. 1993;34(4):517-24.
75. Jostins L, Ripke S, Weersma RK, Duerr RH, McGovern DP, Hui KY, et al. Host-microbe interactions have shaped the genetic architecture of inflammatory bowel disease. Nature. 2012;491(7422):119-24.
76. Khor B, Gardet A, Xavier RJ. Genetics and pathogenesis of inflammatory bowel disease. Nature. 2011;474(7351):307-17.
77. Turner JR. Molecular basis of epithelial barrier regulation: from basic mechanisms to clinical application. The American journal of pathology. 2006;169(6):1901-9.
78. Prasad S, Mingrino R, Kaukinen K, Hayes KL, Powell RM, MacDonald TT, et al. Inflammatory processes have differential effects on claudins 2, 3 and 4 in colonic epithelial cells. Laboratory investigation; a journal of technical methods and pathology. 2005;85(9):1139-62.
79. Guan Q, Zhang J. Recent Advances: The Imbalance of Cytokines in the Pathogenesis of Inflammatory Bowel Disease. Mediators Inflamm. 2017;2017:4810258.
80. Bouma G, Strober W. The immunological and genetic basis of inflammatory bowel disease. Nature reviews Immunology. 2003;3(7):521-33.
81. Galvez J. Role of Th17 Cells in the Pathogenesis of Human IBD. ISRN inflammation. 2014;2014:928461.
82. Jiang W, Su J, Zhang X, Cheng X, Zhou J, Shi R, et al. Elevated levels of Th17 cells and Th17-related cytokines are associated with disease activity in patients with inflammatory bowel disease. Inflammation research : official journal of the European Histamine Research Society [et al]. 2014;63(11):943-50.
83. Strober W, Fuss IJ. Proinflammatory cytokines in the pathogenesis of inflammatory bowel diseases. Gastroenterology. 2011;140(6):1756-67.

84. Eckburg PB, Relman DA. The role of microbes in Crohn's disease. Clinical infectious diseases : an official publication of the Infectious Diseases Society of America. 2007;44(2):256-62.
85. Sokol H, Lay C, Seksik P, Tannock GW. Analysis of bacterial bowel communities of IBD patients: what has it revealed? Inflammatory bowel diseases. 2008;14(6):858-67.
86. Duchmann R, Schmitt E, Knolle P, Meyer zum Buschenfelde KH, Neurath M. Tolerance towards resident intestinal flora in mice is abrogated in experimental colitis and restored by treatment with interleukin-10 or antibodies to interleukin-12. European journal of immunology. 1996;26(4):934-8.
87. Rath HC, Herfarth HH, Ikeda JS, Grenther WB, Hamm TE, Jr., Balish E, et al. Normal luminal bacteria, especially Bacteroides species, mediate chronic colitis, gastritis, and arthritis in HLA-B27/human beta2 microglobulin transgenic rats. The Journal of clinical investigation. 1996;98(4):945-53.
88. Sellon RK, Tonkonogy S, Schultz M, Dieleman LA, Grenther W, Balish E, et al. Resident enteric bacteria are necessary for development of spontaneous colitis and immune system activation in interleukin-10-deficient mice. Infect Immun. 1998;66(11):5224-31.
89. Madsen KL, Doyle JS, Tavernini MM, Jewell LD, Rennie RP, Fedorak RN. Antibiotic therapy attenuates colitis in interleukin 10 gene-deficient mice. Gastroenterology. 2000;118(6):1094-105.
90. Manichanh C, Borruel N, Casellas F, Guarner F. The gut microbiota in IBD. Nature reviews Gastroenterology & hepatology. 2012;9(10):599-608.
91. Feller M, Huwiler K, Schoepfer A, Shang A, Furrer H, Egger M. Long-term antibiotic treatment for Crohn's disease: systematic review and meta-analysis of placebo-controlled trials. Clinical infectious diseases : an official publication of the Infectious Diseases Society of America. 2010;50(4):473-80.
92. Atarashi K, Tanoue T, Shima T, Imaoka A, Kuwahara T, Momose Y, et al. Induction of colonic regulatory T cells by indigenous Clostridium species. Science (New York, NY). 2011;331(6015):337-41.
93. Round JL, Lee SM, Li J, Tran G, Jabri B, Chatila TA, et al. The Toll-like receptor 2 pathway establishes colonization by a commensal of the human microbiota. Science (New York, NY). 2011;332(6032):974-7.
94. Fukuda S, Toh H, Hase K, Oshima K, Nakanishi Y, Yoshimura K, et al. Bifidobacteria can protect from enteropathogenic infection through production of acetate. Nature. 2011;469(7331):543-7.
95. Chassaing B, Darfeuille-Michaud A. The commensal microbiota and enteropathogens in the pathogenesis of inflammatory bowel diseases. Gastroenterology. 2011;140(6):1720-28.
96. Mukhopadhya I, Hansen R, El-Omar EM, Hold GL. IBD-what role do Proteobacteria play? Nature reviews Gastroenterology & hepatology. 2012;9(4):219-30.
97. Oh SY, Cho KA, Kang JL, Kim KH, Woo SY. Comparison of experimental mouse models of inflammatory bowel disease. International journal of molecular medicine. 2014;33(2):333-40.
98. Valatas V, Bamias G, Kolios G. Experimental colitis models: Insights into the pathogenesis of inflammatory bowel disease and translational issues. European journal of pharmacology. 2015;759:253-64.
99. Eckmann L. Animal models of inflammatory bowel disease: lessons from enteric infections. Annals of the New York Academy of Sciences. 2006;1072:28-38.
100. Heffernan EJ, Fierer J, Chikami G, Guiney D. Natural history of oral Salmonella dublin infection in BALB/c mice: effect of an 80-kilobase-pair plasmid on virulence. The Journal of infectious diseases. 1987;155(6):1254-9.
101. Brennan PC, Fritz TE, Flynn RJ, Poole CM. Citrobacter Freundii associated with diarrhea in a laborytory mice. Laboratory animal care. 1965;15:266-75.

102. Petty NK, Bulgin R, Crepin VF, Cerdeno-Tarraga AM, Schroeder GN, Quail MA, et al. The Citrobacter rodentium genome sequence reveals convergent evolution with human pathogenic Escherichia coli. Journal of bacteriology. 2010;192(2):525-38.
103. Chandrakesan P, Roy B, Jakkula LU, Ahmed I, Ramamoorthy P, Tawfik O, et al. Utility of a bacterial infection model to study epithelial-mesenchymal transition, mesenchymal-epithelial transition or tumorigenesis. Oncogene. 2014;33(20):2639-54.
104. Collins JW, Keeney KM, Crepin VF, Rathinam VA, Fitzgerald KA, Finlay BB, et al. Citrobacter rodentium: infection, inflammation and the microbiota. Nature reviews Microbiology. 2014;12(9):612-23.
105. Pickard JM, Maurice CF, Kinnebrew MA, Abt MC, Schenten D, Golovkina TV, et al. Rapid fucosylation of intestinal epithelium sustains host-commensal symbiosis in sickness. Nature. 2014;514(7524):638-41.
106. Barthold SW, Coleman GL, Jacoby RO, Livestone EM, Jonas AM. Transmissible murine colonic hyperplasia. Veterinary pathology. 1978;15(2):223-36.
107. Wiles S, Clare S, Harker J, Huett A, Young D, Dougan G, et al. Organ specificity, colonization and clearance dynamics in vivo following oral challenges with the murine pathogen Citrobacter rodentium. Cellular microbiology. 2004;6(10):963-72.
108. Wales AD, Pearson GR, Roe JM, Hayes CM, La Ragione RM, Woodward MJ. Attaching-effacing lesions associated with Escherichia coli O157:H7 and other bacteria in experimentally infected conventional neonatal goats. Journal of comparative pathology. 2005;132(2-3):185-94.
109. Bry L, Brenner MB. Critical role of T cell-dependent serum antibody, but not the gut-associated lymphoid tissue, for surviving acute mucosal infection with Citrobacter rodentium, an attaching and effacing pathogen. Journal of immunology (Baltimore, Md : 1950). 2004;172(1):433-41.
110. Luperchio SA, Schauer DB. Molecular pathogenesis of Citrobacter rodentium and transmissible murine colonic hyperplasia. Microbes and infection. 2001;3(4):333-40.
111. Mundy R, MacDonald TT, Dougan G, Frankel G, Wiles S. Citrobacter rodentium of mice and man. Cellular microbiology. 2005;7(12):1697-706.
112. Maaser C, Housley MP, Iimura M, Smith JR, Vallance BA, Finlay BB, et al. Clearance of Citrobacter rodentium requires B cells but not secretory immunoglobulin A (IgA) or IgM antibodies. Infect Immun. 2004;72(6):3315-24.
113. Wlodarska M, Willing B, Keeney KM, Menendez A, Bergstrom KS, Gill N, et al. Antibiotic treatment alters the colonic mucus layer and predisposes the host to exacerbated Citrobacter rodentium-induced colitis. Infect Immun. 2011;79(4):1536-45.
114. Gibson DL, Ma C, Bergstrom KS, Huang JT, Man C, Vallance BA. MyD88 signalling plays a critical role in host defence by controlling pathogen burden and promoting epithelial cell homeostasis during Citrobacter rodentium-induced colitis. Cellular microbiology. 2008;10(3):618-31.
115. Lebeis SL, Bommarius B, Parkos CA, Sherman MA, Kalman D. TLR signaling mediated by MyD88 is required for a protective innate immune response by neutrophils to Citrobacter rodentium. Journal of immunology (Baltimore, Md : 1950). 2007;179(1):566-77.
116. Gibson DL, Ma C, Rosenberger CM, Bergstrom KS, Valdez Y, Huang JT, et al. Toll-like receptor 2 plays a critical role in maintaining mucosal integrity during Citrobacter rodentium-induced colitis. Cellular microbiology. 2008;10(2):388-403.
117. Khan MA, Ma C, Knodler LA, Valdez Y, Rosenberger CM, Deng W, et al. Toll-like receptor 4 contributes to colitis development but not to host defense during Citrobacter rodentium infection in mice. Infect Immun. 2006;74(5):2522-36.
118. Ahmed I, Chandrakesan P, Tawfik O, Xia L, Anant S, Umar S. Critical roles of Notch and Wnt/beta-catenin pathways in the regulation of hyperplasia and/or colitis in response to bacterial infection. Infect Immun. 2012;80(9):3107-21.
119. Higgins LM, Frankel G, Douce G, Dougan G, MacDonald TT. Citrobacter rodentium infection in mice elicits a mucosal Th1 cytokine response and lesions similar to those in murine inflammatory bowel disease. Infect Immun. 1999;67(6):3031-9.

120. Alipour M, Lou Y, Zimmerman D, Bording-Jorgensen MW, Sergi C, Liu JJ, et al. A balanced IL-1beta activity is required for host response to Citrobacter rodentium infection. PloS one. 2013;8(12):e80656.
121. Li L, Shi QG, Lin F, Liang YG, Sun LJ, Mu JS, et al. Cytokine IL-6 is required in Citrobacter rodentium infection-induced intestinal Th17 responses and promotes IL-22 expression in inflammatory bowel disease. Molecular medicine reports. 2014;9(3):831-6.
122. Buschor S, Cuenca M, Uster SS, Scharen OP, Balmer ML, Terrazos MA, et al. Innate immunity restricts Citrobacter rodentium A/E pathogenesis initiation to an early window of opportunity. PLoS pathogens. 2017;13(6):e1006476.
123. Simmons CP, Goncalves NS, Ghaem-Maghami M, Bajaj-Elliott M, Clare S, Neves B, et al. Impaired resistance and enhanced pathology during infection with a noninvasive, attaching-effacing enteric bacterial pathogen, Citrobacter rodentium, in mice lacking IL-12 or IFN-gamma. Journal of immunology (Baltimore, Md : 1950). 2002;168(4):1804-12.
124. Symonds EL, Riedel CU, O'Mahony D, Lapthorne S, O'Mahony L, Shanahan F. Involvement of T helper type 17 and regulatory T cell activity in Citrobacter rodentium invasion and inflammatory damage. Clinical and experimental immunology. 2009;157(1):148-54.
125. Mangan PR, Harrington LE, O'Quinn DB, Helms WS, Bullard DC, Elson CO, et al. Transforming growth factor-beta induces development of the T(H)17 lineage. Nature. 2006;441(7090):231-4.
126. Geddes K, Rubino SJ, Magalhaes JG, Streutker C, Le Bourhis L, Cho JH, et al. Identification of an innate T helper type 17 response to intestinal bacterial pathogens. Nat Med. 2011;17(7):837-44.
127. Singer SJ, Nicolson GL. The fluid mosaic model of the structure of cell membranes. Science (New York, NY). 1972;175(4023):720-31.
128. and DAB, London E. Functions of lipid rafts in biological membranes. Annual Review of Cell and Developmental Biology. 1998;14(1):111-36.
129. Simons K, Ikonen E. Functional rafts in cell membranes. Nature. 1997;387(6633):569-72.
130. Watson H. Biological membranes. Essays in Biochemistry. 2015;59:43-69.
131. Sezgin E, Levental I, Mayor S, Eggeling C. The mystery of membrane organization: composition, regulation and roles of lipid rafts. Nature reviews Molecular cell biology. 2017;18(6):361-74.
132. Futerman AH, Hannun YA. The complex life of simple sphingolipids. EMBO reports. 2004;5(8):777-82.
133. Lippincott-Schwartz J, Phair RD. Lipids and Cholesterol as Regulators of Traffic in the Endomembrane System. Annual Review of Biophysics. 2010;39:559-78.
134. Gault CR, Obeid LM, Hannun YA. An overview of sphingolipid metabolism: from synthesis to breakdown. Advances in experimental medicine and biology. 2010;688:1-23.
135. Zhang Y, Li X, Becker KA, Gulbins E. Ceramide-enriched membrane domains--structure and function. Biochimica et biophysica acta. 2009;1788(1):178-83.
136. Gatt S. ENZYMIC HYDROLYSIS AND SYNTHESIS OF CERAMIDES. The Journal of biological chemistry. 1963;238:3131-3.
137. Levran O, Desnick RJ, Schuchman EH. Niemann-Pick disease: a frequent missense mutation in the acid sphingomyelinase gene of Ashkenazi Jewish type A and B patients. Proceedings of the National Academy of Sciences of the United States of America. 1991;88(9):3748-52.
138. Kitatani K, Idkowiak-Baldys J, Hannun YA. The sphingolipid salvage pathway in ceramide metabolism and signaling. Cellular signalling. 2008;20(6):1010-8.
139. Ogretmen B, Hannun YA. Biologically active sphingolipids in cancer pathogenesis and treatment. Nature reviews Cancer. 2004;4(8):604-16.
140. Hannun YA, Obeid LM. Principles of bioactive lipid signalling: lessons from sphingolipids. Nature reviews Molecular cell biology. 2008;9(2):139-50.

141. Bao JX, Jin S, Zhang F, Wang ZC, Li N, Li PL. Activation of membrane NADPH oxidase associated with lysosome-targeted acid sphingomyelinase in coronary endothelial cells. Antioxidants & redox signaling. 2010;12(6):703-12.
142. Herz J, Pardo J, Kashkar H, Schramm M, Kuzmenkina E, Bos E, et al. Acid sphingomyelinase is a key regulator of cytotoxic granule secretion by primary T lymphocytes. Nature immunology. 2009;10(7):761-8.
143. Fowler S. Lysosomal localization of sphingomyelinase in rat liver. Biochimica et biophysica acta. 1969;191(2):481-4.
144. Schissel SL, Jiang X, Tweedie-Hardman J, Jeong T, Camejo EH, Najib J, et al. Secretory sphingomyelinase, a product of the acid sphingomyelinase gene, can hydrolyze atherogenic lipoproteins at neutral pH. Implications for atherosclerotic lesion development. The Journal of biological chemistry. 1998;273(5):2738-46.
145. Schissel SL, Keesler GA, Schuchman EH, Williams KJ, Tabas I. The cellular trafficking and zinc dependence of secretory and lysosomal sphingomyelinase, two products of the acid sphingomyelinase gene. The Journal of biological chemistry. 1998;273(29):18250-9.
146. Beckmann N, Sharma D, Gulbins E, Becker KA, Edelmann B. Inhibition of acid sphingomyelinase by tricyclic antidepressants and analogons. Frontiers in physiology. 2014;5:331.
147. Menaldino DS, Bushnev A, Sun A, Liotta DC, Symolon H, Desai K, et al. Sphingoid bases and de novo ceramide synthesis: enzymes involved, pharmacology and mechanisms of action. Pharmacological research. 2003;47(5):373-81.
148. Bose R, Verheij M, Haimovitz-Friedman A, Scotto K, Fuks Z, Kolesnick R. Ceramide synthase mediates daunorubicin-induced apoptosis: an alternative mechanism for generating death signals. Cell. 1995;82(3):405-14.
149. Jenkins GM, Cowart LA, Signorelli P, Pettus BJ, Chalfant CE, Hannun YA. Acute activation of de novo sphingolipid biosynthesis upon heat shock causes an accumulation of ceramide and subsequent dephosphorylation of SR proteins. The Journal of biological chemistry. 2002;277(45):42572-8.
150. Kitatani K, Nemoto M, Akiba S, Sato T. Stimulation by de novo-synthesized ceramide of phospholipase A2-dependent cholesterol esterification promoted by the uptake of oxidized low-density lipoprotein in macrophages. Cellular signalling. 2002;14(8):695-701.
151. Gomez del Pulgar T, Velasco G, Sanchez C, Haro A, Guzman M. De novo-synthesized ceramide is involved in cannabinoid-induced apoptosis. The Biochemical journal. 2002;363(Pt 1):183-8.
152. Don AS, Lim XY, Couttas TA. Re-configuration of sphingolipid metabolism by oncogenic transformation. Biomolecules. 2014;4(1):315-53.
153. Mao C, Obeid LM. Ceramidases: regulators of cellular responses mediated by ceramide, sphingosine, and sphingosine-1-phosphate. Biochimica et biophysica acta. 2008;1781(9):424-34.
154. Shtraizent N, Eliyahu E, Park JH, He X, Shalgi R, Schuchman EH. Autoproteolytic cleavage and activation of human acid ceramidase. The Journal of biological chemistry. 2008;283(17):11253-9.
155. Franzen R, Pautz A, Brautigam L, Geisslinger G, Pfeilschifter J, Huwiler A. Interleukin-1beta induces chronic activation and de novo synthesis of neutral ceramidase in renal mesangial cells. The Journal of biological chemistry. 2001;276(38):35382-9.
156. Houben E, Holleran WM, Yaginuma T, Mao C, Obeid LM, Rogiers V, et al. Differentiation-associated expression of ceramidase isoforms in cultured keratinocytes and epidermis. Journal of lipid research. 2006;47(5):1063-70.
157. Xu R, Jin J, Hu W, Sun W, Bielawski J, Szulc Z, et al. Golgi alkaline ceramidase regulates cell proliferation and survival by controlling levels of sphingosine and S1P. FASEB journal : official publication of the Federation of American Societies for Experimental Biology. 2006;20(11):1813-25.

158. Coant N, Sakamoto W, Mao C, Hannun YA. Ceramidases, roles in sphingolipid metabolism and in health and disease. Advances in biological regulation. 2017;63:122-31.
159. Maceyka M, Harikumar KB, Milstien S, Spiegel S. Sphingosine-1-phosphate signaling and its role in disease. Trends in cell biology. 2012;22(1):50-60.
160. Hurwitz R, Ferlinz K, Vielhaber G, Moczall H, Sandhoff K. Processing of human acid sphingomyelinase in normal and I-cell fibroblasts. The Journal of biological chemistry. 1994;269(7):5440-5.
161. Jenkins RW, Canals D, Hannun YA. Roles and regulation of secretory and lysosomal acid sphingomyelinase. Cellular signalling. 2009;21(6):836-46.
162. Schuchman EH, Levran O, Pereira LV, Desnick RJ. Structural organization and complete nucleotide sequence of the gene encoding human acid sphingomyelinase (SMPD1). Genomics. 1992;12(2):197-205.
163. Hannun YA, Newcomb B. A new twist to the emerging functions of ceramides in cancer: novel role for platelet acid sphingomyelinase in cancer metastasis. EMBO molecular medicine. 2015;7(6):692-4.
164. Qiu H, Edmunds T, Baker-Malcolm J, Karey KP, Estes S, Schwarz C, et al. Activation of human acid sphingomyelinase through modification or deletion of C-terminal cysteine. The Journal of biological chemistry. 2003;278(35):32744-52.
165. Niemann A. Ein unbekanntes krankheitsbild. Jahrb Kinderheilkd. 1914;79(1).
166. Pick L. Über die lipoidzellige splenohepatomegalie typus Niemann-Pick als stoffwechselerkrankung. Med Klin. 1927;23:1483-6.
167. Klenk E. Über die natur der phosphatide und anderer lipoide des gehirns und der leber bei der Niemann-Pickschen krankheit.[12. Mitteilung über phosphatide.]. Hoppe-Seyler´ s Zeitschrift für physiologische Chemie. 1935;235(1-2):24-36.
168. Koch J, Gartner S, Li CM, Quintern LE, Bernardo K, Levran O, et al. Molecular cloning and characterization of a full-length complementary DNA encoding human acid ceramidase. Identification Of the first molecular lesion causing Farber disease. The Journal of biological chemistry. 1996;271(51):33110-5.
169. Ferlinz K, Kopal G, Bernardo K, Linke T, Bar J, Breiden B, et al. Human acid ceramidase: processing, glycosylation, and lysosomal targeting. The Journal of biological chemistry. 2001;276(38):35352-60.
170. Schulze H, Schepers U, Sandhoff K. Overexpression and mass spectrometry analysis of mature human acid ceramidase. Biological chemistry. 2007;388(12):1333-43.
171. Azuma N, O'Brien JS, Moser HW, Kishimoto Y. Stimulation of acid ceramidase activity by saposin D. Archives of biochemistry and biophysics. 1994;311(2):354-7.
172. Zalba S, ten Hagen T. Cell membrane modulation as adjuvant in cancer therapy2016.
173. Keller P, Simons K. Cholesterol is required for surface transport of influenza virus hemagglutinin. The Journal of cell biology. 1998;140(6):1357-67.
174. Sot J, Bagatolli LA, Goni FM, Alonso A. Detergent-resistant, ceramide-enriched domains in sphingomyelin/ceramide bilayers. Biophysical journal. 2006;90(3):903-14.
175. Gulbins E. Regulation of death receptor signaling and apoptosis by ceramide. Pharmacological research. 2003;47(5):393-9.
176. Bollinger CR, Teichgraber V, Gulbins E. Ceramide-enriched membrane domains. Biochimica et biophysica acta. 2005;1746(3):284-94.
177. Stancevic B, Kolesnick R. CERAMIDE-RICH PLATFORMS IN TRANSMEMBRANE SIGNALING. FEBS letters. 2010;584(9):1728-40.
178. Grassme H, Jekle A, Riehle A, Schwarz H, Berger J, Sandhoff K, et al. CD95 signaling via ceramide-rich membrane rafts. The Journal of biological chemistry. 2001;276(23):20589-96.
179. Grassme H, Jendrossek V, Bock J, Riehle A, Gulbins E. Ceramide-rich membrane rafts mediate CD40 clustering. Journal of immunology (Baltimore, Md : 1950). 2002;168(1):298-307.

180. Gulbins E, Dreschers S, Wilker B, Grassmé H. Ceramide, membrane rafts and infections. Journal of Molecular Medicine. 2004;82(6):357-63.
181. Grassme H, Riethmuller J, Gulbins E. Ceramide in cystic fibrosis. Handbook of experimental pharmacology. 2013(216):265-74.
182. Dinoff A, Herrmann N, Lanctot KL. Ceramides and depression: A systematic review. Journal of affective disorders. 2017;213:35-43.
183. Barth BM, Cabot MC, Kester M. Ceramide-based therapeutics for the treatment of cancer. Anti-cancer agents in medicinal chemistry. 2011;11(9):911-9.
184. Reynolds CP, Maurer BJ, Kolesnick RN. Ceramide synthesis and metabolism as a target for cancer therapy. Cancer letters. 2004;206(2):169-80.
185. Morad SA, Cabot MC. Ceramide-orchestrated signalling in cancer cells. Nature reviews Cancer. 2013;13(1):51-65.
186. Rhein C, Tripal P, Seebahn A, Konrad A, Kramer M, Nagel C, et al. Functional implications of novel human acid sphingomyelinase splice variants. PloS one. 2012;7(4):e35467.
187. Kolzer M, Arenz C, Ferlinz K, Werth N, Schulze H, Klingenstein R, et al. Phosphatidylinositol-3,5-Bisphosphate is a potent and selective inhibitor of acid sphingomyelinase. Biological chemistry. 2003;384(9):1293-8.
188. Perrotta C, De Palma C, Clementi E. Nitric oxide and sphingolipids: mechanisms of interaction and role in cellular pathophysiology. Biological chemistry. 2008;389(11):1391-7.
189. Kornhuber J, Tripal P, Gulbins E, Muehlbacher M. Functional inhibitors of acid sphingomyelinase (FIASMAs). Handbook of experimental pharmacology. 2013(215):169-86.
190. Kornhuber J, Tripal P, Reichel M, Terfloth L, Bleich S, Wiltfang J, et al. Identification of new functional inhibitors of acid sphingomyelinase using a structure-property-activity relation model. Journal of medicinal chemistry. 2008;51(2):219-37.
191. Trapp S, Rosania GR, Horobin RW, Kornhuber J. Quantitative modeling of selective lysosomal targeting for drug design. European biophysics journal : EBJ. 2008;37(8):1317-28.
192. Kornhuber J, Retz W, Riederer P. Slow accumulation of psychotropic substances in the human brain. Relationship to therapeutic latency of neuroleptic and antidepressant drugs? Journal of neural transmission Supplementum. 1995;46:315-23.
193. Kolzer M, Werth N, Sandhoff K. Interactions of acid sphingomyelinase and lipid bilayers in the presence of the tricyclic antidepressant desipramine. FEBS Lett. 2004;559(1-3):96-8.
194. Zhou YF, Metcalf MC, Garman SC, Edmunds T, Qiu H, Wei RR. Human acid sphingomyelinase structures provide insight to molecular basis of Niemann-Pick disease. Nature communications. 2016;7:13082.
195. Kornhuber J, Muehlbacher M, Trapp S, Pechmann S, Friedl A, Reichel M, et al. Identification of novel functional inhibitors of acid sphingomyelinase. PloS one. 2011;6(8):e23852.
196. Kornhuber J, Tripal P, Reichel M, Muhle C, Rhein C, Muehlbacher M, et al. Functional Inhibitors of Acid Sphingomyelinase (FIASMAs): a novel pharmacological group of drugs with broad clinical applications. Cellular physiology and biochemistry : international journal of experimental cellular physiology, biochemistry, and pharmacology. 2010;26(1):9-20.
197. Elojeimy S, Holman DH, Liu X, El-Zawahry A, Villani M, Cheng JC, et al. New insights on the use of desipramine as an inhibitor for acid ceramidase. FEBS Lett. 2006;580(19):4751-6.
198. Merck Sharp. aD. Amitriptyline Hydrochloride: An antidepressive Agent: Résumé of Essential Information. Rahway, NJ: Merck & CO. 1961.
199. Carette S, McCain GA, Bell DA, Fam AG. Evaluation of amitriptyline in primary fibrositis. A double-blind, placebo-controlled study. Arthritis and rheumatism. 1986;29(5):655-9.

200. Couch JR, Ziegler DK, Hassanein R. Amitriptyline in the prophylaxis of migraine. Effectiveness and relationship of antimigraine and antidepressant effects. Neurology. 1976;26(2):121-7.
201. Egbunike IG, Chaffee BJ. Antidepressants in the management of chronic pain syndromes. Pharmacotherapy. 1990;10(4):262-70.
202. Mishra PC, Agarwal VK, Rahman H. Therapeutic trial of amitryptiline in the treatment of nocturnal enuresis--a controlled study. Indian pediatrics. 1980;17(3):279-85.
203. Friedman G. Treatment of the irritable bowel syndrome. Gastroenterology clinics of North America. 1991;20(2):325-33.
204. Mandal A, Sinha C, Kumar Jena A, Ghosh S, Samanta A. An Investigation on in vitro and in vivo Antimicrobial Properties of the Antidepressant: Amitriptyline Hydrochloride. Brazilian journal of microbiology : [publication of the Brazilian Society for Microbiology]. 2010;41(3):635-45.
205. Roumestan C, Michel A, Bichon F, Portet K, Detoc M, Henriquet C, et al. Anti-inflammatory properties of desipramine and fluoxetine. Respiratory research. 2007;8:35.
206. Breyer-Pfaff U. The metabolic fate of amitriptyline, nortriptyline and amitriptylinoxide in man. Drug metabolism reviews. 2004;36(3-4):723-46.
207. Gillman PK. Tricyclic antidepressant pharmacology and therapeutic drug interactions updated. British journal of pharmacology. 2007;151(6):737-48.
208. Glowinski J, Axelrod J. Inhibtion ofuptake of tritiated-noradrenaline in the intactrat brain by imipramine and structurally related compounds. Nature. 1964;204:1318-9.
209. Owens MJ, Morgan WN, Plott SJ, Nemeroff CB. Neurotransmitter receptor and transporter binding profile of antidepressants and their metabolites. The Journal of pharmacology and experimental therapeutics. 1997;283(3):1305-22.
210. Arenz C. Small molecule inhibitors of acid sphingomyelinase. Cellular physiology and biochemistry : international journal of experimental cellular physiology, biochemistry, and pharmacology. 2010;26(1):1-8.
211. Riethmuller J, Anthonysamy J, Serra E, Schwab M, Doring G, Gulbins E. Therapeutic efficacy and safety of amitriptyline in patients with cystic fibrosis. Cellular physiology and biochemistry : international journal of experimental cellular physiology, biochemistry, and pharmacology. 2009;24(1-2):65-72.
212. Schuchman EH. Acid ceramidase and the treatment of ceramide diseases: The expanding role of enzyme replacement therapy. Biochimica et biophysica acta. 2016;1862(9):1459-71.
213. Schulze H, Kolter T, Sandhoff K. Principles of lysosomal membrane degradation: Cellular topology and biochemistry of lysosomal lipid degradation. Biochimica et biophysica acta. 2009;1793(4):674-83.
214. Adams C, Icheva V, Deppisch C, Lauer J, Herrmann G, Graepler-Mainka U, et al. Long-Term Pulmonal Therapy of Cystic Fibrosis-Patients with Amitriptyline. Cellular physiology and biochemistry : international journal of experimental cellular physiology, biochemistry, and pharmacology. 2016;39(2):565-72.
215. Teichgraber V, Ulrich M, Endlich N, Riethmuller J, Wilker B, De Oliveira-Munding CC, et al. Ceramide accumulation mediates inflammation, cell death and infection susceptibility in cystic fibrosis. Nat Med. 2008;14(4):382-91.
216. Brady RO, Kanfer JN, Mock MB, Fredrickson DS. The metabolism of sphingomyelin. II. Evidence of an enzymatic deficiency in Niemann-Pick diseae. Proceedings of the National Academy of Sciences of the United States of America. 1966;55(2):366-9.
217. Schuchman EH, Desnick RJ. Types A and B Niemann-Pick disease. Molecular genetics and metabolism. 2017;120(1-2):27-33.
218. Beckmann N, Gulbins E, Becker KA, Carpinteiro A. Sphingomyelinase, Acidic. Encyclopedia of Signaling Molecules. 2017:1-8.

219. Hurwitz R, Ferlinz K, Sandhoff K. The tricyclic antidepressant desipramine causes proteolytic degradation of lysosomal sphingomyelinase in human fibroblasts. Biological chemistry Hoppe-Seyler. 1994;375(7):447-50.
220. Grassme H, Jernigan PL, Hoehn RS, Wilker B, Soddemann M, Edwards MJ, et al. Inhibition of Acid Sphingomyelinase by Antidepressants Counteracts Stress-Induced Activation of P38-Kinase in Major Depression. Neuro-Signals. 2015;23(1):84-92.
221. Gulbins A, Grassme H, Hoehn R, Wilker B, Soddemann M, Kohnen M, et al. Regulation of Neuronal Stem Cell Proliferation in the Hippocampus by Endothelial Ceramide. Cellular physiology and biochemistry : international journal of experimental cellular physiology, biochemistry, and pharmacology. 2016;39(2):790-801.
222. Gulbins E, Palmada M, Reichel M, Luth A, Bohmer C, Amato D, et al. Acid sphingomyelinase-ceramide system mediates effects of antidepressant drugs. Nat Med. 2013;19(7):934-8.
223. Okayasu I, Hatakeyama S, Yamada M, Ohkusa T, Inagaki Y, Nakaya R. A novel method in the induction of reliable experimental acute and chronic ulcerative colitis in mice. Gastroenterology. 1990;98(3):694-702.
224. Chassaing B, Aitken JD, Malleshappa M, Vijay-Kumar M. Dextran sulfate sodium (DSS)-induced colitis in mice. Current protocols in immunology. 2014;104:Unit-15.25.
225. Fischbeck A, Leucht K, Frey-Wagner I, Bentz S, Pesch T, Kellermeier S, et al. Sphingomyelin induces cathepsin D-mediated apoptosis in intestinal epithelial cells and increases inflammation in DSS colitis. Gut. 2011;60(1):55-65.
226. Ohnishi T, Hashizume C, Taniguchi M, Furumoto H, Han J, Gao R, et al. Sphingomyelin synthase 2 deficiency inhibits the induction of murine colitis-associated colon cancer. FASEB journal : official publication of the Federation of American Societies for Experimental Biology. 2017;31(9):3816-30.
227. Oertel S, Scholich K, Weigert A, Thomas D, Schmetzer J, Trautmann S, et al. Ceramide synthase 2 deficiency aggravates AOM-DSS-induced colitis in mice: role of colon barrier integrity. Cellular and molecular life sciences : CMLS. 2017;74(16):3039-55.
228. Sandborn WJ, Feagan BG, Wolf DC, D'Haens G, Vermeire S, Hanauer SB, et al. Ozanimod Induction and Maintenance Treatment for Ulcerative Colitis. The New England journal of medicine. 2016;374(18):1754-62.
229. Horinouchi K, Erlich S, Perl DP, Ferlinz K, Bisgaier CL, Sandhoff K, et al. Acid sphingomyelinase deficient mice: a model of types A and B Niemann-Pick disease. Nat Genet. 1995;10(3):288-93.
230. Zhang J, Zhao J, Jiang W-j, Shan X-w, Yang X-m, Gao J-g. Conditional gene manipulation: Cre-ating a new biological era. Journal of Zhejiang University Science B. 2012;13(7):511-24.
231. Eliyahu E, Shtraizent N, Shalgi R, Schuchman EH. Construction of conditional acid ceramidase knockout mice and in vivo effects on oocyte development and fertility. Cellular physiology and biochemistry : international journal of experimental cellular physiology, biochemistry, and pharmacology. 2012;30(3):735-48.
232. Quillin RC, 3rd, Wilson GC, Nojima H, Freeman CM, Wang J, Schuster RM, et al. Inhibition of acidic sphingomyelinase reduces established hepatic fibrosis in mice. Hepatol Res. 2015;45(3):305-14.
233. Zhang X, Goncalves R, Mosser DM. The Isolation and Characterization of Murine Macrophages. Current protocols in immunology / edited by John E Coligan [et al]. 2008;CHAPTER:Unit-14.1.
234. Weigmann B, Tubbe I, Seidel D, Nicolaev A, Becker C, Neurath MF. Isolation and subsequent analysis of murine lamina propria mononuclear cells from colonic tissue. Nature protocols. 2007;2(10):2307-11.
235. Wu Y, Gulbins E, Grassme H. The function of sphingomyelinases in mycobacterial infections. Biological chemistry. 2018.

236. Becker KA, Riethmuller J, Seitz AP, Gardner A, Boudreau R, Kamler M, et al. Sphingolipids as targets for inhalation treatment of cystic fibrosis. Advanced drug delivery reviews. 2018.
237. Grassme H, Becker KA, Zhang Y, Gulbins E. Ceramide in bacterial infections and cystic fibrosis. Biological chemistry. 2008;389(11):1371-9.
238. Woodcock J. Sphingosine and ceramide signalling in apoptosis. IUBMB life. 2006;58(8):462-6.
239. Ruvolo PP. Intracellular signal transduction pathways activated by ceramide and its metabolites. Pharmacological research. 2003;47(5):383-92.
240. Gerdes J, Schwab U, Lemke H, Stein H. Production of a mouse monoclonal antibody reactive with a human nuclear antigen associated with cell proliferation. International journal of cancer. 1983;31(1):13-20.
241. Gerdes J, Stein H, Pileri S, Rivano MT, Gobbi M, Ralfkiaer E, et al. Prognostic relevance of tumour-cell growth fraction in malignant non-Hodgkin's lymphomas. Lancet (London, England). 1987;2(8556):448-9.
242. Fischer H, Ellstrom P, Ekstrom K, Gustafsson L, Gustafsson M, Svanborg C. Ceramide as a TLR4 agonist; a putative signalling intermediate between sphingolipid receptors for microbial ligands and TLR4. Cellular microbiology. 2007;9(5):1239-51.
243. Matsunaga N, Tsuchimori N, Matsumoto T, Ii M. TAK-242 (resatorvid), a small-molecule inhibitor of Toll-like receptor (TLR) 4 signaling, binds selectively to TLR4 and interferes with interactions between TLR4 and its adaptor molecules. Molecular pharmacology. 2011;79(1):34-41.
244. Wang Z, Friedrich C, Hagemann SC, Korte WH, Goharani N, Cording S, et al. Regulatory T cells promote a protective Th17-associated immune response to intestinal bacterial infection with C. rodentium. Mucosal immunology. 2014;7(6):1290-301.
245. Schneider-Schaulies J, Beyersdorf N. CD4+ Foxp3+ regulatory T cell-mediated immunomodulation by anti-depressants inhibiting acid sphingomyelinase. Biological chemistry. 2018;399(10):1175-82.
246. Matricon J, Barnich N, Ardid D. Immunopathogenesis of inflammatory bowel disease. Self/nonself. 2010;1(4):299-309.
247. Bock J, Liebisch G, Schweimer J, Schmitz G, Rogler G. Exogenous sphingomyelinase causes impaired intestinal epithelial barrier function. World journal of gastroenterology. 2007;13(39):5217-25.
248. Bouhet S, Hourcade E, Loiseau N, Fikry A, Martinez S, Roselli M, et al. The mycotoxin fumonisin B1 alters the proliferation and the barrier function of porcine intestinal epithelial cells. Toxicological sciences : an official journal of the Society of Toxicology. 2004;77(1):165-71.
249. Cheng ZJ, Singh RD, Sharma DK, Holicky EL, Hanada K, Marks DL, et al. Distinct mechanisms of clathrin-independent endocytosis have unique sphingolipid requirements. Molecular biology of the cell. 2006;17(7):3197-210.
250. Tafazoli F, Magnusson KE, Zheng L. Disruption of epithelial barrier integrity by Salmonella enterica serovar typhimurium requires geranylgeranylated proteins. Infect Immun. 2003;71(2):872-81.
251. Bryan P-F, Karla C, Edgar Alejandro M-T, Sara Elva E-P, Gemma F, Luz C. Sphingolipids as Mediators in the Crosstalk between Microbiota and Intestinal Cells: Implications for Inflammatory Bowel Disease. Mediators of inflammation. 2016;2016:9890141-.
252. Schulze H, Sandhoff K. Sphingolipids and lysosomal pathologies. Biochimica et biophysica acta. 2014;1841(5):799-810.
253. Bruewer M, Luegering A, Kucharzik T, Parkos CA, Madara JL, Hopkins AM, et al. Proinflammatory cytokines disrupt epithelial barrier function by apoptosis-independent mechanisms. Journal of immunology (Baltimore, Md : 1950). 2003;171(11):6164-72.
254. Homaidan FR, Chakroun I, El-Sabban ME. Regulation of nuclear factor-kappaB in intestinal epithelial cells in a cell model of inflammation. Mediators Inflamm. 2003;12(5):277-83.

255. Bauer J, Liebisch G, Hofmann C, Huy C, Schmitz G, Obermeier F, et al. Lipid alterations in experimental murine colitis: role of ceramide and imipramine for matrix metalloproteinase-1 expression. PloS one. 2009;4(9):e7197.
256. Furuya H, Ohkawara S, Nagashima K, Asanuma N, Hino T. Dietary sphingomyelin alleviates experimental inflammatory bowel disease in mice. International journal for vitamin and nutrition research Internationale Zeitschrift fur Vitamin- und Ernahrungsforschung Journal international de vitaminologie et de nutrition. 2008;78(1):41-9.
257. Andersson D, Kotarsky K, Wu J, Agace W, Duan RD. Expression of alkaline sphingomyelinase in yeast cells and anti-inflammatory effects of the expressed enzyme in a rat colitis model. Digestive diseases and sciences. 2009;54(7):1440-8.
258. Chen Y, Xu SC, Duan RD. Mevalonate inhibits acid sphingomyelinase activity, increases sphingomyelin levels and inhibits cell proliferation of HepG2 and Caco-2 cells. Lipids in health and disease. 2015;14:130.
259. Xiong Y, Zhu XD, Wan P, Ren YP, Wang C, Yan RW, et al. Inhibition of ASM activity ameliorates DSS-induced colitis in mice. Prostaglandins & other lipid mediators. 2019;140:26-30.
260. Bock J, Liebisch G, Schweimer J, Schmitz G, Rogler G. Exogenous sphingomyelinase causes impaired intestinal epithelial barrier function. World journal of gastroenterology. 2007;13(39):5217-25.
261. Arango Duque G, Descoteaux A. Macrophage cytokines: involvement in immunity and infectious diseases. Frontiers in immunology. 2014;5:491-.
262. Sakata A, Ochiai T, Shimeno H, Hikishima S, Yokomatsu T, Shibuya S, et al. Acid sphingomyelinase inhibition suppresses lipopolysaccharide-mediated release of inflammatory cytokines from macrophages and protects against disease pathology in dextran sulphate sodium-induced colitis in mice. Immunology. 2007;122(1):54-64.
263. Tafesse FG, Rashidfarrokhi A, Schmidt FI, Freinkman E, Dougan S, Dougan M, et al. Disruption of Sphingolipid Biosynthesis Blocks Phagocytosis of Candida albicans. PLoS pathogens. 2015;11(10):e1005188-e.
264. McQuiston T, Luberto C, Del Poeta M. Role of sphingosine-1-phosphate (S1P) and S1P receptor 2 in the phagocytosis of Cryptococcus neoformans by alveolar macrophages. Microbiology (Reading, England). 2011;157(Pt 5):1416-27.
265. Lee WL, Harrison RE, Grinstein S. Phagocytosis by neutrophils. Microbes and infection. 2003;5(14):1299-306.
266. Suchard SJ, Mansfield PJ, Boxer LA, Shayman JA. Mitogen-activated protein kinase activation during IgG-dependent phagocytosis in human neutrophils: inhibition by ceramide. Journal of immunology (Baltimore, Md : 1950). 1997;158(10):4961-7.
267. Qureshi A, Subathra M, Grey A, Schey K, Del Poeta M, Luberto C. Role of sphingomyelin synthase in controlling the antimicrobial activity of neutrophils against Cryptococcus neoformans. PloS one. 2010;5(12):e15587-e.
268. McCollister BD, Myers JT, Jones-Carson J, Voelker DR, Vazquez-Torres A. Constitutive acid sphingomyelinase enhances early and late macrophage killing of Salmonella enterica serovar Typhimurium. Infect Immun. 2007;75(11):5346-52.
269. Balreira A, Lacerda L, Miranda CS, Arosa FA. Evidence for a link between sphingolipid metabolism and expression of CD1d and MHC-class II: monocytes from Gaucher disease patients as a model. Br J Haematol. 2005;129(5):667-76.
270. Church LD, Hessler G, Goodall JE, Rider DA, Workman CJ, Vignali DA, et al. TNFR1-induced sphingomyelinase activation modulates TCR signaling by impairing store-operated Ca2+ influx. Journal of leukocyte biology. 2005;78(1):266-78.
271. Bai A, Kokkotou E, Zheng Y, Robson SC. Role of acid sphingomyelinase bioactivity in human CD4+ T-cell activation and immune responses. Cell death & disease. 2015;6:e1828.
272. Bai A, Moss A, Kokkotou E, Usheva A, Sun X, Cheifetz A, et al. CD39 and CD161 modulate Th17 responses in Crohn's disease. Journal of immunology (Baltimore, Md : 1950). 2014;193(7):3366-77.

273. Kharel Y, Lee S, Snyder AH, Sheasley-O'neill S L, Morris MA, Setiady Y, et al. Sphingosine kinase 2 is required for modulation of lymphocyte traffic by FTY720. The Journal of biological chemistry. 2005;280(44):36865-72.
274. Daniel C, Sartory N, Zahn N, Geisslinger G, Radeke HH, Stein JM. FTY720 ameliorates Th1-mediated colitis in mice by directly affecting the functional activity of CD4+CD25+ regulatory T cells. Journal of immunology (Baltimore, Md : 1950). 2007;178(4):2458-68.
275. Zhou Y, Salker MS, Walker B, Munzer P, Borst O, Gawaz M, et al. Acid Sphingomyelinase (ASM) is a Negative Regulator of Regulatory T Cell (Treg) Development. Cellular physiology and biochemistry : international journal of experimental cellular physiology, biochemistry, and pharmacology. 2016;39(3):985-95.
276. Hollmann C, Werner S, Avota E, Reuter D, Japtok L, Kleuser B, et al. Inhibition of Acid Sphingomyelinase Allows for Selective Targeting of CD4+ Conventional versus Foxp3+ Regulatory T Cells. Journal of immunology (Baltimore, Md : 1950). 2016;197(8):3130-41.
277. Utermohlen O, Karow U, Lohler J, Kronke M. Severe impairment in early host defense against Listeria monocytogenes in mice deficient in acid sphingomyelinase. Journal of immunology (Baltimore, Md : 1950). 2003;170(5):2621-8.
278. Yu H, Zeidan YH, Wu BX, Jenkins RW, Flotte TR, Hannun YA, et al. Defective acid sphingomyelinase pathway with Pseudomonas aeruginosa infection in cystic fibrosis. American journal of respiratory cell and molecular biology. 2009;41(3):367-75.
279. Li C, Wu Y, Riehle A, Orian-Rousseau V, Zhang Y, Gulbins E, et al. Regulation of Staphylococcus aureus Infection of Macrophages by CD44, Reactive Oxygen Species, and Acid Sphingomyelinase. Antioxidants & redox signaling. 2017.
280. Faulstich M, Hagen F, Avota E, Kozjak-Pavlovic V, Winkler AC, Xian Y, et al. Neutral sphingomyelinase 2 is a key factor for PorB-dependent invasion of Neisseria gonorrhoeae. Cellular microbiology. 2015;17(2):241-53.
281. Simonis A, Hebling S, Gulbins E, Schneider-Schaulies S, Schubert-Unkmeir A. Differential activation of acid sphingomyelinase and ceramide release determines invasiveness of Neisseria meningitidis into brain endothelial cells. PLoS pathogens. 2014;10(6):e1004160.
282. Grassme H, Gulbins E, Brenner B, Ferlinz K, Sandhoff K, Harzer K, et al. Acidic sphingomyelinase mediates entry of N. gonorrhoeae into nonphagocytic cells. Cell. 1997;91(5):605-15.
283. Grassme H, Jendrossek V, Riehle A, von Kurthy G, Berger J, Schwarz H, et al. Host defense against Pseudomonas aeruginosa requires ceramide-rich membrane rafts. Nat Med. 2003;9(3):322-30.
284. Heaver SL, Johnson EL, Ley RE. Sphingolipids in host-microbial interactions. Current opinion in microbiology. 2018;43:92-9.
285. Franzosa EA, Sirota-Madi A, Avila-Pacheco J, Fornelos N, Haiser HJ, Reinker S, et al. Gut microbiome structure and metabolic activity in inflammatory bowel disease. Nature microbiology. 2018.
286. Di Marzio L, Di Leo A, Cinque B, Fanini D, Agnifili A, Berloco P, et al. Detection of alkaline sphingomyelinase activity in human stool: proposed role as a new diagnostic and prognostic marker of colorectal cancer. Cancer epidemiology, biomarkers & prevention : a publication of the American Association for Cancer Research, cosponsored by the American Society of Preventive Oncology. 2005;14(4):856-62.
287. Duan RD, Hertervig E, Nyberg L, Hauge T, Sternby B, Lillienau J, et al. Distribution of alkaline sphingomyelinase activity in human beings and animals. Tissue and species differences. Digestive diseases and sciences. 1996;41(9):1801-6.
288. Chauvier D, Morjani H, Manfait M. Ceramide involvement in homocamptothecin- and camptothecin-induced cytotoxicity and apoptosis in colon HT29 cells. International journal of oncology. 2002;20(4):855-63.
289. Soo I, Madsen KL, Tejpar Q, Sydora BC, Sherbaniuk R, Cinque B, et al. VSL#3 probiotic upregulates intestinal mucosal alkaline sphingomyelinase and reduces

inflammation. Canadian journal of gastroenterology = Journal canadien de gastroenterologie. 2008;22(3):237-42.

Appendix

8.1 Abbreviations

AC	Acid ceramidase (human AC, murine Ac)
ACER1-3	Alkaline ceramidase 1-3
Asm	Acid sphingomyelinase (human ASM, murine Asm)
AJ	Adherents junctions
AJC	Apical junctional complex
APC	Antigen presenting cell
BM	Bone marrow
BMDMs	Bone marrow derived macrophages
C1PP	Ceramide-1-phosphate phosphatase
C. rodentium	*Citrobacter rodentium*
CD	Cluster of differentiation
CDases	Ceramidases
CK	Ceramide kinase
cKO	Conditional knockout
CoA	Coenzyme A
CR	*Citrobacter rodentium*
CRS	Cerebrosides
CS	Ceramide synthases
DC	Dendritic cell
DE	Desmosome
DES	Dihydroceramide desaturase
DNA	Deoxyribonucleic acid
DNase	Deoxyribonuclease
dNTP	Deoxy-Nucleotide-Triphosphate
dp	Days post
DSS	Dextran-sodium sulphate
E-cadherin	Epithelial-cadherin
E. coli	*Escherichia coli*
EDTA	Ethylenediaminetetraacetic acid
EGTA	Ethyleneglycol-bis(β-aminoethyl ether)-N,N,N',N'-tetraacetic acid
EHEC	Enterohemorrhagic *E. coli*
EPEC	Enteropathogen *E. coli*
FACS	Fluorescence-activated cell sorting
FCS	Fetal calf serum
FIASMAs	Functional inhibitor of acid sphingomyelinase

FITC-Dextranbeads	Fluorescein isothiocyanate-dextran beads
FoxP3	Forkhead-box 3
GFP	Green florescence protein
GJ	gap junctions
H&E	Hematoxylin and eosin stain
H_2O_2	Hydrogen peroxide
i.p.	Intraperitoneal
i.v.	Intravenous
IFNγ	Interferon-γ
IgA	Immunoglobulin A
IL	Interleukin
iNOS	Inducible nitric oxide synthases
IVC	Individually ventilated cages
JAM	Junctional adherents molecules
Kb	Kilobases
KM	Michaelis-Menten constant
KO	Knock out
LP	Lamina propria
LPL	Lamina propria lymphocytes
LPS	Lipopolysaccharide
MACS	Magnetic cell separation
MFI	Mean fluorescence intensity
MHCII	Major histocompatibility complex class II
mLN	Mesenteric lymph node
mRNA	Messenger RNA
MUC	Mucin glycoprotein
MyD88	Myeloid differentiation primary response gene 88
NADPH	Nicotinamide adenine dinucleotide phosphate
NC	Neutral ceramidase
NfκB	Nuclear-factor-κB
NK	Natural killer cells
NLR	NOD-like receptor
NO	Nitric oxide
NO_2	Nitrogen dioxide
N_2O_3	Dinitrogen trioxide
NOD	Nucleotide binding oligomerization domain
O_2^-	Superoxide

$ONOO^-$	Peroxynitrite
PC	Phosphatidylcholine
PAMP	Pathogen associated molecular pattern
PBS	Phosphate buffered saline
PCR	Polymerase chain reaction
RNA	Ribonucleic acid
RNS	Reactive nitric oxide
ROS	Reactive oxygen species
RT	Real time
S1P	Sphingosine-1-phosphate
S1PP	S1P phosphatase
SI	Small intestine
SKs	Sphingosine kinases
SMase	Sphingomyelinase
SMS	Sphingomyelin synthase
SPH	Sphingosine
SPT	Serine palmitoyl transferase
TCA	Tricycle antidepressant
TGF-ß	Transforming growth factor ß
T_h	T helper cells
TJ	Tight junctions
TLR	Toll like receptor
TMCH	Transmissible murine crypt hyperplasia
TNBS	Trinitrobenzenesulfonic acid
TNFα	Tumour-necrosis Factoring-α
T_{reg}	Regulatory T cell
TCR	T cell receptor
WT	Wilde type
ZO-1-3	Zona occludens 1-3

8.2 List of figures

8.3 List of tables

8.4 Acknowledgments

By writing this acknowledgment, an intense and exciting chapter is about to end, which brings me to addressee a huge thanks to all the people participating, supporting and encouraging me in the last years.

First and foremost I would like to thank Prof. Dr. Astrid Westendorf for giving me the opportunity to work on these exciting projects. Not only I am really grateful for your help and support during this project but also for your guidance to reach my scientific and personal goals.

Furthermore, I thank Jan Buer for giving me the possibility to work in his institute, Wiebke Hansen and Richard Kolesnick for their professional support.

I would also like to thank Dr. Fabian Schumacher at the Department of Toxicology/Institute of Nutritional Science in Potsdam, Prof. Dr. Dirk Hermann and Ayan Mohamud Yusuf at the Department of Neurology, Dr. med. Alexander Carpinteiro and Eyad Naser, Prof. Dr. Karl Lang and Judith Bezgovsek at the Institute for Immunology in Essen and finally Prof. Dr. Robert Klopfleisch at the Institute of Veterinary Pathology in Berlin for their time and effort supporting my project.

Further, I would also like to thank the members of the thesis committee for taking the time to evaluate my PhD thesis.

A huge thank you is also owed to my past and present colleagues and friends at the Department of Medical Mircobiology, for supporting me. Sina, Christian, Christina and Benny thanks for the support in the lab and the fun I had with you whenever I couldn't motivate myself. A special and huge thanks I owe to you, Mechthild. Thanks Mechthild, for always helping me out, supporting me and taking so much care. I really enjoyed working with you. With all my heart I want to thank Romy, Katarina and Eva, thanks for proof reading, your constant support and friendship. Especially Romy, thanks for always being there for me, no matter what! I will really miss all the delicious food we enjoyed together.

I would also like to thank my family, for their love and their unconditional support. Mum, dad thanks for being such a wonderful role model to me, the confidence you always gave me and your endless trust in me. A huge thanks to my friends back home for dancing through the night whenever I needed to get a clear head. I really hope we all will never get tired of laughing and dancing. Thanks Tina, for the walks and talks, the ice cream and your support. Finally, thank you Hinnerk, for giving me this special kind of support, the endless freedom during this adventure and the trust in me and my work. You truly made me smile whenever things were mad. I am absolutely looking forward to our next adventures and as you can imagine, I cannot wait for all of them to come.

8.5 Curriculum Vitae

Der Lebenslauf ist in der Online-Version aus Gründen des Datenschutzes nicht enthalten.

8.6 Declarations

Erklärung:

Hiermit erkläre ich, gem. § 6 Abs. (2) g) der Promotionsordnung der Fakultät für Biologie zur Erlangung des Dr. rer. nat., dass ich das Arbeitsgebiet, dem das Thema „The effect of the acid sphingomyelinase/ceramidase system on bacterial induced colitis“ zuzuordnen ist, in Forschung und Lehre vertrete und den Antrag von Jana Meiners befürworte.

Essen, den_____ _____

Prof. Dr. Astrid Westendorf

Erklärung:

Hiermit erkläre ich, gem. § 7 Abs. (2) d) + f) der Promotionsordnung der Fakultät für Biologie zur Erlangung des Dr. rer. nat., dass ich die vorliegende Dissertation selbständig verfasst und mich keiner anderen als der angegebenen Hilfsmittel bedient, bei der Abfassung der Dissertation nur die angegebenen Hilfsmittel benutzt und alle wörtlichen oder inhaltlich übernommen Stellen als solche gekennzeichnet habe.

Essen, den_____ _____

Jana Meiners

Erklärung:

Hiermit erkläre ich, gem. § 7 Abs. (2) e) + g) der Promotionsordnung der Fakultät für Biologie zur Erlangung des Dr. rer. nat., dass ich keine anderen Promotionen bzw. Promotionsversuche in der Vergangenheit durchgeführt habe und dass diese Arbeit von keiner anderen Fakultät/Fachbereich abgelehnt worden ist.

Essen, den_____ _____

Jana Meiners